STATE OF NEW MEXICO
BEFORE THE ENVIRONMENTAL IMPROVEMENT BOARD

IN THE MATTER OF PROPOSED REGULATION
20.2.350 NMAC – *GREENHOUSE GAS CAP AND TRADE PROVISIONS*

No. EIB 10-04 (R)

REBUTTAL TESTIMONY OF JONATHAN PATZ

I will focus in my rebuttal testimony on the testimony of Dr. Howard Maccabee, the only witness to question my testimony about the public health impacts of climate change. As described more fully below, Dr. Maccabee's testimony runs counter to the science and ignores key aspects of the issue.

Dr. Maccabee begins and ends his testimony with the claim that warmer temperature will be beneficial to the the public health. He opens his testimony with the statement that "[a]n overall benefit, in terms of decreased overall mortality, as average temperatures rise by one to four degrees centigrade as predicted by various IPCC projections. This is due to the physiological fact that there is less "sludging" of the blood in small vessels in warmer temperature and therefore significantly less heart attacks, strokes and pneumonia." Maccabee at 1-2 (emphasis added). He then claims that "Different sources estimate that the excess mortality from cold is six to nine times the excess mortality from heat waves." Maccabee at 2 (emphasis added). And finally, he concludes that "In fact, the dominant health effect of potential increases in climatic temperatures would be beneficial in New Mexico, the US, and the developed and developing

countries for which we have data. The lives saved by decreasing deaths from winter cold will far exceed the increased deaths from summer heat waves. Quantitative estimates of the magnitude of the benefit may be obtained from recent publications, including my own. (J.Amer.Phy.Surg., summer 2011) Similar calculations were presented by the British Department of Health, in a comprehensive report that predicted decreased mortality with climate warming." Maccabee at 5 (emphasis added).

There are several reasons why these statements are problematic. First, the medical explanation of higher winter mortality is far from resolved, and not at all a "physiologic fact." "Sludging of blood" is but one of several theories and based on a limited number of studies. Humans are not reptiles, after all, but warm-blooded mammals that maintain a relatively constant body temperature throughout the year.

Second, it is difficult to compare the net annual effect of temperature-related deaths due to differences in the methods of data compilation and types of exposure that cause heat-related versus cold-related (and often storm-related) mortality deaths. For example, Dixon et al. (2005) report that "The number of heat- or cold-related mortality are quite divergent. Consequently, in general, these separate mortality databases should not be combined or compared in policy determination." NMED-Patz Rebuttal Exhibit 1.

Finally, and perhaps most importantly, Dr. Maccabee does not even mention one of the most important determinants of winter mortality: seasonal influenza. From 1979-2001, an annual average of 41,400 deaths were attributed to influenza in the U.S., according to a study published by Dushoff et al. in the American Journal of Epidemiology. NMED-Patz Rebuttal Exhibit 2. The authors concluded that "No consistent relationships were found between various combinations of monthly mean

temperatures and normalized excess deaths." They also found that "On an annual timescale, we find preliminary evidence that cold weather does not predict winter deaths." (emphasis added). In other words, the study found that "the triggering of deaths by cold weather may be a short-term phenomenon that has much less impact on an annual timescale."

The Dushoff study contradicts the British studies cited by Dr. Maccabee, which attribute most excess winter deaths to cold. I will not attempt to deconstruct the British studies or their data, but simply caution against applying those studies to the Southwestern U.S., which differs significantly in climatic terms from the United Kingdom, which is dominated by maritime weather with a narrow temperature range .

Dr. Maccabee questions the data collection techniques of EPA which support the finding of no significant difference in deaths related to temperature, claiming that "[t]he EPA analysts blundered by counting death certificates from heat stroke, etc. but ignored all the deaths from heart attacks, strokes, etc. that are triggered by cooler temperatures, but are not announced as cold deaths on certificates." Maccabee at 2. The claim is not true, and in any event, this is not how heat wave statistics are calculated. It is well known that many deaths from heat waves are from cardiac and respiratory-related deaths. In fact, heat stroke deaths themselves are a tiny fraction of the real mortality figures in a heat wave, which are generally derived by calculating excess mortality beyond an expected norm (over the study period) for a given date.

Maccabee also discounts concern about morbidity and mortality associated with weather events and disease transmission:

> Furthermore, there has been speculation about increases in morbidity and mortality that might occur with more extreme weather events related to climate change. Anxiety about this is probably misplaced. Despite the fact that our climatic temperature has increased by 1.3°C over the 20th century, the death rate from extreme weather events has steadily decreased, according to US Government data. It would be surprising if warming of another one or two C would reverse this trend, especially given steady improvement in detection and response of our society to weather events. The same argument holds true for the threat of increased disease transmission, as predicted by Professors Epstein, Patz, et al. Why are we not seeing increased disease transmission after 1.3 C of warming?

Maccabee at 3.

Dr. Maccabee's question is not unreasonable, but it misses the point. We all know the multi-factorial nature of disease emergence, and therefore that the multiple "confounding factors" of any disease must be controlled for in order to assess relationships between exposures (in this case, temperatures) and disease outcome. If multiple decades of reliable data on trends in health care, human migration, drug resistance, and vector control were as available and reliable as weather data, we could attempt to answer this question of long term responses to climate change. NMED-Patz Rebuttal Exhibit 3.

Because this data is not available, we must rely on location-specific or short-term studies that show just how sensitive diseases are to climate variability. Studies demonstrating this relationship include childhood diarrheal disease in Lima (NMED-Patz Rebuttal Exhibit 4; waterborne diseases in the U.S. (NMED-Patz Rebuttal Exhibit 5); and cholera in Bangladesh (NMED-Patz Rebuttal Exhibit 6). We also find much higher rates of water contamination following extreme rainfall and runoff (extremes of

the hydrologic cycle being part of the climate change story). NMED-Patz Rebuttal Exhibit 7 (see Figure 4).

Dr. Maccabee seems to believe that the changing temperature will move in small and incremental steps when he states "It would be surprising if warming of another one or two C would reverse this trend" (referring to the death rate from extreme weather events). Maccabee at 3. This statment suggests that temperature is a finite quantity or fixed target on which we can focus our decisionmaking. A study published this year in the Proceedings of the National Academy of Sciences shows that unmitigated climate change could deliver temperatures that are beyond human adaptability. NMED-Patz Rebuttal Exhibit 8. Another recent study shows a much higher frequency of heat waves, especially in the western U.S., occurring within the next 30 years. NMED-Patz Rebuttal Exhibit 9. Heatwaves in Los Angeles, according to another study, are expected to quadruple by the end of this century. NMED-Patz Rebuttal Exhibit 10.

Finally, Dr. Maccabee opines that "It is also clear that there can be enormous economic costs involved in attempting to decrease carbon emissions, whether by carbon taxation or 'cap and trade' measures." Maccabee at 4. This concern misses a key dimension to the rationale behind reducing carbon emissions: focusing solely on the "costs" without including the "benefits" is to miss half (or more) of the story. For example, Nemet et al. (2010) examined the major cost-benefit analyses of CO_2 reduction conducted across the world. NMED-Patz Rebuttal Exhibit 11. The authors found that while the <u>costs</u> of

mitigation averaged $30 per ton of CO2 reduced, the benefits (e.g, improved air quality) averaged $49 per ton CO2 reduced. We have found similar results in more localized actions, for instance, the air pollution and physical exercise benefits of removing a small portion of internal combustion engines from the roadways in the Midwest region rises into the billions of dollars (Grabow et al. in preparation). These findings should be considered when evaluating claims about the cost of changing energy policies.

HEAT MORTALITY VERSUS COLD MORTALITY

A Study of Conflicting Databases in the United States

BY P. G. DIXON, D. M. BROMMER, B. C. HEDQUIST, A. J. KALKSTEIN, G. B. GOODRICH, J. C. WALTER, C. C. DICKERSON IV, S. J. PENNY, AND R. S. CERVENY

Studies of heat- and cold-related mortality in the United States produce widely ranging results due to inconsistent data sources, and this paper describes the methods, assets, and limitations of the most common temperature-related mortality sources.

When set against the backdrop of the massive death toll associated with the August 2003 heat wave in Europe, weather-related mortality and the comparison of the various causes is important in regard to preparation, policy determination, and the allocation of resources. However, discussion of cross-disciplinary statistics is difficult due to the lack of knowledge and communication between different areas of interest. Even in a country such as the United States, where substantial documentation of mortality exists, significant errors and marked differences can occur. A classic case is the number of fatalities associated with "excessive cold" or "excessive heat," where statistics have been independently compiled by weather sources of information (e.g., National Climatic Data Center) and by medical authorities (e.g., Centers for Disease Control and Prevention's National Center for Health Statistics). Such comparisons set the number of heat stroke victims, and other sources of life-ending heat-related conditions, against hypothermia and other sources of life-ending cold-related conditions. The adequate allocation of medical resources, formulation of advance warning and prediction systems, and other policy decisions are fundamentally linked to questions of the following type: "Do more people die from heat than die from cold?" and even more basically, "How many people die due to heat or cold?"

Interestingly, depending on the database used and the compiling U.S. agency, completely different results can be obtained. Several studies show that heat-related deaths outnumber cold-related deaths, while other studies conclude the exact opposite. We are not suggesting that any particular study is consistently inferior to another, but, rather, that it is absolutely critical to identify the exact data source, as well as the benefits and limitations of the database, used in these studies.

AFFILIATIONS: DIXON, BROMMER, HEDQUIST, KALKSTEIN, GOODRICH, WALTER, DICKERSON, PENNY, AND CERVENY—Office of Climatology, Department of Geography, Arizona State University, Tempe, Arizona
CORRESPONDING AUTHOR: Randy Cerveny, Department of Geography, Arizona State University, P.O. Box 870101, Tempe, AZ 85287-0104
E-mail: cerveny@asu.edu
DOI:10.1175/BAMS-86-7-937

In final form 19 January 2005
©2005 American Meteorological Society

DISCUSSION OF DATABASES. *Centers for Disease Control and Prevention.* The Centers for Disease

NMED - PATZ
REBUTTAL EXHIBIT 1

Control and Prevention's (CDC's) National Center for Health Statistics (NCHS) maintains electronic records for identified causes of death. Each state is responsible for compiling their death certificates and entering the information into a series of computer programs—such as the Automated Classification of Medical Entities (ACME); Translation of Axis, (TRANSAX); Mortality Medical Indexing, Classification, and Retrieval system (MICAR); and Super MICAR. Such programs scan for common terms and then code the data based on keywords. In some cases, however, such as those with multiple causes of death, human review may be necessary. Additionally, in a few cases, human evaluation under strict regulations might reorder the cause of death as stated on the death certificate and override the examining doctor's diagnosis of ultimate cause of death.

To quote a practicing physician, "death certificates are pretty straightforward." Much like any other official paperwork, the death certificate consists of a series of blanks that must be filled with specific information regarding the deceased. The forms tend to vary by state and are meant to record the fundamental cause of death, as well as unambiguously identify the person in question. The space on the certificate that is provided to state the cause of death is not particularly large. Rather, there is generally a single blank for the "immediate cause," as well as another small space used to list any underlying causes that may have led to the immediate cause. There may also be a small space for the explanation of other contributing factors (e.g., substance abuse, disease, smoking, etc.) that were not related to the immediate cause. However, each of these spaces is separate, and mortality compilations based on the immediate cause usually exclude information about underlying or complicating factors. Unfortunately, for most users the acquisition of death certificate copies is cost prohibitive, and the use of a secondary dataset, a codified analysis of death certificates such as the Compressed Mortality Index, is necessary.

Consequently, the CDC NCHS maintains a database that is structured on the cause of death as denoted by the deceased's death certificate. Deaths are classified as to the underlying cause, using the International Classification of Disease (ICD) [ninth edition for 1979–98 (ICD-9) and tenth edition for 1999–present]. The World Health Organization (1992) defines the underlying cause of death as "the disease or injury that initiated the train of events leading directly to death, or the circumstances of the accident or violence, which produced the fatal injury." Weather-related mortality categories according to the ICD-9 classification scheme include "excessive heat," "excessive cold," "lightning," and "high and low air pressure and changes in air pressure" (Table 1) among others. Most of the excessive cold and excessive heat mortality studies presented in the CDC's publication *Morbidity and Mortality Weekly Report* employ this database (Donoghue et al. 2003; Grey et al. 2002; Mirchandani et al. 2003; Sathyavagiswaran et al. 2001).

Kalkstein (1991) proposed the use of standardized gross mortality values as a method to determine the

Table 1. Selected categories of various databases containing weather-related mortality.

Selected major categories of the ICD-9	Selected weather categories from NCDC's *Storm Data*
Excessive heat	Drought
Excessive cold	Dust storm
High and low air pressure and changes in air pressure	Fog
Hunger, thirst, exposure, and neglect	Hail
Lightning	Hurricane/tropical storm
Cataclysmic storms, and floods resulting from storms	Lightning
Cataclysmic Earth surface movements and eruptions	Tornado
Accidental drowning and submersion	Wild/forest fire
Struck accidentally by falling object	Ocean/lake surf
Exposure to radiation	Precipitation
Overexertion and strenuous movements	Snow/ice
Other and unspecified environmental and accidental causes	Temperature extremes
Late effects of accidental injury	Thunderstorms and high winds

number of people dying from heat-related events. Using this method, total daily mortality within a metropolitan area is standardized first for population change, and then for time of year, because more deaths occur during the winter months (Fig. 1). A residual is then computed from the difference of the specific date/year of mortality and its standardized counterpart. It has been shown that heat waves exhibit an increased number of deaths over the standardized values (excess deaths), and this excess will be more reflective of the actual number of heat-related deaths (Kalkstein 1991). It is important to note that the gross mortality method takes all causes of death into account, and evidence has shown that overall mortality rates of numerous causes, such as heart attack and stroke, increase during heat waves. Thus, there is no need for stratification by cause of death.

Storm Data *index.* *Storm Data,* maintained by the National Climatic Data Center (NCDC), lists mortality values that are compiled (based on reports from trained spotters, law enforcement agents, emergency managers, and various media sources) by local National Weather Service (NWS) offices. *Storm Data* publications are easily accessible online through the NCDC Web site for 1994–present. However, a search function allows users to query the Storm Events Database for certain weather phenomena back to 1950, with more detailed information from *Storm Data* comprising all of the years since 1993. Included in both the online *Storm Data* publications and the Storm Events Database is the number of direct weather-related casualties, injuries, and property damage, including the location and date of each event. Also included for significant weather events are narratives that provide detailed information regarding casualties, weather records, and other anecdotal information. The Storm Events Database is updated monthly and generally lags 90–120 days behind the current month. The coupling of online data with the relatively quick updates makes *Storm Data* a very accessible data source. An example of a study based on *Storm Data* information is Curran et al.'s (2000) study on lightning deaths across the United States.

Because the source of each event is not given in the database, users of *Storm Data* must be cautious. The NWS cannot verify the accuracy and validity of all events. Once data from the various NWS offices are compiled, they are categorized by weather event type (Table 1). While data regarding tornadoes, thunderstorm winds, and hail are available from the 1950s, all other weather events in Table 1 are only available since 1993.

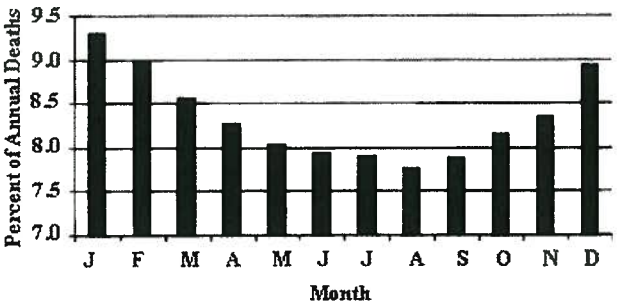

FIG. 1. Gross mortality (in percentage of annual deaths) for 12 cities across the United States for 1975–98.

In contrast to CDC reports, the operation manual for NCDC's *Storm Data* (Mandt 2002) includes detailed instructions on how to categorize direct and indirect causes for dozens of weather-related deaths. Regardless of the type of weather event, the manual clearly indicates that only deaths caused directly by the given weather event can be entered into the *Storm Data* archive. Any death that is indirectly caused by a weather event will be noted in the narrative that accompanies each entry, but will not be entered into the database.

For excessive heat to be considered the direct cause of a death in *Storm Data,* there must be a "fatality where heat-related or heat stress was the primary, secondary, or major contributing factor as determined by a medical examiner or coroner" (Mandt 2002). Hypothermia and cold-related deaths must meet similar criteria. The weather event itself must also achieve locally established values for heat or cold for the death to be considered direct. Deaths due solely to exposure to excessive temperatures are found in the "temperature extremes" category. Another category in *Storm Data* that can include excessive cold deaths is "snow and ice." If the death was the result of excessive cold and there were other weather conditions that led to the disorientation of the individual (such as blowing snow or icy roads), the death is not counted under the temperature extremes category and is, instead, listed under the category of snow and ice, which includes deaths by blizzards, heavy snow, and winter storms. For example, if the individual dies of exposure to cold after a traffic accident, the death is counted as a direct cause under snow and ice, but not temperature extremes.

Indirect deaths that are related to excessive cold and heat include those due to man-made heat or cold or, for example, when an individual dies of a heart attack while shoveling snow. Also included as indirect deaths are those related to excessive cold and heat that occur when the ambient weather conditions do

Table 2. Total number of heat-related deaths reported by the media (*Chicago Sun-Times*) for the Chicago 1995 heat wave event.

Date	Total deaths reported
13 Jul 1995	20
15 Jul 1995	56
16 Jul 1995	116
17 Jul 1995	179
18 Jul 1995	376
19 Jul 1995	402
20 Jul 1995	456
21 Jul 1995	457
22 Jul 1995	466
23 Jul 1995	468
25 Jul 1995	484
27 Jul 1995	529
3 Aug 1995	549
10 Aug 1995	562
30 Aug 1995	568

not surpass the locally established thresholds for an excessive cold or heat event. *Storm Data* also considers deaths from snow- or ice-related traffic accidents where exposure to excessive cold is not a factor in the death to be indirectly caused by weather, and, thus, they are not counted in the database. Therefore, defined criteria for death by heat or cold must be considered before data selection can begin.

Unfortunately, even with a well-defined standard for classifying direct and indirect causes of death, it is possible for problems to occur. There are several instances in *Storm Data* where traffic-related deaths were classified as directly caused by weather in contrast to the official guidelines. A random sample of two months from early 1995 snow and ice deaths shows that three deaths in January in Kentucky, two in February in Pennsylvania, and six in February in Texas were all from traffic accidents where exposure to excessive cold was not a factor in the death. These 11 incorrectly labeled deaths make up more than half of the total (17) snow-and-ice-related deaths during January/February 1995.

Media reports. Media accounts of heat- or cold-related deaths are primarily comprised of mortality numbers obtained from pertinent authorities and, given the nature of the media, are obtained quickly after, or even during, a given event. For example, the media-reported mortality numbers during the Chicago, Illinois, heat wave of 1995 were primarily made up of daily reports from the Cook County Chief Medical Examiner. During that event, the media reported daily heat-related death statistics (Table 2). In addition to medical examiners, the media also garnered death statistics from personal interviews with local funeral homes.

A common problem with the use of weather-related death totals as reported in the media is that major events are often underreported and rarely revised after publication. Further, because the media use county medical examiners as primary information sources, it should be noted that a medical examiner generally is involved only with deaths of an unknown cause or of a suspicious nature. Consequently, many heat-related deaths are not sent for collaboration to the medical examiner. Also, as with other methods, media reports can be taken out of context and tend to lack reliable evidence of direct or indirect causes of death. See Changnon et al. (1996) for a comprehensive discussion of media reporting on the Chicago 1995 heat wave.

COMPARISON OF DATABASES FOR HOT/COLD DEATHS. *Compressed Mortality Index.* Using CDC NCHS's compressed mortality database during the 21-yr period of 1979–99 (the most recent years for which national data are available), a total of 8015 deaths in the United States were heat related (Fig. 2). Of that total, 3829 (47.8%) were "due to weather conditions," while 3809 (47.5%) were "of unspecified origin" and 377 (4.7%) were "of man-made origins" (e.g., heat generated in vehicles, kitchens, boiler rooms, furnace rooms, and factories) (Donoghue et al. 2003; Sathyavagiswaran et al. 2001). Consequently, the CDC NCHS dataset's category of "excessive heat resulting from weather conditions" creates an average of 182 deaths per year.

Conversely, again using the compressed mortality database during the 21-yr period of 1979–99, a total of 13,970 deaths were attributed to hypothermia (excluding anthropogenic cold deaths) (Grey et al. 2002; Mirchandani et al. 2003) (Fig. 2). In 1999, exposure to excessive natural cold was listed as the underlying

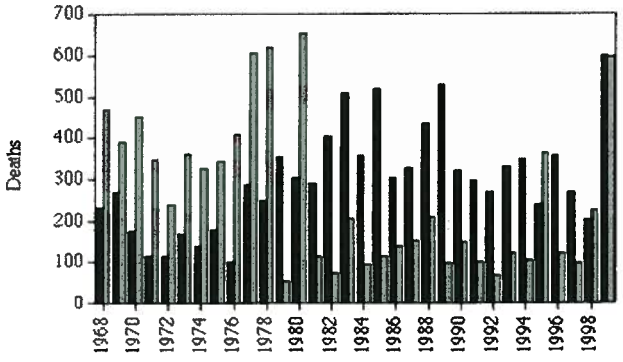

FIG. 2. CDC NCHS Compressed Mortality Index. Total deaths by excessive heat (gray bars) and total deaths by excessive cold (black bars) for 1968–99.

cause of death for 598 persons in the United States, and hypothermia was listed as a "nature" of injury (i.e., an injury that occurred to the deceased) in 1139 deaths. Totaling these numbers, the database lists a total of 15,707 people who have died from extreme cold from 1979 to 1999. Therefore, this dataset's category of "excessive cold resulting from weather conditions" lists an average of 748 persons killed per year.

Storm Data. Temperature extreme deaths listed in NCDC's *Storm Data* are skewed heavily toward heat-related deaths (Fig. 3). Even when snow and ice events are combined with cold temperature extremes, the number of heat-related deaths far outweighs cold-related deaths during the period 1993–2003 by a 3-to-1 margin. Of course, the data are heavily linked to two specific heat-wave events in 1995 and 1999. If these events are removed from the list, the numbers of hot and cold extreme deaths are nearly equal.

Gross mortality. Daily gross mortality data from 12 cities (Fig. 4) across the United States were provided by the CDC NCHS for the years 1975–98. The data are organized by age group, and daily mortality is broken down into those younger than 65 and those 65 and older. A simple linear regression was conducted for each of the metropolitan areas to adjust for any changes in population.

One of the key points regarding total, or gross, mortality is the prevalence of higher deaths in the winter months (Fig. 3). Such deaths cannot be solely linked to atmospheric conditions (i.e., cold) and are a function of socioeconomic conditions, psychological state, influenza, etc. (Kalkstein 1991). Therefore, before performing analyses of mortality associated with abnormal hot/cold conditions, gross mortality numbers must be detrended to account for population change and a strong seasonal cycle.

For this study, gross mortality numbers were detrended using two methods. The first is based on computing the residual of the actual day's mortality for a specific year from its long-term mean mortality. For example, to calculate the residual for 1 January 1975, its mortality is subtracted from the average mortality value for every 1 January from 1975 to 1998. The second method utilizes a first-order harmonic wave fitted to the annual mortality data and computes the residual of the actual day's mortality for a specific year from the harmonic.

Once detrended, excess heat- or cold-related deaths can be analyzed more effectively, and specific heat waves and cold events between 1975 and 1998 were examined for each of the cities. Severe heat waves often produce large "spikes" in mortality, especially during the 1995 heat wave across the Midwest. However, abnormally cold conditions have little effect on the standardized daily mortality. For example, February 1996, a cold period across much of the United States, produced no spikes in winter mortality levels.

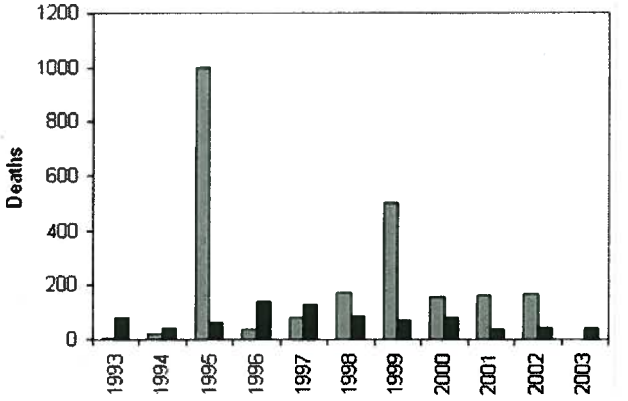

FIG. 3. NCDC *Storm Data*. Total deaths by excessive heat (gray bars) and total deaths by excessive cold (black bars) for the period of 1993–2003.

FIG. 4. Twelve cities for which gross mortality data (see Fig. 1) were used in this study.

Overall. It is apparent from the numbers shown above that these databases have different degrees of "correctness," and this is likely due to multiple methodological differences. For example, *Storm Data,* which is often based on media reports, tends to be biased to the media's (and consequently the public's) overall awareness of the event. As such, weather-related catastrophic "group kills" rather than "individual kills" are more likely to be included in *Storm Data.* Therefore, this may tend to give more complete numbers for weather-related categories, such as tornadoes, hurricanes, or heat waves, than for deaths from winter cold, and the multiple categories for excessive cold deaths can also introduce an underreporting of cold deaths. However, *Storm Data* is updated each month, and consequently, information on a given weather event is added into the database fairly quickly after its occurrence.

The CDC NCHS's Compressed Mortality Database is, in general, a more comprehensive database. As such, it would more likely include weather-related "single kills" than would *Storm Data.* However, the Compressed Mortality Database is limited by the medical personnel's actual determination of the "weather relatedness" of death, and the database often runs years behind current events. The latest mortality values that are used in recent medical studies are from 1999 (Donoghue et al. 2003; Grey et al. 2002; Mirchandani et al. 2003; Sathyavagiswaran et al. 2001).

The calculation of deviations from the daily norm in gross mortality does not suffer from many of the subjective death determinations associated with other datasets. However, it can be problematic to classify the causes of death using these data. In addition, gross mortality data are generally available only for metropolitan areas and are not easily obtainable on a daily time scale for large regions.

CHICAGO 1995 HEAT WAVE. As an example of the disparity between datasets, we review the wide range of mortality numbers reported for the Chicago 1995 major heat-wave event. By 27 July 1995, the media (*Chicago Sun-Times*) reported 529 heat-related deaths in the Chicago metropolitan area (Table 2). *Storm Data* lists 583 heat-related deaths in Illinois for the entire month of July 1995 (heat-related deaths from Chicago are erroneously placed under the state of Idaho in the online NCDC database). However, a subsequent NOAA natural disaster survey report lists 465 heat-related deaths for Chicago for the period 11–27 July (NOAA Disaster Survey Team 1995). Yet, according to the CDC NCHS Compressed Mortality Index, the total number of reported deaths due to "excessive heat" in Cook County, Illinois for all of 1995 was only 85.

When gross mortality values are examined in Cook County for the period associated with the 1995 heat wave, a tremendous spike in daily mortality is indeed apparent (Fig. 5). While the background "baseline" mortality for that time of year is around 120 deaths per day, the daily total mortality greatly exceeds that baseline value for five days (14–18 July) by approximately 840 individuals.

Certainly, if such a wide range of values exists for a single event in a single city, compiled mortality databases are more likely to have even greater

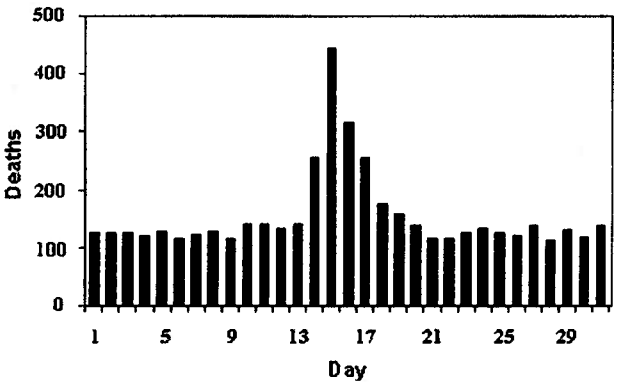

FIG. 5. Gross mortality (number of deaths) for July 1995 in Chicago, IL. (Adapted from Whitman et al. 1997.)

disparity. Fundamentally, the vast differences in these mortality numbers exist because of the various sources on which the mortality databases rely. For example, mortality numbers coming from a medical examiner are limited to only the cases in which that medical examiner was involved. The markedly low number of deaths reported by the CDC NCHS also suggests that, on many death certificates, the cause of death was likely determined not to be directly heat related.

CONCLUSIONS. Depending on the compilation nature of the dataset, the numbers of heat- or cold-related mortality are quite divergent. Consequently, in general, these separate mortality datasets should not be combined or compared in policy determination, and the specific dataset used in a given study should be clearly identified. All of the datasets suffer from some major limitations, such as the potential incompleteness of source information, long compilation time, limited quality control, and subjective determination of the direct versus indirect cause of death. These factors must

be considered if the data are used in policy determination or resource allocation.

Of the datasets identified in this study, the one that appears to be least influenced by the above limitations is gross mortality. However, the gross mortality data must be detrended in order to remove a persistent winter-dominant death maximum. Another major limitation of gross mortality is in obtaining regional daily mortality as opposed to only daily mortality for metropolitan areas. Therefore, any users of weather-related mortality data must determine which source is most suitable for their needs, and they should fully understand the limitations associated with the data.

ACKNOWLEDGMENTS. We greatly appreciate the information and comments provided by Dr. Edmund R. Donoghue, Dr. R. C. Patel, Dr. David Berglund, D. Kenneth Kochanek, Pamela Monroe, and Charles J. Dastych.

REFERENCES

Changnon, S. A., K. E. Kunkel, and B. C. Reinke, 1996: Impacts and responses to the 1995 heat wave: A call to action. *Bull. Amer. Meteor. Soc.*, **77**, 1497–1506.

Curran, E. G., R. L. Holle, and R. E. Lopez, 2000: Lightning casualties and damages in the United States from 1959 to 1994. *J. Climate*, **13**, 3448–3464.

Donoghue, E. R., M. Nelson, G. Rudis, R. I. Sabogal, J. T. Watson, G. Huhn, and G. Luber, 2003: Heat-related deaths—Chicago, Illinois, 1996–2001, and United States, 1979–1999. *Morbid. Mortal. Weekly Rep.*, **52**, 610–613.

Grey, T. C., R. Rolfs, M. A. Chambers, and A. S. Niskar, 2002: Hypothermia-related deaths—Utah, 2000, and United States, 1979–1998. *Morbid. Mortal. Weekly Rep.*, **51**, 76–78.

Kalkstein, L. S., 1991: A new approach to evaluate the impact of climate on human mortality. *Environ. Health Perspectives*, **96**, 145–150.

Mandt, G. A., 2002: *Storm Data* preparation. National Weather Service, National Oceanic and Atmospheric Administration, Department of Commerce, National Weather Service Instruction 10-1605, NWSFD 10-16, 79 pp.

Mirchandani, H., C. Johnson, C. Newbern, and C. Canchez, 2003: Hypothermia-related deaths—Philadelphia, 2001, and United States, 1999. *Morbid. Mortal. Weekly Rep.*, **52**, 86–87.

NOAA Disaster Survey Team, 1995: July 1995 Heat Wave. Natural Disaster Survey Report, 52 pp.

Sathyavagiswaran, L., J. E. Fielding, and D. Dassy, 2001: Heat-related deaths—Los Angeles County, California, 1999–2000, and United States, 1979–1998. *Morbid. Mortal. Weekly Rep.*, **50**, 623–626.

World Health Organization, 1992: *International Statistical Classification of Diseases and Related Health Problems*. World Health Organization, 1243 pp.

American Journal of Epidemiology
Copyright © 2005 by the Johns Hopkins Bloomberg School of Public Health
All rights reserved; printed in U.S.A.
Vol. 163, No. 2
DOI: 10.1093/aje/kwj024
Advance Access publication November 30, 2005

Practice of Epidemiology

Mortality due to Influenza in the United States—An Annualized Regression Approach Using Multiple-Cause Mortality Data

Jonathan Dushoff[1,2], Joshua B. Plotkin[3], Cecile Viboud[2], David J. D. Earn[4], and Lone Simonsen[5]

[1] Department of Ecology and Evolutionary Biology, Princeton University, Princeton, NJ.
[2] Fogarty International Center, National Institutes of Health, Bethesda, MD.
[3] Harvard University, Cambridge, MA.
[4] Department of Mathematics and Statistics, McMaster University, Hamilton, Ontario, Canada.
[5] National Institute of Allergy and Infectious Diseases, National Institutes of Health, Bethesda, MD.

Received for publication March 2, 2005; accepted for publication September 14, 2005.

Influenza is an important cause of mortality in temperate countries, but there is substantial controversy as to the total direct and indirect mortality burden imposed by influenza viruses. The authors have extracted multiple-cause death data from public-use data files for the United States from 1979 to 2001. The current research reevaluates attribution of deaths to influenza, by use of an annualized regression approach: comparing measures of excess deaths with measures of influenza virus prevalence by subtype over entire influenza seasons and attributing deaths to influenza by a regression model. This approach is more conservative in its assumptions than is earlier work, which used weekly regression models, or models based on fitting baselines, but it produces results consistent with these other methods, supporting the conclusion that influenza is an important cause of seasonal excess deaths. The regression model attributes an annual average of 41,400 (95% confidence interval: 27,100, 55,700) deaths to influenza over the period 1979–2001. The study also uses regional death data to investigate the effects of cold weather on annualized excess deaths.

cause of death; influenza; linear regression; mortality; seasons; temperature; time series; United States

Abbreviations: NAD, normalized annual death series; T_{thresh}, threshold temperature.

In temperate countries, more people die in the winter than in the summer (1). The contribution of influenza to these seasonal excess deaths remains a subject of controversy, with some authors arguing that influenza epidemics trigger the majority of excess deaths (1, 2) and others arguing that they trigger only a small minority (3). Retrospective cohort studies have shown a surprisingly large protective effect of influenza vaccination against deaths from any cause (4–6).

Deaths caused by influenza must be estimated indirectly because most influenza infections are not confirmed virologically (7). Moreoever, deaths triggered by influenza may occur as a result of a number of final causes, including pneumonia and a wide variety of respiratory and circulatory causes, and may occur weeks after initial infection (1, 8–11). Serfling (12) developed a method to infer influenza deaths based on seasonal patterns in the deaths attributed to pneumonia and influenza. Serfling's approach has been further developed by Simonsen et al. (13, 14). Influenza deaths are estimated as the number of deaths (either among all deaths or among pneumonia and influenza deaths) above an epidemic threshold based on a sinusoidal function fitted to summer deaths. Simonsen et al. (13) estimated that influenza caused approximately 21,000 deaths per year in the United States for the period 1972–1992. More recently, Simonsen et al. (14) estimated influenza deaths by use of winter excess mortality, controlling for changes in age

Correspondence to Dr. Jonathan Dushoff, Department of Ecology and Evolutionary Biology, Princeton University, Guyot Hall, Princeton, NJ 08544 (e-mail: dushoff@eno.princeton.edu).

NMED - PATZ
REBUTTAL EXHIBIT 2

Downloaded from http://aje.oxfordjournals.org at University of Wisconsin Madison - General Library System on August 23, 2010

TABLE 1. Mean monthly deaths from 1979 to 2001 for the US mortality time series investigated in this study

Name	Definition	Deaths/month
All deaths	All deaths	181,721
Pneumonia and influenza deaths	Any ICD-9* cause 480–487, any ICD-10* cause J10–J18	16,405
Respiratory and circulatory deaths	Any ICD-9 cause 390–519, any ICD-10 category I or J	129,275
Underlying pneumonia and influenza deaths	Underlying ICD-9 cause 480–487, underlying ICD-10 cause J10–J18	5,849
Underlying respiratory and circulatory deaths	Underlying ICD-9 cause 390–519, underlying ICD-10 category I or J	95,313

* ICD-9, *International Classification of Diseases,* Ninth Revision; ICD-10, *International Classification of Diseases,* Tenth Revision.

structure and for dominant viral subtype, and argued that the population-level burden of influenza is not consistent with the high protective values of vaccination found in cohort studies.

In a recent paper, Thompson et al. (11) introduced a new approach for estimating deaths attributable to influenza: They fit a regression model to death time series that combined a sinusoidal function with weekly virologic surveillance data from the United States. They attributed an average of 34,000 deaths per year to influenza for the period 1976–1999, consistent with the 37,500 deaths per year estimated by Serfling-type models for this period (14). Thompson et al. also estimated deaths due to both influenza and respiratory syncytial virus for the period 1990–1999.

This work by Thompson et al. (11) represents an advance over baseline methods, because it quantifies the relation between deaths attributed to influenza infection and virologic surveillance data. The work also has significant limitations. Both influenza prevalence and mortality are highly seasonal. Therefore, fitting a weekly regression between deaths and influenza virus surveillance has the potential to produce spurious correlations: Even if the annual pattern of deaths were exactly the same every year, unaffected by changes in influenza prevalence, a weekly regression against influenza prevalence would likely indicate a significant correlation. Thompson et al. address this problem by including sinusoidal terms in their regression. Since noninfluenza-related mortality is not expected to follow an exact exponentiated sinusoidal pattern, this reduces, but does not eliminate, the potential for spurious correlation and spurious attribution of deaths to influenza.

Another limitation of the weekly approach is the difficulty of correctly adjusting for time delays. It has been shown that peak mortality lags roughly 2 weeks behind the peak of influenza activity (8). This is likely the result of several different time delays from different influenza mortality pathways (1). The model of Thompson et al. (11) does not attempt to correct for these lags.

Nicholson (15) included viral and clinical surveillance data in a model of mortality in England and Wales using a 4-week timescale. This model, built on earlier models by Tillett et al. (16), used dummy variables for some time periods (but not others) to control for seasonal trends. Interpretation of the results is complicated by the complexity of the model (27 independent variables overall).

Sophisticated time-series methods attempt to separate seasonal components, by use of autoregressive integrated moving average models, for example (17), before applying regression. Carrat and Valleron (18) fit such models to time series of noninfluenza deaths and modeled the residuals against influenza deaths, in an attempt to attribute the total number of deaths caused by influenza in France. The usefulness of this approach is limited by the unreliability of attribution of influenza deaths on death certificates, however (19). Recently, increasingly sophisticated methods including generalized additive modeling (20), hierarchical modeling (21), and distributed-lag modeling (22) have been applied to mortality time series to assess the impact of air pollution on deaths (21, 22), with the work of Braga et al. (20) explicitly attempting to control for epidemics of respiratory disease. Removing seasonal confounding remains a complex issue, however (22). Further, influenza surveillance data for this time period at daily, weekly, or even monthly scales are not available in the public domain.

In this paper, we take a robust, conservative approach to the problem of seasonal confounding by investigating the relation between influenza virus surveillance data and mortality at an annual timescale. We aggregate excess deaths and prevalence measures over an entire influenza season and estimate the number of deaths attributable to influenza infection in the United States. Additionally, we applied our method to two regions of the United States to investigate the contribution of cold temperatures to seasonal excess mortality on an annualized basis.

MATERIALS AND METHODS

Using public-use mortality data files for the United States, obtained from the Centers for Disease Control and Protection's National Center for Health Statistics, we created a database of all US deaths from 1979 to 2001 that can be queried by age, gender, underlying cause of death, and contributing cause of death, among other variables. Using this database, we generated several monthly time series of US mortality (available at http://mortality.princeton.edu/annualflu/) by use of different disease categories from the *International Classification of Diseases,* Ninth Revision and Tenth Revision, that were based on either the underlying cause of death or the underlying and contributing cause of death (table 1). We divide the calendar into "flu years," each containing a single influenza season, that run from July to June. Deaths were corrected multiplicatively to a standard month length of $1,461/48 \approx 30.44$ days.

Downloaded from http://aje.oxfordjournals.org at University of Wisconsin Madison - General Library System on August 23, 2010

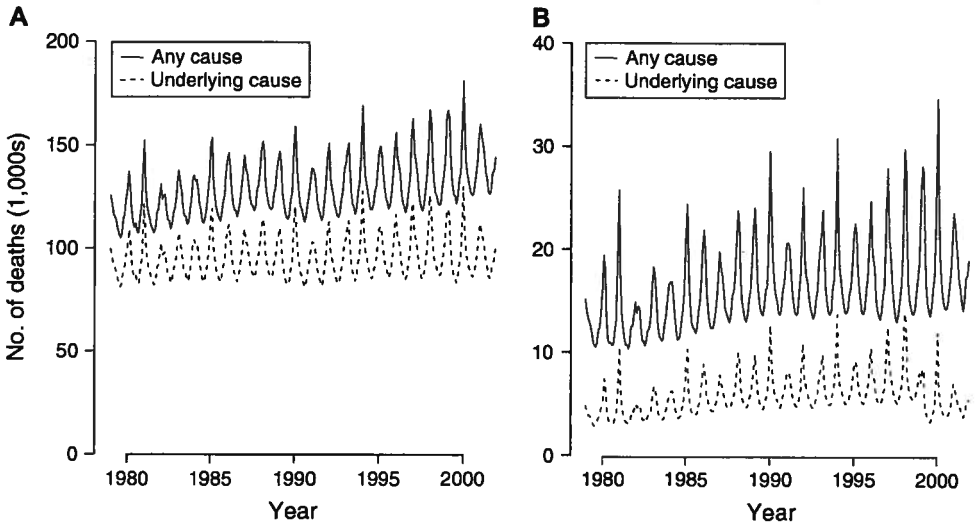

FIGURE 1. Reported respiratory and circulatory (A) and pneumonia and influenza (B) deaths, by underlying cause and by multiple causes, United States, 1979–2001.The sharp drop in underlying pneumonia and influenza deaths in 1999 is due to the change in coding under the *International Classification of Diseases* system from the Ninth Revision to the Tenth Revision. In general, the series that consider multiple causes are expected to be less sensitive to changes in coding methodologies.

Estimates based on mortality data depend on the consistency of mortality reports. This study takes a novel approach within the influenza epidemiology literature to the categorization of causes of death. Instead of using only the listed "underlying" cause of death, we tabulate all deaths with a specific cause—either pneumonia and influenza causes or all respiratory and circulatory causes—listed anywhere on the death certificate. We expect these "multiple-cause" data series to be more robust, both because more deaths are included and because considering all causes on the death certificate should make these series less sensitive to coding and nosologic changes (figure 1).

Annual virologic surveillance data (aggregated by influenza season) for the United States were obtained from Thompson et al. (11) and *Morbidity and Mortality Weekly Report* (23, 24). Following Thompson et al., we use the proportion of tested samples positive as a proxy for prevalence of each influenza subtype. Although this proportion is an imperfect measure of prevalence, we feel that it is the best influenza-specific measure available. The model of Thompson et al. makes use of weekly virus surveillance data, but these data have not been made available in the public domain.

To remove long-term trends from our mortality data, we fit a least-squares quadratic model to the time series of all deaths in each age category studied and divided the number of deaths in each category by this quadratic fit to all deaths to obtain "normalized" deaths by month and category. This form of normalization is an alternative to dividing by population estimates, and it has the advantages of being robust to changes in population estimation methods and of allowing us to conveniently divide our population by age and region.

Annual excess deaths were defined as the total number of deaths in a selected set of "influenza months" above the monthly average of a disjoint set of "baseline months." For the main analysis, we used November to April as the flu months and the remaining 6 months as the baseline months (figure 2).

The main statistical model used was as follows:

$$\mathrm{NAD} = \alpha + \beta_{H3}\mathrm{H3} + \beta_{H1}\mathrm{H1} + \beta_{B}\mathrm{B},$$

where "NAD" is any normalized annual death series; "H3," "H1," and "B" refer to the proportions of samples positive for influenza A subtypes H3N2 and H1N1 and influenza B; α is the intercept; and the βs are regression coefficients.

Regional studies used deaths from 16 large counties in the New York metropolitan area, linked to temperature data from Newark International Airport, and deaths from the states of Illinois and Indiana, linked to temperature data from O'Hare International Airport. We chose regions that are densely populated, were expected to have similar weather across the region, and had complete monthly temperature series available at the International Research Institute for Climate Prediction (25). Cold was measured on a monthly basis as the average number of degrees below a threshold temperature (T_{thresh}) or cold (C) = $\min(T_{\mathrm{thresh}} - T, 0)$, where T is the mean monthly temperature. Cold was measured for each flu year as the average of monthly cold values from November through April. The statistical model used was as follows:

$$\mathrm{NAD} = \alpha + \beta_{H3}\mathrm{H3} + \beta_{H1}\mathrm{H1} + \beta_{B}\mathrm{B} + \beta_{C}\mathrm{C}.$$

Because virus surveillance data were not available with age structure or regional breakdowns, we used national virus surveillance data for all regressions involving surveillance data.

Downloaded from http://aje.oxfordjournals.org at University of Wisconsin Madison - General Library System on August 23, 2010

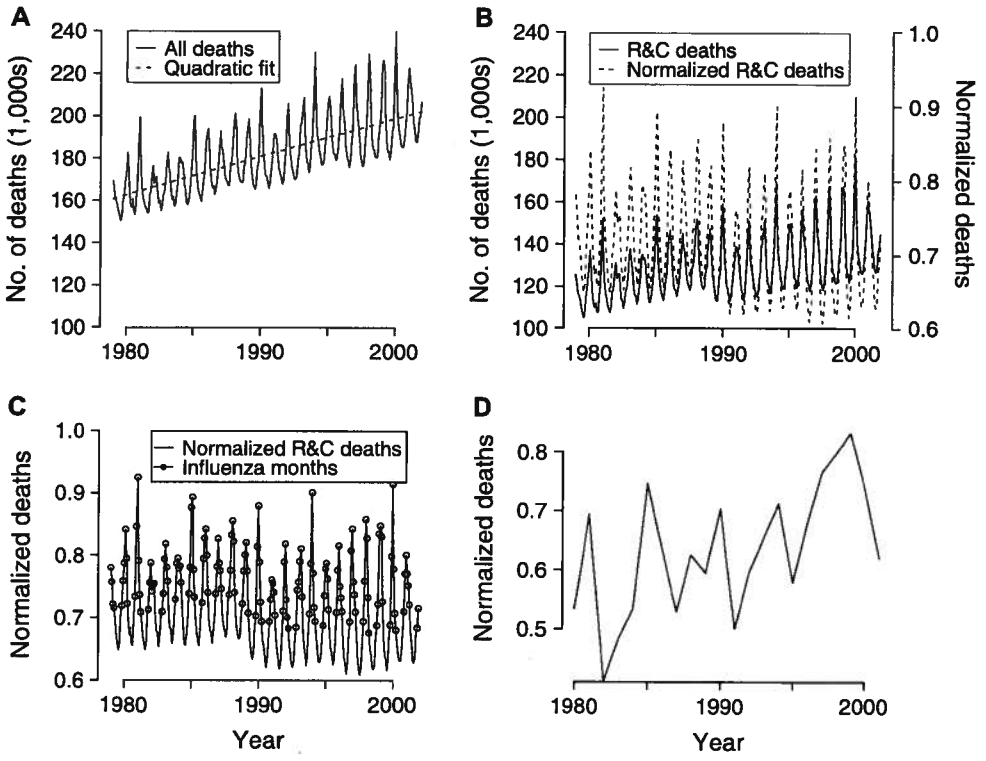

FIGURE 2. A normalized, detrended annual time series of excess deaths from monthly mortality data, United States, 1979–2001. Respiratory and circulatory (R&C) deaths for the whole population are used in this example. In A, a quadratic is fit to all deaths for a given age class (or the whole population); in B, deaths from a given cause are normalized by dividing by this quadratic fit; in C and D, normalized annualized winter deaths are defined as normalized deaths in "influenza" months above the monthly average for "baseline" months in the same season.

Statistical analyses were performed using the statistical package R (26). Deaths attributed to an independent variable in a regression model were calculated by the difference between the number of normalized deaths predicted by the regression model and the number predicted when the independent variable is set to zero. Normalized deaths attributed in each year were then multiplied by the appropriate normalization factor. Because this method assumes that each cofactor has the same effect each year (e.g., no strain of a given subtype is more virulent than any other), estimates of attributable deaths in a particular season are less reliable than the estimates of average annual deaths over the entire time period. R scripts used in the analysis are available at http://mortality.princeton.edu/annualflu/.

RESULTS

We find positive correlations between excess deaths and the annual prevalence of each of the three influenza subtypes, for each category of deaths that we study. Using these correlations, we can estimate the average number of deaths in each category caused by influenza over a 20-year period (table 2) (Web table 1). (This latter tabular material is described in the first of seven supplementary tables; each is referred to as "Web table" in the text and is posted on the *Journal*'s website (http://aje.oxfordjournals.org/).) The regression model attributes an annual average of 41,400 (95 percent confidence interval: 27,100, 55,700) deaths to influenza over the period 1979–2001.

To investigate the effects of cold, we compared death records for two regions of the United States with winter temperature records from these regions. We found associations between normalized excess regional pneumonia and influenza deaths and the national prevalence of H3 and B viruses in both regions (table 3). Pneumonia and influenza deaths were used with these smaller samples because they showed more robust correlations with surveillance data in all analyses. No consistent relations were found between various combinations of monthly mean temperatures and normalized excess deaths, however, whether or not nationwide influenza virus surveillance data were used in the regression models (the example of cold over the whole winter season is shown in table 3).

Confidence intervals on the number of deaths attributed to cold weather are large, so we cannot conclude that influenza is a more important cause of winter mortality on an annual timescale than is cold weather. The result is suggestive, however, because the weather data used are more localized and more precise than the influenza surveillance data, so we

Downloaded from http://aje.oxfordjournals.org at University of Wisconsin Madison - General Library System on August 23, 2010

TABLE 2. Annual deaths attributed by the surveillance regression model, categorized by pneumonia and influenza or by all respiratory and circulatory causes appearing anywhere in the death record, United States, 1979–2001

Cause	Pneumonia and influenza deaths	Other respiratory and circulatory deaths	All respiratory and circulatory deaths	Non-respiratory and circulatory deaths	All deaths
H3N2	10,266***	13,331**	23,597***	5,282***	28,878***
H1N1	1,045	1,731	2,775	1,184†	3,960
B	3,165*	3,562	6,727†	1,821†	8,547*
Total	14,475***	18,624**	33,099***	8,287**	41,386***

* $p < 0.05$; ** $p < 0.01$; *** $p < 0.001$.
† $p < 0.1$.

might have expected more statistical power in weather analyses. Results in table 3 are for $T_{thresh} = 10°C$. Results setting T_{thresh} to the mean temperature for each month, or to 20°C, are similar, but with much smaller and much larger confidence intervals, respectively.

We performed a sensitivity analysis to test our expectation that attributing deaths using annualized regression would be relatively insensitive to our choice of influenza months and baseline months, by examining several different such choices (Web tables 2, 3, 4, 5, and 6). For all choices, each of the 15 estimates of deaths in a category attributed to a subtype was positive, and all produced estimated totals within 10 percent of the estimate in the main text.

Over the time span that we studied, the average surveyed prevalence of influenza increases through time, possibly because of better prescreening or improved test sensitivity. We constructed normalized surveillance time series, by fitting a linear trend through total measured influenza prevalence and dividing the surveillance observations for H3, H1, and B for each year by this trend line, thus removing overall prevalence trends. These normalized data showed a qualitatively similar pattern, with significantly positive regression coefficients for two of the three subtypes, and predicted a total number of influenza deaths around 90 percent of the number predicted by the raw prevalence estimates (Web table 7).

If, instead of using normalized excess deaths, we apply our regression model to Serfling estimates generated by the method of Simonsen et al. (14), the model attributes 33,100 (95 percent confidence interval: 20,500, 45,600) annual deaths to influenza infection.

DISCUSSION

The total number of deaths attributed to influenza by our surveillance model (41,400 per year from 1979 to 2001) is similar to that found in other studies (11, 13, 14). The fact that our estimate of the mortality burden of influenza, based on our conservative methodology, is similar to earlier estimates provides support for classical assumptions about the role of influenza in seasonal excess mortality. Our estimates are not consistent, however, with much lower estimates from authors who attribute most excess winter deaths to cold (3, 27) or with much higher numbers that can be inferred from cohort studies (2, 4–6, 14).

Although our results are consistent with other ecologic estimates, the conservative, annualized method used here increases the certainty that deaths attributed to influenza are in fact caused by influenza. Methods based on seasonal pattern begin from the assumption that influenza is the major source of excess winter death. Daily, weekly, and monthly regressions are powerful, but they are in danger of being confounded by other seasonal factors.

The annualized approach also measures effects at a different timescale than daily or weekly regressions. A person

TABLE 3. Annual pneumonia and influenza deaths, with 95% confidence intervals, categorized by causes appearing anywhere in the death record, attributed by the regional surveillance regression model for the New York metropolitan area and the states of Illinois and Indiana, 1979–2001*

Cause	New York metropolitan area		Illinois and Indiana	
	No. of deaths	95% confidence interval	No. of deaths	95% confidence interval
H3N2	1,492	361, 2,624	2,126	1,004, 3,249
H1N1	−88	−560, 384	127	−338, 592
B	774	−21, 1,571	549	−173, 1,271
Cold	1,640	−1,815, 5,097	1,646	−2,504, 5,796
Total	3,819	66, 7,572	4,447	62, 8,832

* Threshold temperature is 10°C.

Downloaded from http://aje.oxfordjournals.org at University of Wisconsin Madison - General Library System on August 23, 2010

whose death in a given week is triggered by influenza or cold weather may be somebody who would otherwise have lived for many more years or somebody who was unlikely to survive the winter anyway. Deaths in the latter category associated with causes by time-series analysis are often referred to as the "harvesting effect," meaning that a particular cause, such as cold or influenza, may be "harvesting" people with very short life expectancies, determining the exact time of death but shortening lives by only a small amount (28). Weekly analyses measure deaths in both categories, whereas an annualized analysis will omit most deaths in the latter category. Measuring at different timescales asks fundamentally different questions: Neither answer is more correct than the other. The annualized approach presented here is, however, a substantially more conservative way of asking whether influenza triggers a substantial proportion of seasonal excess deaths.

By making use of multiple-cause death information, we have more than doubled the number of pneumonia and influenza deaths available for analysis and made our analysis less sensitive to coding choices. We suggest that, where multiple-cause death data are available, all pneumonia and influenza deaths and all respiratory and circulatory deaths may be useful time series for investigating influenza-caused mortality.

On an annual timescale, we find preliminary evidence that cold weather does not predict winter deaths. A full-scale spatial analysis of influenza mortality, ideally incorporating spatial surveillance data, remains to be done. If this result holds up, however, it does not necessarily contradict the large body of evidence relating cold stress to mortality (27, 29, 30). It is likely that temperature determines the timing of deaths on a shorter timescale; that is, people whose deaths are triggered by a particular cold spell may be people who are unlikely to survive until June. It is also possible that cold weather has indirect effects on mortality, by accelerating the spread of influenza (1, 31).

We believe that we have made a simple, robust, and conservative model of influenza deaths. The price, however, is that our model is rather crude. The fact that we have only one data point per year limits the power and precision of our analysis. Our surveillance-based regression model does not allow for the fact that different strains of a given subtype may be more or less deadly from year to year. Additionally, virus surveillance by the Centers for Disease Control and Prevention is based largely on contributed samples and therefore does not reflect a systematic sampling scheme (32). On at least one occasion, the 1985–1986 season, the epidemic in the total US population was largely dominated by the B virus, while most cases in the elderly, and thus influenza-triggered deaths, were due to the more lethal influenza A(H3) virus (33).

In summary, a conservative, annualized analysis finds evidence that influenza virus infections are causing mortality on an annual timescale. Our estimates support earlier estimates of influenza burden based on direct excess deaths (13, 14) and weekly regressions (11), but they do not support higher estimates based on cohort studies (4–6). Our results suggest that the triggering of deaths by cold weather (3) may be a short-term phenomenon that has much less impact on an annual timescale. Further analyses based on disaggregated, systematic viral surveillance data have the potential to shed further light on these questions, as such data become publicly available.

ACKNOWLEDGMENTS

The authors thank Dr. Mark Miller for helpful conversations.

Conflict of interest: none declared.

REFERENCES

1. Reichert TA, Simonsen L, Sharma A, et al. Influenza and the winter increase in mortality in the United States, 1959–1999. Am J Epidemiol 2004;160:492–502.
2. Poland GA. If you could halve the mortality rate, would you do it? Clin Infect Dis 2002;35:378–80.
3. Donaldson GC, Keatinge WR. Excess winter mortality: influenza or cold stress? Observational study. BMJ 2002; 324:89–90.
4. Nichol KL, Goodman M. The health and economic benefits of influenza vaccination for healthy and at-risk persons aged 65 to 74 years. Pharmacoeconomics 1999;16:63–71.
5. Hak E, Nordin J, Wei FF, et al. Influence of high-risk medical conditions on the effectiveness of influenza vaccination among elderly members of 3 large managed-care organizations. Clin Infect Dis 2002;35:370–7.
6. Nichol KL, Nordin J, Mullooly J, et al. Influenza vaccination and reduction in hospitalizations for cardiac disease and stroke among the elderly. N Engl J Med 2003;348:1322–32.
7. Cox NJ, Subbarao K. Influenza. Lancet 1999;354:1277–82.
8. Glezen WP, Payne AA, Snyder DN, et al. Mortality and influenza. J Infect Dis 1982;146:313–21.
9. Woodhouse PR, Khaw KT, Plummer M, et al. Seasonal variations of plasma fibrinogen and factor-VII. Activity in the elderly: winter infections and death from cardiovascular disease. Lancet 1994;343:435–9.
10. Meier CR, Jick SS, Derby LE, et al. Acute respiratory-tract infections and risk of first-time acute myocardial infarction. Lancet 1998;351:1467–71.
11. Thompson WW, Shay DK, Weintraub E, et al. Mortality associated with influenza and respiratory syncytial virus in the United States. JAMA 2003;289:179–86.
12. Serfling RE. Methods for current statistical analysis of excess pneumonia influenza deaths. Public Health Rep 1963; 78:494–506.
13. Simonsen L, Clarke MJ, Williamson GD, et al. The impact of influenza epidemics on mortality: introducing a severity index. Am J Public Health 1997;87:1944–50.
14. Simonsen L, Reichert TA, Viboud C, et al. Impact of influenza vaccination on seasonal mortality in the US elderly population. Arch Intern Med 2005;165:265–72.
15. Nicholson KG. Impact of influenza and respiratory syncytial virus on mortality in England and Wales from January 1975 to December 1990. Epidemiol Infect 1996;116:51–63.
16. Tillett HE, Smith JWG, Gooch CD. Excess deaths attributable to influenza in England and Wales: age at death and certified cause. Int J Epidemiol 1983;12:344–52.

Downloaded from http://aje.oxfordjournals.org at University of Wisconsin Madison - General Library System on August 23, 2010

17. Helfenstein U. Detecting hidden relations between time series of mortality rates. Methods Inf Med 1990;29:57–60.
18. Carrat F, Valleron AJ. Influenza mortality among the elderly in France, 1980–90: how many deaths may have been avoided through vaccination? J Epidemiol Community Health 1995; 49:419–25.
19. Fleming DM, Cross KW, Watson JM, et al. Excess winter mortality. Method of calculating mortality attributed to influenza is disputed. (Letter). BMJ 2002;324:1337.
20. Braga ALF, Zanobetti A, Schwartz J. Do respiratory epidemics confound the association between air pollution and daily deaths? Eur Resp J 2000;16:723–8.
21. Dominici F, Daniels M, Zeger SL, et al. Air pollution and mortality: estimating regional and national dose-response relationships. J Am Stat Assoc 2002;97:100–11.
22. Welty LJ, Zeger SL. Are the acute effects of particulate matter on mortality in the National Morbidity, Mortality, and Air Pollution Study the result of inadequate control for weather and season? A sensitivity analysis using flexible distributed lag models. Am J Epidemiol 2005;162:80–8.
23. Centers for Disease Control and Prevention (CDC). Update: influenza activity—United States and worldwide, 1999–2000 season, and composition of the 2000–01 influenza vaccine. MMWR Morb Mortal Wkly Rep 2000;49:375–81.
24. Centers for Disease Control and Prevention (CDC). Update: influenza activity—United States and worldwide, 2000–2001 season, and composition of the 2001–02 influenza vaccine. MMWR Morb Mortal Wkly Rep 2000;50:466–70.
25. International Research Institute for Climate Prediction. IRI/LDEO climate data library. New York, NY: Columbia University, 2004. (http://iridl.ldeo.columbia.edu/).
26. R Development Core Team. The R project for statistical computing. Madison, WI: University of Wisconsin, 2003–2004. (http://www.r-project.org/).
27. Keatinge WR, Donaldson GC, Bucher K, et al. Cold exposure and winter mortality from ischaemic heart disease, cerebrovascular disease, respiratory disease, and all causes in warm and cold regions of Europe. Lancet 1997;349:1341–6.
28. Murphy BR, Morens DM, Simonsen L, et al. Reappraisal of the association of intussusception with the licensed live rotavirus vaccine challenges initial conclusions. J Infect Dis 2003;187:1301–8.
29. Huntington E. The control of pneumonia and influenza by weather. Ecology 1920;1:6–23.
30. Wilkinson P, Pattenden S, Armstrong B, et al. Vulnerability to winter mortality in elderly people in Britain: population based study. BMJ 2004;329:647–51.
31. Eccles R. An explanation for the seasonality of acute upper respiratory tract viral infections. Acta Otolaryngol 2002;122: 183–91.
32. Brammer TL, Izurieta HS, Fukuda K, et al. Surveillance for influenza—United States, 1994–95, 1995–96, and 1996–97 seasons. MMWR CDC Surveill Summ 2000;49:13–28.
33. Centers for Disease Control (CDC). Influenza—United States, 1985–1986 season. MMWR Morb Mortal Wkly Rep 1986; 35:470, 475–9.

Downloaded from http://aje.oxfordjournals.org at University of Wisconsin Madison - General Library System on August 23, 2010

Commentary

A human disease indicator for the effects of recent global climate change

Jonathan A. Patz*

Department of Environmental Health Sciences, Johns Hopkins Bloomberg School of Public Health, 615 North Wolfe Street, Baltimore, MD 21205-2179

Connections between weather and disease are well established, with many diseases occurring during certain seasons or erupting from unseasonable flood or drought conditions. With new concerns about global warming, accompanied by greater climate variability, many recent studies have focused on disease fluctuations related to short-term or interannual climate oscillations (e.g., from weather extremes driven by El Niño). Yet, the nagging question remains as to whether or not there has been any documented change in human disease trends in response to long-term climate change, since warming has already occurred over the last century (1, 2).

This trend analysis has been elusive because of the scarcity or inconsistent quality of health databases over long periods. Additionally, strong confounding factors especially complicate long-term trend analysis. Some of these include increasing trends in travel, trade and migration, erratic disease control efforts, emerging drug or pesticide resistance, human population growth, urban sprawl, agricultural development, and variable reporting biases. But Rodo *et al.* (3) have now succeeded in finding a robust relationship between progressively stronger El Niño events and cholera prevalence in Bangladesh, spanning a 70-year period; their use of a uniquely high quality extensive cholera database and innovative statistical methods were key. This study likely represents the first piece of evidence that warming trends over the last century are affecting human disease.

This study likely represents the first piece of evidence that warming trends over the last century are affecting human disease.

The investigators used innovative statistical methods to conduct a time-series analysis of historical cholera data dating back to 1893 to examine the effect of nonstationary interannual variability possibly associated with climate change. In the last two decades, the El Niño Southern Oscillation (ENSO) differed from previous decades (3). Since the 1980's, there has been a marked intensification of the ENSO beyond that expected from the known shift in the Pacific basin temperature regime that began in the mid 1970s. The authors found that the association of cholera incidence in the earlier half of the century (1893–1940) is weak and uncorrelated with ENSO, whereas late in the century (1980–2001), the relationship is strong and consistent with ENSO. Past climate change, therefore, may have already affected cholera trends in the region through intensified ENSO events.

Recent Climate Change and Trends in El Niño

According to the United Nations Intergovernmental Panel on Climate Change (IPCC), evidence of past warming is building. Since the late 1950s, global average surface temperature has increased by 0.6°C (Fig. 1), snow cover and ice extent have diminished, and ocean heat content has increased (2). Also, sea level has risen on average by 10–20 cm during the past century. Relevant to Bangladesh, the Indian ocean has progressively warmed since 1960 (4), and the subcontinent has warmed by 2–3°C over the last century (5). Rodo *et al.* found an increase over time in the frequency and amplitude in the ENSO; although debate remains about the relationship between climate change and ENSO intensification, the observations of Rodo *et al.* are consistent with model projections of greenhouse gas warming (6). The rate of change in climate is faster now than in any period in the last thousand years (2), making the findings of Rodo *et al.* of progressively more intense ENSO in the region pertinent to climate scientists as well as health professionals.

Human Disease and Short-Term Climate Variability

Seasonality in disease incidence can often infer an association with weather factors. Epidemics of meningococcal meningitis in subSaharan Africa consistently erupt during the hot dry season and subside soon after the onset of the rainy season (7). Mosquito-borne diseases, such as dengue fever, show strong seasonal patterns; transmission is highest in the months of heavy rainfall and humidity. Enteric diseases also show significant seasonal fluctuations. In the U.S., Rotavirus peaks in the winter, and, in Scotland, *Campylobacter* infections are characterized by short peaks in the spring (8). In Peru, Cyclospora infections peak in the summer and subside in the winter months (9). Also, in Peru, Checkley *et al.* (10) used harmonic regression to control for seasonality, and found childhood diarrheal disease to be significantly affected by elevated El Niño temperatures; the number of daily admissions for diarrhea increased by more than twofold in winter, compared with expected trends based on the prior 5 years. For each degree centigrade of increase in mean annual temperature, the number of admissions increased by 8%.

El Niño is a natural interannual climate phenomenon that originates in the Pacific ocean every 3–7 years and, next to the seasons, is the strongest short-term driving force of climate throughout many regions of the world. The 1997–98 El Niño event was one of the two strongest this century. The accompanying absence of the monsoon brought extremely dry conditions resulting in devastating fires and hazardous air pollution in Southeast Asia (11). At the other extreme, the same El Niño event caused severe flooding in East Africa, triggering a mosquito-borne Rift Valley fever epidemic (12). Because the mosquitoes that transmit Rift Valley fever lay their eggs at the tops of grasses, only during periods of flooding are the eggs submersed, allowing for development. The link between malaria and extreme climatic episodes also has long been the subject of study in the Indian subcontinent. Historical analyses have shown that the risk of a malaria epidemic is increased approximately fivefold during the year after an El Niño in this region (13, 14).

The long-term ENSO trend analysis of Rodo *et al.* expands upon previous work by Pascual *et al.* (15), who showed a strong

See companion article on page 12901.

*E-mail: jpatz@jhsph.edu.

www.pnas.org/cgi/doi/10.1073/pnas.212467899

NMED - PATZ
REBUTTAL EXHIBIT 3

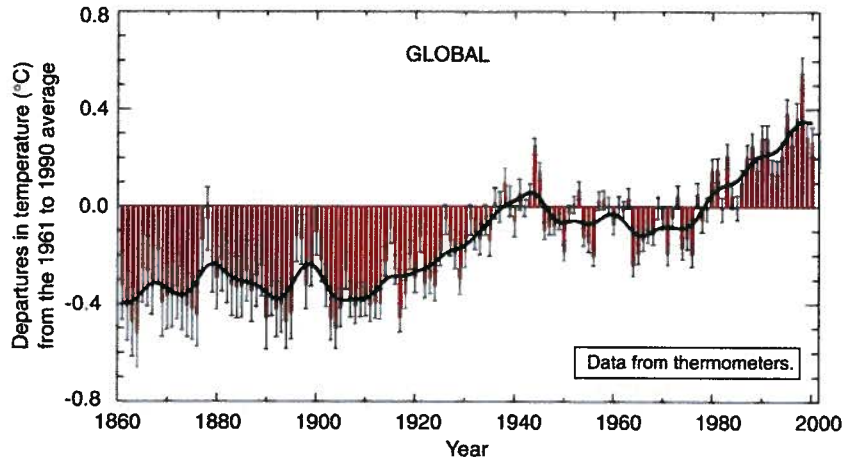

Fig. 1. Average global surface temperatures (in centigrade) from 1860–2000, showing deviation from the baseline 1961–1990 average temperature. [Reproduced with permission from ref. 19 (Copyright 2001, Intergovernmental Panel on Climate Change).]

relationship between ENSO and cholera by using 18 years of data from the ICDDR,B (International Center for Diarrhoeal Disease Research, Bangladesh; Fig. 2). Colwell (16) discovered the biological basis for a link between sea surface temperature (SST), marine ecology, and human cholera. Copepods (or zooplankton), which feed on algae, serve as reservoirs for *Vibrio cholerae* and other enteric pathogens. This observation may explain why cholera follows seasonal warming of SST that can enhance plankton blooms. *Vibrio* spp. in general are influenced by temperature and salinity (17), which, along with SST, is consistent with the role played by sea surface height (18).

Difficulties in Determining Human Disease Indicators Linked to Long-Term Climate Trends

Many physical and biological indicators of long-term climate change effects have been documented. Some examples include the thawing of permafrost, later freezing and earlier break-up of ice on rivers and lakes, poleward and altitudinal shifts in the ranges of a variety of plants and animals, earlier flowering of trees, emergence of insects, and egg-laying of birds (19).

However, human health outcomes depend on many "upstream" physical and biological systems. Adding complexity to disease analyses is the potential for numerous response options by human populations to reduce risk (ref. 20; Fig. 3). Even if disease does occur, variability in detection and/or reporting remain major obstacles to determining valid trends in human disease incidence. Rodo *et al.* studied cholera percentages (rather than cases) to reduce varying denominators and minimize reporting bias.

Reported linear correlations between disease and climate variability typically have been low (15). Rodo *et al.* posit that standard statistical techniques will fail to reveal even a strong climate/health relationship, assuming nonlinearity or a discontinuous association. The authors implemented innovative statistical techniques, such as Singular Spectrum Analysis to decompose a "noisy" time series into a nonlinear trend, oscillatory components, and remaining noise, followed by Scale-Dependent Correlation analysis, a time-series method developed to isolate possible transient signals. The association between cholera and ENSO was strong but transient, suggesting a *threshold* phenomenon. A linear correlation, therefore, would be entirely uninformative in this case and illustrates the inadequacies of using conventional statistical methods to decipher long-term climate/health relationships. Given such a threshold effect, higher average global temperatures and more extreme climate variability would not bode well for controlling cholera under a scenario of climate change. On the optimistic side, this new knowledge improves the potential for prediction of and early response to cholera risk in the region.

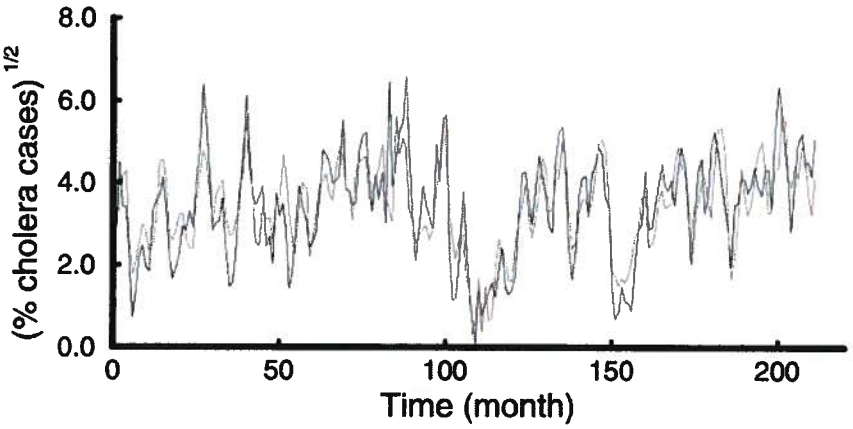

Fig. 2. Model relationship between ENSO and cholera in Bangladesh. The (square-root-transformed) cholera data (black line) and the 2-months-ahead prediction of the fitted model incorporating both seasonality and ENSO at a lag $f = 11$ (red line). [Reproduced with permission from ref. 15 (Copyright 2000, AAAS).]

While this study by Rodo *et al.* quantitatively analyzed a long human health dataset for a climate signal, shorter time series studies have been conducted. In Sweden, Lindgren *et al.* (21) studied whether the increasing incidence of tick-borne encephalitis (TBE) could be linked to changes in climate during the period 1960–1998. One conclusion of the study was that the increased incidence of TBE can be explained by climate changing toward milder winters and early spring arrival. For example, the highest rates of TBE—a threefold increase from the annual average—were reported for Sweden in the year 1994, which was preceded by five consecutive mild winters and seven early spring arrivals. But, growing human population, changing land use patterns, and increased reporting may confound these findings (22).

In addition to confounding factors, pitfalls can arise from a mismatch in the scale of climate vs. health databases. Hay *et al.* (23) found no statistically significant change in climate in four villages in the East African Highlands where an increase in malaria incidence has been documented over the last century. Therefore, the authors concluded a lack of a climate effect. However, results were derived from interpolating a broad-scale gridded regional climate data set based on very sparse historical weather station data; such data are intended for upward aggregation for regional and subcontinental climate trend analysis, not for individual village sites (24). Drug resistance of the malaria parasite has received much attribution for

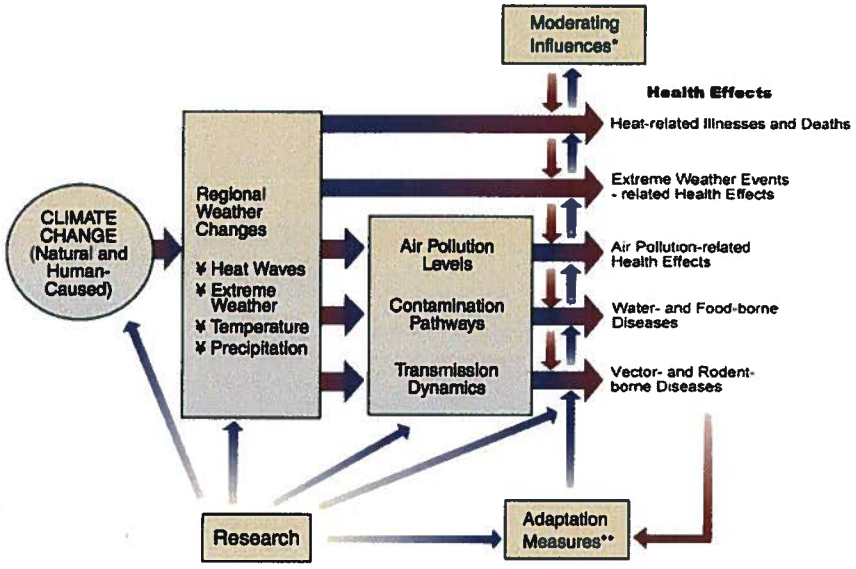

Fig. 3. Potential health effects of climate variability and change. *, moderating influences include nonclimate factors that affect climate-related health outcomes, such as population growth and demographic change, standards of living, access to health care, improvements in health care, and public health infrastructure. **, adaptation measures include actions to reduce risks of adverse health outcomes, such as vaccination programs, disease surveillance, monitoring, use of protective technologies (e.g., air conditioning, pesticides, water filtration/treatment), use of climate forecasts, development of weather warning systems, emergency management and disaster preparedness programs, and public education. (Reproduced with permission from ref. 20.)

increasing malaria in the region; however, drug resistance may disproportionately affect disease severity more than incidence which, at a minimum, requires suitable climatic conditions. In short, the question of vectorborne diseases and long-term climate change remains unresolved; there is a lack of unequivocal quantitative evidence in either direction. Kovats *et al.* (25) describe this as an "absence of evidence, rather than evidence of absence of a (climate) effect."

Kovats *et al.* also offer criteria for assessing the evidence for a causal association between infectious diseases and observed climate change: (*i*) evidence for biological sensitivity to climate, requiring both field and lab research on important vectors and pathogens; (*ii*) meteorological evidence of climate change, requiring sufficient measurements for specific study regions; and (*iii*) evidence for epidemiological or entomological change with climate change, accounting for potential confounding factors.

In conclusion, the study by Rodo *et al.* reported in this issue of PNAS meets these rigorous criteria by applying sophisticated statistical tools to one of the longest quality disease databases available. With this landmark climate/health analysis, we are much better positioned to enter a new phase of inquiry into the links between human disease incidence and realized long-term climate change.

I thank Dr. Diarmid Campbell-Lendrum, Disease Control and Vector Biology Unit, Infectious Diseases Department, London School of Hygiene and Tropical Medicine, for comments on the manuscript drafts.

1. Folland, C. K., Karl, T. R. (2001) in *Climate Change 2001: The Scientific Basis*, eds. Houghton, J., Ding, Y., Griggs, M., Noguer, M., van der Linden, P. & Dai, X. (Cambridge Univ. Press, Cambridge, U.K.), p. 881.
2. Easterling, D. R., Horton, B., Jones, P. D., Peterson, T. C., Karl, T. R., Parker, D. E., Salinger, M. J., Razuvayev, V., Plummer, N., Jamason, P. & Folland, C. K. (1997) *Science* **277**, 364–367.
3. Rodó, X., Pascual, M., Fuchs, G. & Faruque, A. S. G. (2002) *Proc. Natl. Acad. Sci. USA* **99**, 12901–12906.
4. Levitus, S., Antonov, J. I. & Boyer, T. P. (2000) *Science* **287**, 2225–2229.
5. Kumar, K. K., Rajagopalan, B. & Cane, M. A. (1999) *Science* **284**, 2156–2159.
6. Timmermann, A. (1999) *Nature (London)* **398**, 694–697.
7. Moore, P. S. (1992) *Clin. Infect. Dis.* **14**, 515–525.
8. Colwell, R. R. & Patz, J. A. (1998) *Climate, Infectious Disease and Human Health: An Interdisciplinary Perspective* (Am. Soc. Microbiol., Washington, DC).
9. Madico, G., McDonald, J., Gilman, R. H., Cabrera, L. & Sterling, C. R. (1997) *Clin. Infect. Dis.* **24**, 977–981.
10. Checkley, W., Epstein, L. D., Gilman, R. H., Figueroa, D., Cama, R. I., Patz, J. A. & Black, R. E. (2000) *Lancet* **355**, 442–450.
11. Patz, J. A., Engelberg, D. & Last, J. (2000) *Annu. Rev. Public Health* **21**, 271–307.
12. Linthicum, K. J., Anyamba, A., Tucker, C. J., Kelley, P. W., Myers, M. F. & Peters, C. J. (1999) *Science* **285**, 397–400.
13. Bouma, M. J. & van der Kaay, H. J. (1994) *Lancet* **344**, 1638–1639.
14. Bouma, M. & van der Kaay, H. (1996) *Trop. Med. Int. Health* **1**, 86–96.
15. Pascual, M., Rodo, X., Ellner, S. P., Colwell, R. & Bouma, M. J. (2000) *Science* **289**, 1766–1769.
16. Colwell, R. R. (1996) *Science* **274**, 2025–2031.
17. Lipp, E. K. & Rose, J. B. (1997) *Rev. Sci. Tech.* **16**, 620–640.
18. Lobitz, B., Beck, L., Huq, A., Wood, B., Fuchs, G., Faruque, A. S. & Colwell, R. (2000) *Proc. Natl. Acad. Sci. USA* **97**, 1438–1443.
19. Intergovernmental Panel on Climate Change (2001) in *Climate Change 2001: Impacts, Adaptation and Vulnerability*, eds. Canziani, O. & McCarthy, J. (Cambridge Univ. Press, Cambridge, U.K.).
20. Patz, J. A., McGeehin, M. A., Bernard, S. M., Ebi, K. L., Epstein, P. R., Grambsch, A., Gubler, D. J., Reiter, P., Romieu, I., Rose, J. B., *et al.* (2000) *Environ. Health Perspect.* **108**, 367–376.
21. Lindgren, E. & Gustafson, R. (2001) *Lancet* **358**, 16–18.
22. Randolph, S. E. (2001) *Philos. Trans. R. Soc. London B* **356**, 1045–1056.
23. Hay, S. I., Cox, J., Rogers, D. J., Randolph, S. E., Stern, D. I., Shanks, G. D., Myers, M. F. & Snow, R. W. (2002) *Nature (London)* **415**, 905–909.
24. Patz, J. A., Hulme, M., Rosenzweig, C., Mitchell, T. D., Goldberg, R. A., Githeko, A. K., Lele, S., McMichael, A. J. & Le Sueur, D. (2002) *Nature*, in press.
25. Kovats, R. S., Campbell-Lendrum, D. H., McMichael, A. J., Woodward, A. & Cox, J. S. (2001) *Philos. Trans. R. Soc. London B* **356**, 1057–1068.

Effects of the *El Niño* phenomenon and ambient temperature on hospital admissions for diarrheal diseases in Peruvian children

William Checkley(1, 2),
Leonardo D Epstein(1, 3),
Robert H Gilman(1, 2),
Dante Figueroa (4),
Rosa I Cama(2),
Jonathan A Patz(5),
and Robert E Black (1).

August 30, 1999

Affiliations:

(1) Department of International Health, The Johns Hopkins School of Public Health, Baltimore, MD.

(2) Proyectos de Informática, Salud, Medicina y Agricultura (A.B. PRISMA), Lima, Perú.

(3) Departamento de Estadistica, Universidad Católica de Chile, Santiago, Chile.

(4) Unidad de Rehidratación Oral, Instituto Nacional de Salud del Niño, Lima, Perú.

(5) Department of Environmental Health Sciences, The Johns Hopkins School of Public Health, Baltimore, MD.

NMED - PATZ
REBUTTAL EXHIBIT 4

Short title : *El Niño* and childhood diarrhea in Peru

Corresponding author:

Robert H Gilman

The Johns Hopkins School of Public Health

615 North Wolfe Street, Room W3503

Baltimore, MD 21205

Telephone: (410) 614-3959

Fax : (410) 614-6060

Keywords: *El Niño* phenomenon, temperature, diarrheal disease, statistics, epidemiology.

Abbreviations: RR (relative risk), CI (confidence Interval), SD (standard deviations), 95% CI (95 percent confidence interval).

Abstract

To investigate whether the *El Niño* phenomenon and ambient temperature had an effect on the epidemiology of childhood diarrhea, we analyzed data on daily admissions to the Oral Rehydration Unit of the Instituto Nacional de Salud del Niño in Lima, Peru, between January 1993 and November 1998. During the 1997-98 *El Niño* episode, mean ambient temperature in Lima increased up to 5 °C above normal, and the number of daily admissions for diarrhea increased up to 200 percent. We found that 6,225 excess admissions were attributable to *El Niño* and that these cost USD 277,000. During the pre-*El Niño* period, diarrheal admissions increased by eight percent per 1 °C increase in mean ambient temperature. The effects of *El Niño* and ambient temperature on the number of admissions for diarrhea were greatest during the winter months. *El Niño*, through its effects on weather, had an effect on admissions greater than that explained by the regular seasonal variability in ambient temperature, and the excess increase in temperature was the main environmental variable affecting admissions. If our findings are reproducible in other regions, then diarrheal diseases may increase by millions of cases worldwide with each degree of increase in ambient temperature above normal.

1 INTRODUCTION

In recent years, the *El Niño* phenomenon has raised concern about the potential effects of extreme weather variability on health and disease transmission (1, 2). *El Niño* is an unusual warming of the equatorial Pacific Ocean that occurs every two to seven years, and is one of the best understood systematic patterns of climate variability. Although *El Niño* has been linked to outbreaks of dengue (3), malaria (4, 5), cholera (6), and other less common diseases (2, 7, 8), its effects on the epidemiology of non-cholera diarrhea have not been studied until recently. The effects of weather alterations on diarrheal diseases, if important, may be of significant public health concern since diarrhea causes one billion episodes and three million deaths annually in children under five worldwide (9).

El Niño may affect the incidence of infectious diseases around the world through its regional effects on weather. Ambient temperature is known to affect mosquito-borne diseases like malaria (10) and dengue (11), and causes of diarrhea like *Vibrio cholerae* (12) and *Cyclospora cayetanensis* (13). Diarrhea presents a highly seasonal pattern, usually with more cases during warmer seasons, among hospital admissions (14, 15) and in community-based studies (16, 17). The effects of ambient temperature on the epidemiology of diarrhea, however, have not been adequately addressed.

This study investigates the effects of the 1997-1998 *El Niño* event and ambient temperature on diarrheal diseases in Lima, Peru, where elevated sea-surface temperatures during *El Niño* have a strong effect on weather. Our study is of public health relevance for Peru because diarrhea is one of the most important causes of infant hospitalization and is a main cause of illness and death during

infancy and early childhood (18). We analyzed data from daily admissions to the Oral Rehydration Unit (ORU) of the Instituto Nacional de Salud del Niño between January 1993 and November 1998 to determine whether childhood diarrhea increased more than expected during the 1997-98 *El Niño* episode.

2 MATERIALS AND METHODS

2.1 Study area:

Lima is located in the tropics, 12 degrees south of the equator, on the coastline of the Pacific Ocean, and has a year-round temperate climate due to the cool Humboldt Current. Mean ambient temperature ranges from 16 to 19 °C in May to November and 20 to 26 °C in December to April. Rainfall rarely exceeds 50 mm per year, and usually is in the form of condensation. Mean relative humidity is 84 percent.

The Instituto Nacional de Salud del Niño, with 600 beds and over 264 staff physicians, is the largest public hospital for children in Lima and is a reference center for child health (19). It is located near downtown Lima and receives patients from the surrounding shantytown communities, and from low- to mid- income neighborhoods. These populations are stable and experience little migration. The ambulatory ORU receives all children with diarrhea who reach the hospital. Children are evaluated by a physician, and then administered oral rehydration. Those with severe dehydrating diarrhea or shock are transferred immediately to the emergency room.

2.2 Data sources:

We obtained data on the daily number of children under 10 years of age who were admitted for diarrhea to the ORU between January 1, 1993 and November 15, 1998. For each child we obtained age, weight and height, and severity status at admission, gender, and calculated height-for-age and weight-for-height at admission (20). We calculated height-for-age and weight-for-age

as the number of standard deviation units above or below the National Center for Health Statistics (NCHS) reference. We defined stunting as a height-for-age two standard deviations below the NCHS reference (20). No information on the cause of diarrhea was available.

Daily admission records were collected by the unit's personnel with a standard form, and then double entered into a spreadsheet by project staff. Mean daily ambient temperature and relative humidity were obtained from the Peruvian National Weather Service for the two weather stations closest to the hospital (Jesus Maria and San Marcos stations).

2.3 Definitions:

Based on meteorological data from the central Pacific, climatologists broadly agree that the 1997-98 *El Niño*-Southern Oscillation (ENSO) episode lasted from March 1997 to May 1998 (21). However, since *El Niño* may have varying effects on weather by region, it is less certain whether this arbitrary time period applies to more localized effects. Sea-surface temperatures along the South American coast are different from the basin wide phenomenon, and are less sensitive to the large-scale dynamics and strongly related to coastal forcing. Therefore, our definition of the *El Niño* period extended that of the global ENSO period to account for possible differences in the local effects of *El Niño* phenomenon on weather in Lima. Based on *a priori* information from previous *El Niño* episodes in the Peruvian coast, which usually manifest between late December and early January, we decided to use January 1, 1997 as the beginning date for the *El Niño* period. The effect of *El Niño* on ambient temperature lasted until about mid-August 1998. Peaks in diarrheal admissions,

however, lagged peaks in ambient temperature by one month. We therefore used August 31, 1998 as the end date for the *El Niño* period to account for a possible lagged effect. We defined the pre-*El Niño* period as January 1, 1993 to December 31, 1996.

2.4 Biostatistical methods:

To measure the effects of *El Niño* on the number of daily admissions for diarrhea, we used linear regression models with autoregressive-moving average (ARMA) errors (22). We approached the analysis in two steps:

Step 1: We developed a time series regression model using only the history of pre-*El Niño* admissions to predict an *expected* pattern of admissions during the *El Niño* event. These expected admissions may be interpreted as the number of admissions for diarrhea had the *El Niño* not occurred. We formulated this regression model via the construction of a harmonic model (23) – a linear combination of sine and cosine functions – for the expected admissions, and ARMA models for the error structure.

The dependent variable for this model was the square root of the number of daily admissions for diarrhea. We used the square root transformation to normalize the count data (24). From this regression model, we predicted the series of *expected* admissions for diarrhea (C_E) for the *El Niño* period. Values for C_E prior to *El Niño* were the fitted values of the regression model. This time series model allowed us to compare the expected with the observed admissions during *El Niño* and

to calculate 95 % pointwise prediction intervals (22).

Step 2: We developed a second regression model using the entire time series to model the attributable effect of *El Niño* on the number of diarrheal admissions. To model this effect, we added a smooth curve (a regression spline) that branched off from the curve fitted in **Step 1** at the onset of *El Niño*, in a manner described elsewhere (25). Hence, our model simultaneously fitted a curve representing the number of admissions had *El Niño* not occurred, and a separate curve reflecting the change in the pattern of admissions brought on by *El Niño*.

The number of admissions attributable to *El Niño* was calculated as the sum of the daily differences between the expected admissions during *El Niño* and the expected admissions had *El Niño* not occurred for January 1, 1997 to August 31, 1998. Using this second model, we calculated the relative risk for diarrheal admissions during *El Niño*. We calculated a 95 % pointwise confidence interval (CI) for the relative risk by the delta method (24). Model testing was based on the likelihood ratio statistic. We also estimated the cost associated with the number of admissions attributable to *El Niño*. The monthly average cost per child admitted to the Oral Rehydration Unit were obtained from the Accounting Office of the Instituto Nacional de Salud del Niño.

We used analytical methods described above to model the effects of *El Niño* on mean monthly age and weight-for-height at the time of admission, and on Lima's ambient temperature. We followed the method outlined in **Step 1** to calculate the *expected* ambient temperature (T_E) during the

study period had *El Niño* not occurred. To examine whether *El Niño* had an effect on admissions that was greater than the effect of ambient temperature alone, we compared the linear relationship between an *excess* increase in ambient temperature and an excess increase in diarrheal admissions prior to *El Niño* period, with the linear relationship between an excess increase in ambient temperature and the excess increase in diarrheal admissions during *El Niño*. We defined an excess increase in diarrheal admissions as the ratio of observed to expected admissions (C_O/C_E) and an excess increase in ambient temperature as the ratio of observed to expected temperature (T_O/T_E). We examined this hypothesis with a Poisson regression model where C_0 was the dependent variable, $\log(T_O/T_E)$ the independent variable, and C_E the offset term. The regression model allows for a change of slope upon the onset of *El Niño* to measure the effect of *El Niño* on daily admisions greater than the effect of ambient temperature.

We used generalized additive models (26) to study the relationship between weather variability and the number of daily admissions for diarrhea, and Poisson regression to calculate the increase in admissions per unit increase in ambient temperature and relative humidity. We estimated a scale parameter to account for overdispersion in Poisson regression. We used additive linear models to study the effects of ambient temperature on mean daily age and nutritional status at admission, and linear regression to estimate changes in mean weight-for-height and height-for-age per unit increase in temperature.

The analyses were performed using EViews (Quantitative Micro Software, Seattle, WA) and S-Plus (MathSoft, Seattle, WA).

3 RESULTS

A total of 57,331 children less than 10 years of age were admitted between January 1, 1993 and November 15, 1998 for diarrhea as outpatients to the ORU. During the 2,145 days of follow-up, 72 percent (41,065/57,331) of the admitted children were less than two years of age; 43 percent (24,625/57,331) were females; nine percent (5,064/57,331) had dehydrating diarrhea; 79 percent (45,243/57,331) of the children had anthropometric data recorded at admission; 13 percent (5,977/45,243) were wasted, and seven percent (2,961/45,243) were stunted. The risk of dehydrating diarrhea was significantly higher among children with stunting (RR = 1.56, 95 % CI 1.43 to 1.70). No children died in the ORU during the study period.

Prior to the onset of *El Niño*, daily admissions for diarrhea (Figure 1A) and mean ambient temperature (Figure 1B) had a clear seasonal pattern. Mean relative humidity was also seasonal (Figure 1C) and varied inversely with mean ambient temperature (Pearson $r = -0.69$, 95 % CI -0.73 to -0.67). Diarrheal admissions peaked between April and May and waned between August and September. The mean annual number of admissions for diarrhea during the pre-*El Niño* period was 8,900 children. Mean ambient temperature peaked between February and March, and waned between July and August.

Mean monthly age and weight-for-height at the time of admission presented a clear seasonal pattern. Age at admission peaked between October and November and waned between April and May (Figure 2A). Weight-for-height at admission peaked between August and September and waned between March and April (Figure 2B). Height-for-age at admission exhibited a weak, seasonal trend

(Figure 2C).

3.1 Effects of the *El Niño* phenomenon

During the 1997-98 *El Niño* episode, mean ambient temperature lost its periodic, pre-*El Niño* pattern and increased up to 5 ^{o}C above normal (Figures 3A-B). The greatest increase took place between the winter, where the mean difference in daily ambient temperature averaged 4.05 ^{o}C above normal. In April 1998, the excess increase in ambient temperature began to decline, and by mid-August 1998 the mean ambient temperature was lower than normal.

The daily number of admissions for diarrhea also lost its periodic, pre-*El Niño* pattern after the onset of *El Niño* and increased up to 200 percent above the *expected* number of admissions (Figure 4A). The relative risk of diarrheal admissions increased significantly during *El Niño* (Figure 4B), and peaked during the winter months. The relative risk of admissions during the *El Niño* winter months ranged from 1.5 to 2 times the expected value. For the entire *El Niño* period, the number of diarrheal admissions during the *El Niño* event was uniformly larger than the what would have been expected had *El Niño* not occurred. We estimated that 6,225 new admissions for diarrhea were attributable to *El Niño* and that they cost the ORU about USD 277,000.

El Niño had an additional effect on the number of diarrheal admissions greater than that explained by the regular seasonal variability in mean ambient temperature ($p < 0.001$; likelihood ratio test). The dose-response relationship between an *excess* increase in ambient temperature (T_O/T_E) and an excess increase in daily admissions (C_O/C_E) was approximately five times greater

during *El Niño* than in the pre-*El Niño* period (Figure 5).

The mean age at admission for diarrhea increased significantly during the *El Niño* period ($p < 0.001$; likelihood ratio test). Between August and October 1997, children were more than 15 months of age older than expected at the time of admission. *El Niño* did not affect mean weight-for-height ($p = 0.42$; likelihood ratio test) or the proportion of admissions for dehydrating diarrhea ($p = 0.68$; likelihood ratio test).

3.2 Effects of weather variability

The daily number of admissions for diarrhea were linearly related to ambient temperature and to relative humidity for most of its range (Figure 6). Prior to the onset of *El Niño*, peaks of diarrheal admissions lagged behind peaks of ambient temperature by 35 to 45 days. We estimated this lag period to be 37 days. An increase of 1 ^{o}C in ambient temperature during the pre-*El Niño* period was associated with an eight percent increase in the number of diarrheal admissions (RR = 1.08, 95 % CI 1.07 to 1.09). An increase of one percent in mean relative humidity was associated with a three percent decrease in the number of diarrheal admissions (RR = 0.97, 95 % CI 0.97 to 0.98). The effect of ambient temperature on the number of diarrheal admissions was month-dependent ($p < 0.001$; likelihood ratio test). A degree centigrade of increase in mean ambient temperature had a greater effect on the number of daily admissions during the cooler months of May to November (RR = 1.12, 95 % CI 1.10 to 1.14) than during the warmer months of December to April (RR = 1.04, 95 % CI 1.02 to 1.05). That is, during the pre-*El Niño* period, a 5 ^{o}C increase in mean

ambient temperature in the winter was associated with a 77 percent increase in the number of diarrheal admissions. A similar 5 °C increase in mean ambient temperature during the pre-*El Niño* summer, however, was only associated with a 21 percent increase in diarrheal admissions.

The relative risk of dehydrating diarrhea increased with ambient temperature between 15 °C and 23 °C, and decreased thereafter (Figure 7A). Mean age at admission decreased as ambient temperature increased from 15 °C to 20 °C, and increased above 20 °C (Figure 7B). Weight-for-height and height-for-age at admission decreased as ambient temperature increased (Figures 7C-D). For each degree of increase in ambient temperature, mean weight-for-height decreased by 0.06 SD (95 % CI 0.05 to 0.06) and mean height-for-age decreased by 0.02 SD (95 % CI 0.01 to 0.02). That is, for a 5 °C increase in ambient temperature, mean weight-for-height and height-for-age decreased by 0.28 and 0.08 SD, respectively.

4 DISCUSSION

There is growing concern about the potential health effects of future *El Niño* episodes and global climate warming. This study demonstrates that the 1997-98 *El Niño* episode increased hospital admissions for diarrheal diseases up to 200 percent above expected during the winter months, and suggests that this concern is well founded. *El Niño* had an effect on diarrheal admissions greater than that explained by the regular seasonal variability in ambient temperature, and the excess increase in temperature was the most important environmental variable affecting admissions. Our results are consistent with a recent report in a different hospital serving a different population base in Lima that found a 28 percent increase in diarrheal admissions between March 1997 and September 1997 (27). For each degree centigrade of increase in mean ambient temperature, diarrheal admissions increased by eight percent. If our findings are reproducible in other geographical regions, then diarrhea may increase by millions of cases worldwide per degree of increase in ambient temperature above normal.

We believe that this is the first study to directly quantify the relationship between ambient temperature and the epidemiology of diarrheal disease. In the past, this relationship has been only indirectly inferred from observed seasonal variations (14-17). A 1 °C increase in ambient temperature had a more significant effect on diarrheal admissions in the winter than in the summer. Similarly, *El Niño* had a more important effect on diarrheal admissions during the winter. These effects differ from the well-known seasonal effect, which increases diarrhea prevalence during warmer weather. The smaller increase per degree of increase in ambient temperature during the warmer

seasons, and the enhanced *El Niño* effect during the cooler seasons, may be explained by changes in the relative presence of diarrheal causes driven by ambient temperature. Higher temperatures increase exposure to bacterial and parasitic diarrhea and lengthens the survival of bacteria like enterotoxigenic *Escherichia coli* in contaminated food (28). Lower temperatures appear to enhance the transmission of viral diarrhea (28, 29). At intermediate temperatures, namely between 18 and 23 ^{o}C, children may be exposed to a wider range of viral, bacterial, and parasitic etiologies. Although data on the cause of diarrheal illness were not available for analysis, we have previously noted a marked increase in the number of admissions for bacterial diarrhea during the summer and a greater number of admissions for rotavirus during the winter (19). Finally, *El Niño* may also bring behavioral patterns more common during warmer weather, such as increased water demand or decreased hygiene practices, that are known to promote diarrheal transmission (28).

Our study provides strong evidence that the 1997-98 *El Niño* event was associated with an increase in the number of diarrheal admissions in Lima. The statistical significance of an *El Niño* effect on admissions for diarrhea indicates that the probability of this effect having taken place by chance alone is very small indeed. These results are consistent with findings of a positive association between *El Niño* and other infectious diseases in different geographical regions (2-8). During the study period, neither the Peruvian Ministry of Health nor the ORU implemented major changes in policy (personal communication, D. Figueroa), making it unlikely that changes in government programs for diarrheal disease may have affected our results. We also observed a strong dose-response relationship between an *excess* increase in ambient temperature and excess increase in

diarrheal admissions during, but not prior to, the *El Niño* period.

The increase of admissions for diarrhea in Lima (12 °S, 77 °E) was associated with an increase in ambient temperature and a decrease in relative humidity. We found that relative humidity, however, was a linear function of ambient temperature, and that ambient temperature was a better predictor of diarrheal admissions than was relative humidity. Rainfall did not increase significantly in Lima throughout *El Niño*, making it very unlikely to affect diarrheal admissions. Flooding in the neighboorhoods surrounding the hospital was minimal too and unlikely to have affected overall rates of diarrheal admissions. Weather changes driven by *El Niño* may vary by geographical area, and consequently may differently affect the dynamics of other diseases. Therefore, we must caution about generalizing these findings to other regions of the world. Interestingly, the 1997-98 *El Niño* event, which increased ambient temperature but decreased rainfall and relative humidity in the Peruvian amazon basin (4 °S, 73 °E), was associated with a decrease in the number of reported malaria cases in the city of Iquitos (personal communication, R.H. Gilman).

To measure the effects of *El Niño* on diarrheal admissions we used time series analyses, which model the correlation structure between adjacent values of the dependent variable. Time series is commonly used in economics for forecasting, and in biostatistics for disease surveillance. Our analytical approach introduces the use of smooth curves (regression splines) to model changes in the pattern of admissions after the onset of *El Niño*. Our method provides a useful tool for the analysis of meteorological effects on health outcomes like diarrhea, acute respiratory infections, or malaria, and can control for confounding variables in the regression model.

The adverse effects of *El Niño* on diarrheal admissions were explained significantly by the excess increase in ambient temperature. Other factors, however, may play an important role in affecting admissions. An increase in relative humidity was related to a decrease in diarrheal admissions, but this effect was not independent from the relationship with ambient temperature. Although *El Niño* had a minimal effect on rainfall and did not cause significant flooding in Lima, we may need to consider the possibility of downstream contamination of the Rimac river from nearby mountainous areas. School attendance may also affect the number of diarrheal admissions, however, less than 10 percent of the children admitted to the ORU were of school age. We currently have a longitudinal study of of diarrheal diseases in birth cohort of children from a Peruvian peri-urban community, and plan to examine the interactions between the *El Niño* phenomenon and other epidemiological variables on the incidence of diarrheal diseases. Understanding the effects of weather variability on the epidemiology of infectious diseases is of special importance for planning of health services. If global climate change occurs as projected, the observed adverse health impacts attributable to *El Niño* may provide an analogue for future environmental health conditions. Accordingly, health services may need to be better prepared to face changes in the epidemiology of diarrheal diseases with preventive public health interventions during future *El Niño* episodes. These interventions may include alerting health workers; aggressive community-based campaigns to promote oral rehydration and chlorination of water sources; increasing staff and number of beds in oral rehydration units in hospitals; implementing *El Niño* forecasts for early warning, and planning and implementing additional diarrheal disease control programs.

Acknowledgments. Work for this study was supported by a National Research Service Award of the National Institutes of Child Health and Development (F31-HD08488), awarded to Mr. Checkley. Partial support was provided by USAID through an Applied Research on Child Health grant awarded to A.B. PRISMA, an EPA Cooperative Agreement grant (CR-823130) awarded to the Johns Hopkins School of Public Health, and by the charitable RG-ER foundation for the advancement of climate research. Special thanks to Drs. D. Burke, MD Chestnut, and J. Friedland for helpful comments, Drs. P. Arkin and C. Ropelewski for expert comments on the definition of the *El Niño* period, Dr. W. Palma for expert advice on time series analysis, Ms. L Kelley for editorial assistance, and Ms. JB Phu and Ms. D Sara for technical support.

REFERENCES

1. World Health Organization. Climate change and human health. Geneva: World Health Organization; 1996.

2. Patz JA, Epstein PR, Burke TA, Balbus JM. Global climate change and emerging infectious diseases. JAMA 1996; 50:217-223.

3. Hales S, Weinstein P, Woodward A. Dengue fever epidemics in the South Pacific: driven by El Niño Southern Oscillation? Lancet 1996; 348:1665.

4. Bouma MJ, van der Kaay HJ. The El Niño Southern Oscillation and the historic malaria epidemics on the Indian subcontinent and Sri Lanka: an early warning system for epidemics? Trop Med Inter Health 1996; 1:86-96.

5. Bouma MJ, Dye C. Cycles of malaria associated with El Niño in Venezuela. JAMA 1997; 278: 1772-1774.

6. Colwell RR, Global climate and infectious disease: the cholera paradigm. Science 1996; 274: 2025-2031.

7. Nicholls N. El Niño-Southern Oscillation and vector-borne disease. Lancet 1993; 342: 1284-1285.

8. Hales S, Weinstein P, Souares Y, Woodward A. El Niño and the dynamics of vector-borne disease transmission. Environ Health Perspect 1998; 107:99-102.

9. Bern C, Martines J, de Zoysa I, Glass I. The magnitude of the global problem of diarrhoeal disease: a ten year update. Bull WHO 1992; 70:705-14.

10. Watts DM, Burke DS, Harrison BA, Whitmire RE, Nisalak A. Effect of temperature on the vector efficiency of Aedes aegypti for dengue 2 virus. Amer J Trop Med Hyg 1987; 36:143-52.

11. Gilles HM. Epidemiology of malaria. In: Gilles HM, Warrell DA, editors. Bruce-Chwatt's Essential Malariology. London: Edward Arnold; 1993.

12. Madico G, Checkley W, Gilman RH, Bravo N, Cabrera L, Calderon M, et al. Active surveillance for Vibrio cholerae O1 and Vibriophages in Sewage Water as a Potential Tool to Predict Cholera Outbreaks. J Clin Microbiol 1996; 34:2968-2972.

13. Madico G, McDonald J, Gilman RH, Cabrera L, Sterling CR. Epidemiology and treatment of *Cyclospora cayetanensis* infection in Peruvian children. Clin Infect Dis 1997; 24:977-981.

14. Black RE, Merson MH, Rahman AS, Yunus M, Alim AR, Huq I, et al. A two-year study of bacterial, viral, and parasitic agents associated with diarrhea in rural Bangladesh. J Infect Dis 1980; 142:660-4.

15. Guerrant RL, Lima NL, Sears CL. Etiologies and epidemiology of childhood diarrhea in Brazil's northeast. In: Guerrant RL, de Souza MA, Nations MK, editors. At the Edge of Development: Health Crisis in a Transitional Society. Durham: Carolina Academic Press; 1996.

16. Black RE, Brown KH, Becker S, Alim AR, Huq I, Longitudinal studies of infection and physical growth of children in rural Bangladesh. II. Incidence of diarrhea and association with known pathogens. Am J Epidemiol 1982; 115:315-324.

17. Guerrant RL, Kirchhoff LV, Shields DS, Nations MK, Leslie J, de Sousa MA, et al. Prospective study of diarrheal illnesses in northeastern Brazil: Patterns of disease, nutritional impact, etiologies, and risk factors. J Infect Dis 1983; 148: 986-987.

18. Panamerican Health Organization. Health Conditions in the Americas. Scientific Publication No. 549. Washington DC: Panamerican Health Organization; 1994.

19. Cama RI, Parashar UD, Taylor DN, Hickey T, Figueroa D, Ortega YR, et al. Enteropathogens and Other Factors Associated with Severe Disease in Children with Acute Watery Diarrhea in Lima, Peru. In press, J Infect Dis.

20. World Health Organization, Physical Status: The use and interpretation of anthropometry. WHO Technical Report No. 854. Geneva: World Health Organization; 1995.

21. Bell GD, Halpert MS. Climate Assessment for 1997. Bull Amer Meteorol Soc 1998; 79:S1-S50.

22. Diggle PJ. Time series: A Biostatistical Introduction. Oxford: Oxford University Press; 1995.

23. Armitage PA, Berry G. Statistical Methods in Medical Research. 3rd ed. Oxford: Blackwell Science; 1996.

24. Rice JA. Mathematical Statistics and Data Analysis. California: Duxbury Press; 1988.

25. Checkley W, Epstein LD, Gilman RH, Black RE, Cabrera L, Sterling CR. Effects of *Cryptosporidium parvum* infection in Peruvian children: Growth faltering and subsequent catch-up growth. Am J Epidemiol 1998; 148: 497-506.

26. Hastie TJ, Tibshirani RJ. Generalized additive models. London: Chapman-Hall, 1995.

27. Salazar-Lindo E, Pinell-Salles P, Maruy A, Chea-Woo E. El Nino and diarrhoea and dehydration in Lima, Peru. Lancet 1997; 350:1597-8.

28. Black RE, Lanata CF. Epidemiology of diarrheal diseases in developing countries. In: MJ Blaser, Smith PD, Ravdin JI, Greenberg HB, Guerrant Rl, editors. Infections of the Gastrointestinal Tract. New York: Raven Press; 1995.

29. Konno T, Suzuki H, Katsushima N, Imai I, Tazawa F, Kutsuzawa T, et al. Influence of temperature and relative humidity on human rotavirus infection in Japan. J Infect Dis 1983; 147: 125-128.

Figure 1. Daily time series between January 1, 1993 and November 15, 1998 for diarrheal admissions (panel A), mean ambient temperature (panel B) and relative humidity (panel C) in Lima, Peru. Data on the number of children less than 10 years of age admitted with diarrhea were obtained from the Oral Rehydration Unit of the Instituto Nacional de Salud del Niño. The shaded region is the time period of the 1997-98 *El Niño* event (January 1, 1997 to August 31, 1998).

Figure 2. Monthly time series between January 1, 1993 and November 15, 1998 of average age (panel A), weight-for-height (panel B), and height-for-age (panel C) at the time of admission with diarrhea to the Oral Rehydration Unit of the Instituto Nacional de Salud del Niño in Lima, Peru. We calculated height-for-age and weight-for-age as the number of standard deviation units above or below the National Center for Health Statistics reference. The shaded region represents the period of the 1997-98 *El Niño* event (January 1, 1997 to August 31, 1998).

Figure 3. Effects of the 1997-98 *El Niño* event on mean ambient temperature in Lima, Peru. Using the pre-*El Niño* data (January 1, 1993 to December 31, 1996), we predicted the series of expected ambient temperature (T_E) between January 1, 1997 and November 15, 1998. T_E estimates the expected ambient temperatures in Lima assuming that *El Niño* did not occur. Panel A shows the series of observed ambient temperatures (T_0) and T_E. The shaded region are 95 percent pointwise prediction intervals for T_E. Panel B shows the difference between T_0 and T_E, i.e., the estimated increase in ambient temperature attributable to *El Niño*.

Figure 4. Effects of the 1997-98 *El Niño* event on the number of daily admissions for diarrhea to the Oral Rehydration Unit of the Instituto Nacional de Salud del Niño in Lima, Peru. Using the pre-*El Niño* data (January 1, 1993 to December 31, 1996), we predicted the series of expected admissions for diarrhea (C_E) between January 1, 1997 and August 31, 1998 (the *El Niño* period). C_E estimates the expected number of admissions assuming that *El Niño* did not occur. Panel A shows the series of observed admissions for diarrhea (C_0) and the series of C_E during the *El Niño* period. The shaded region are 95 % pointwise prediction intervals for C_E. Using the entire time series (January 1, 1993 to November 15, 1998), we fit a time series model to estimate the expected number of diarrheal admissions during the *El Niño* period and the conditional expected number of diarrheal admissions had *El Niño* not occurred. We calculated the relative risk for the number of diarrheal admissions during the *El Niño* period as the ratio of the expected number of diarrheal admissions during the *El Niño* period and the expected number of diarrheal admissions had *El Niño* not occurred. Panel B shows how the relative risk changes during the months of the *El Niño* period. The dashed lines are 95 % pointwise confidence interval for the relative risk.

Figure 5. Graphical representation of the *El Niño* effect greater than that explained by ambient temperature alone on diarrheal admissions in Lima, Peru. Using the pre-*El Niño* data (January 1, 1993 to December 31, 1996), we predicted the series of expected ambient temperature (T_E) and the series of expected admissions for diarrhea (C_E) between January 1, 1997 and August 31, 1998 (the *El Niño* period). The figure shows the dose-response relationship between the log excess of ambient temperature (T_O/T_E) and the log excess of daily admissions for diarrhea (C_O/C_E) before (panel A) and during (panel B) the *El Niño* period. The relationship between T_O/T_E and C_O/C_E was significantly larger during the *El Niño* than prior to the onset of *El Niño*, and provides evidence for an additional effect of *El Niño* on diarrheal admissions which is greater than the effect of ambient temperature.

Figure 6. Relationship between climate variability and diarrheal admissions to the Oral Rehydration Unit of the Instituto Nacional de Salud del Niño in Lima, Peru (January 1, 1993 to November 15, 1998). Panels A and B show the relationship between mean ambient temperature and the number of diarrheal admissions. Panels C and D show the relationship between relative humidity and the number of diarrheal admissions. The upper panels show non-parametric fits of the relative risk for the number of children admitted with diarrhea as a function of each weather variable. The dashed lines are 95 percent pointwise confidence intervals. The lower panels shows the scatterplots of diarrheal admissions by each weather variable.

Figure 7. Relationship between ambient temperature: and 1) the daily number of children with dehydrating diarrhea (panel A), 2) daily average age (panel B), 3) weight-for-height (panel C), and 4) height-for-age (panel D) at the time of admission to the Oral Rehydration Unit of the Instituto Nacional de Salud del Niño in Lima, Peru (January 1, 1993 to November 15, 1998). Panel A shows a non-parametric fit of the relative risk for the number of children admitted with dehydrating diarrhea as a function of ambient temperature. The remaining panels show the non-parametric relationship between mean age and nutritional status at the time of admission and ambient temperature. Dashed lines are 95 percent pointwise confidence intervals.

The Association Between Extreme Precipitation and Waterborne Disease Outbreaks in the United States, 1948–1994

Frank C. Curriero, PhD, Jonathan A. Patz, MD, MPH, Joan B. Rose, PhD, and Subhash Lele, PhD

Objectives. Rainfall and runoff have been implicated in site-specific waterborne disease outbreaks. Because upward trends in heavy precipitation in the United States are projected to increase with climate change, this study sought to quantify the relationship between precipitation and disease outbreaks.

Methods. The US Environmental Protection Agency waterborne disease database, totaling 548 reported outbreaks from 1948 through 1994, and precipitation data of the National Climatic Data Center were used to analyze the relationship between precipitation and waterborne diseases. Analyses were at the watershed level, stratified by groundwater and surface water contamination and controlled for effects due to season and hydrologic region. A Monte Carlo version of the Fisher exact test was used to test for statistical significance.

Results. Fifty-one percent of waterborne disease outbreaks were preceded by precipitation events above the 90th percentile ($P = .002$), and 68% by events above the 80th percentile ($P = .001$). Outbreaks due to surface water contamination showed the strongest association with extreme precipitation during the month of the outbreak; a 2-month lag applied to groundwater contamination events.

Conclusions. The statistically significant association found between rainfall and disease in the United States is important for water managers, public health officials, and risk assessors of future climate change. (*Am J Public Health.* 2001;91:1194–1199)

According to the US National Assessment on the Potential Consequences of Climate Variability and Change,[1] determining the role of weather in the incidence of waterborne disease outbreaks is a priority public health research issue for this country. Rainfall and runoff have been implicated in individual outbreaks in the United Kingdom and the United States. A waterborne disease outbreak of giardiasis in Montana was related to rainfall,[2] as was the largest reported waterborne disease outbreak ever documented, which occurred in Milwaukee, Wis, in 1993. There, an estimated 403 000 cases of intestinal illness and 54 deaths occurred,[3] and the outbreak was preceded by a period of heavy rainfall and runoff with a subsequent turbidity load that compromised the efficiency of the drinking water treatment plant.[4,5]

Even outbreaks of *Escherichia coli,* generally considered a foodborne pathogen, have been linked to rainfall events. In fact, the largest reported outbreak of *E coli* O157:H7 occurred at a fairground in the state of New York in September 1999 and was linked to contaminated well water. Unusually heavy rainfall, which was preceded by a drought, coincided with this major outbreak.[1] Under conditions of high soil saturation, rapid transport of microbial organisms can be enhanced.

Part of the rationale for this study, conducted through a US Environmental Protection Agency grant for studying the effects of global climate change on public health, comes from projections of more intense rainfall that may accompany global warming. In the past century, average daily temperatures in the conterminous United States increased by approximately 1°F.[6] Warmer air can hold more moisture, and changes in the hydrologic cycle in the United States have been evidenced by increases in cloud cover[7] and total precipitation.[8] Moreover, the type of precipitation has been changing in the United States, with increases in extreme precipitation events (those with an intensity of more than 2 inches per day).[9,6,10] These rainfall patterns are consistent with expectations of a more vigorous hydrologic cycle caused by anthropogenic greenhouse gas warming of the earth's surface.[11–13]

The purpose of our study was to analyze the relationship between precipitation and waterborne diseases, using the complete database of all reported waterborne disease outbreaks in the United States from 1948 to 1994. Rainfall intensity is assumed to be a key determining factor in the fate and transport of pathogenic microorganisms, but the relationship has never been analyzed at the national level.

METHODS

US Waterborne Disease Outbreaks and Precipitation Data Sets

Data on all reported waterborne disease outbreaks in the United States between 1948 and 1994 were obtained from the US Environmental Protection Agency's Office of Research and Development. Included in this data set were the etiologic agent, the community and state where the outbreak occurred, and the month and year of each outbreak. The outbreak source was designated as either surface water or groundwater contamination. The community and state information was geocoded and expressed as longitude and latitude coordinates marking the affected city or county.

A waterborne disease outbreak is defined as an outbreak in which epidemiologic evidence points to a drinking water source from which 2 or more persons become ill at similar times. All recreational outbreaks and outbreaks associated with cross-connections or back-siphonage between sewage and drinking water in the distribution system, including chemical outbreaks, were removed from the database. We excluded these outbreaks to focus the analysis on source waters and watershed contamination and to exclude acci-

NMED - PATZ
REBUTTAL EXHIBIT 5

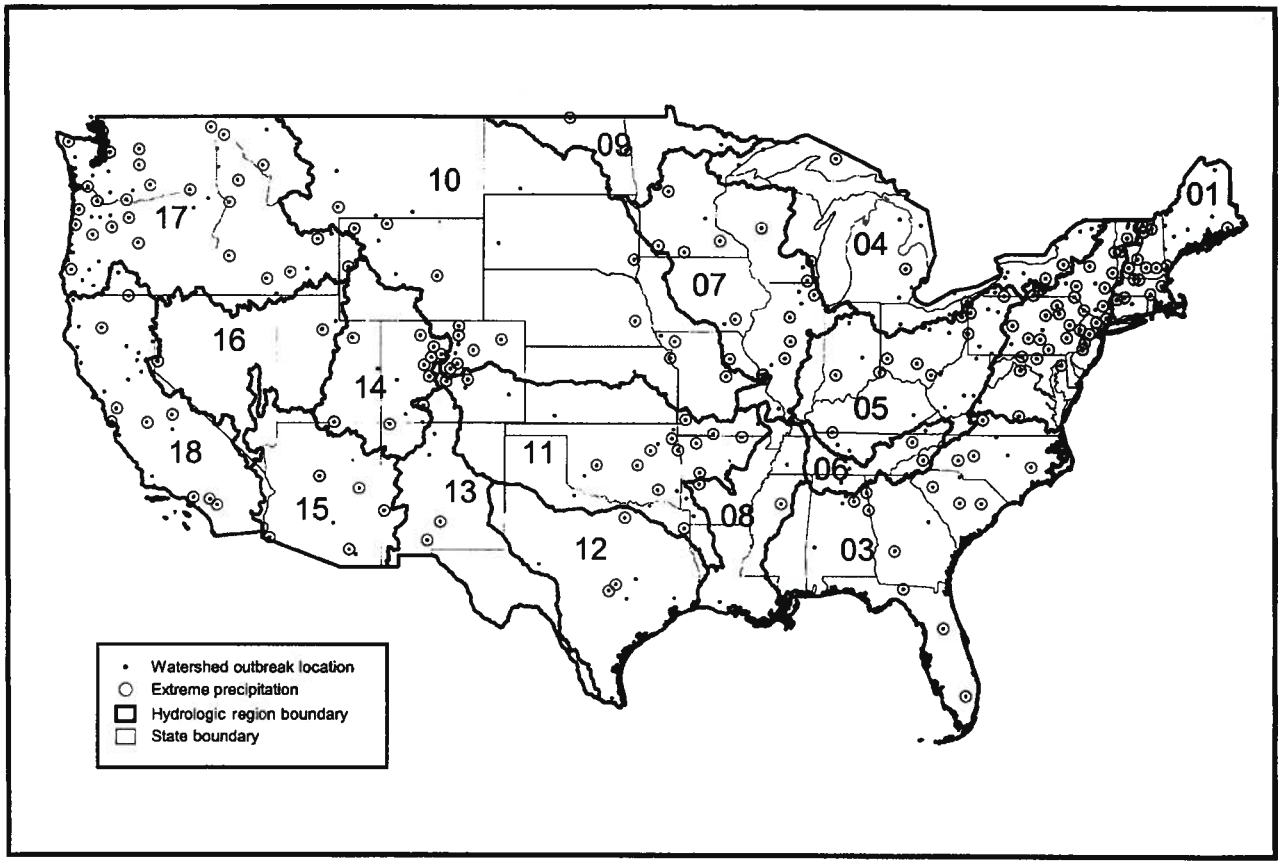

Note. Outbreak locations represent the centroid of the affected watershed.

FIGURE 1—Waterborne disease outbreaks and associated extreme levels of precipitation (precipitation in the highest 10% [90th percentile]) within a 2-month lag preceding the outbreak month: United States, 1948–1994.

dental fecal releases associated with recreational outbreaks and infrastructure problems in the distribution system.

The conterminous United States is subdivided into 2105 hydrologic cataloging units called *watersheds*, which are geographic areas representing part or all of a surface drainage basin, a combination of drainage basins, or a distinct hydrologic feature. Watersheds act as the drinking water source for the surrounding area; thus, we chose watersheds as the geographic units for our investigation. Outbreak locations, originally designating the affected city or county, were recoded to correspond to the centroid of the associated watershed. Data on US hydrologic units, a hierarchy of geographic subdivisions including watersheds, were downloaded from the US Geological Survey.[14] Figure 1 includes boundaries for the largest subdivision in this hierarchy (watersheds are the smallest), which divides the United States into 18 distinct hydrologic regions, each containing the drainage area of a major river or the combined drainage areas of a series of rivers.

Total monthly precipitation readings for the more than 16 000 weather stations located across the United States from 1948 through 1994 were downloaded from the National Climatic Data Center.[15] The weather station locations were also coded to the watershed level; each watershed, on the average, contained approximately 7 weather stations. To account for local variations, we replaced recorded total monthly precipitation for each weather station with its corresponding *z* score, which was computed on the basis of the distribution of values recorded for that month from 1948 to 1997. We considered there to be sufficient information to compute *z* scores only if the corresponding distributions contained at least 20 years of recorded data. The *z* score thresholds were chosen to indicate extreme levels of precipitation. For example, *z* scores greater than 0.84, 1.28, and 1.65 correspond, respectively, to total monthly precipitation in the highest 20%, 10%, and 5% observed for that station and month from 1948 to 1994. The maximum *z* score determined from weather station–specific *z* scores within a watershed was used as a measure of extreme precipitation for that watershed.

Statistical Analysis

Figure 1 displays the 548 waterborne disease outbreaks, plotted using the centroid of the affected watershed, within the contermi-

TABLE 1—Waterborne Disease Outbreaks, With Associated Extreme Levels of Precipitation[a] In the Preceding 2 Months: United States, 1948–1994

	Extreme Precipitation		
Outbreak	Yes	No	Total
Yes	268	257	525
No	NC	NC	1 186 695
Total	NC	NC	1 187 220

Note. There were 1 187 220 watershed outbreak possibilities. Shown are the 525 outbreaks for which extreme precipitation data were available. Information regarding extreme precipitation status for watersheds not experiencing an outbreak was not compiled (NC).
[a]Precipitation in the highest 10% (90th percentile).

nous United States that were reported from 1948 to 1994. Of these outbreaks, 51% were preceded within a 2-month lag by an extreme level of precipitation in the highest 10% (or 90th percentile), as indicated in the figure. Several methods, and an accompanying large body of literature, are available to test for spatial clustering of disease events.[16] In this study we were interested in testing whether the outbreaks cluster around extreme precipitation events, as opposed to solely investigating geographic clustering of outbreaks.

Information in Figure 1 can be represented with a 2×2 contingency table, watershed outbreak status×watershed extreme precipitation status. Since this information is collapsed over time, there are a total of 1 187 220 watershed outbreak possibilities (47 years×12 months×2105 watersheds). Table 1 displays extreme precipitation status for only those watersheds known to have experienced an outbreak. Enumerating the bottom row would require determining the extreme precipitation status within a 2-month lag for the remaining watershed outbreak possibilities, a computational burden we wished to avoid. The total number of outbreaks is shown to be 525, not 548, because sufficient precipitation data were not available for 23 outbreak-associated watersheds.

Associations between events in contingency tables are usually described with odds ratios followed by a χ^2-based test of independence. Proceeding in this fashion, however, would require a completely enumerated table. Note that the percentage of coincident events reported (51%) is simply the (1,1) cell (outbreak and extreme precipitation) divided by its marginal total (number of outbreaks). Since the row and column totals in Table 1 are fixed, the (1,1) cell determines the remaining cells and hence the odds ratio; thus, the percentage of coincident events and the odds ratio are equivalent descriptors of association. Also, because the marginal totals are fixed, the Fisher exact test[17] can be used to assess the significance of the association based on the percentage of coincident events. Although the calculation of *P* values in the Fisher exact test requires fully enumerated information as well, the rationale behind the calculation can be approximated with the following Monte Carlo simulation.

The general idea is to repeatedly generate sets of "outbreaks" in a random fashion, tabulating the percentage of these artificial outbreaks that coincide with extreme levels of precipitation at each step. Such a process would produce a distribution of coincident percentages under the assumption of no association, which can then be compared with the observed percentage to compute a *P* value. The following algorithm describes the process for a given set of outbreaks overlaid with extreme precipitation events.

1. Generate a set of outbreaks.
   a. Randomly select watersheds.
   b. Randomly select a month (1–12) and year (1948–1994) for each watershed.
2. Calculate and store the percentage of these outbreaks coincident with extreme levels of precipitation within a given preceding monthly lag.
3. Repeat steps 1 and 2 one thousand times.

The expected percentage of outbreaks coincident with extreme levels of precipitation within a given preceding monthly lag, under the assumption of no association, can be estimated by averaging the Monte Carlo distribution of percentages in step 2.

For the data shown in Table 1, if the 525 waterborne disease outbreaks are clustered both spatially and temporally within watersheds experiencing extreme levels of precipitation, then the observed 51% would be higher than the percentage expected under the assumption of no association. We were therefore interested in testing the one-sided alternative representing a positive association between outbreaks and extreme precipitation. *P* values for such a test can be obtained by dividing by 1000 the number of percentages in step 2 that are higher than their respective observed percentages.

RESULTS

Table 2 cross-tabulates the 548 reported waterborne disease outbreaks by the 18 hydrologic regions and 4 seasons. The distribution of outbreaks across the seasons (column totals) shows that the number of outbreaks is highest during the summer months and lowest during the winter months. The distribution across the hydrologic regions (row totals) may be due to specific hydrologic features present in these regions. The distributional variations across regions and seasons can be controlled for in the Monte Carlo test by restricting the randomization scheme in step 1 of that algorithm to adhere to the marginal totals shown in Table 2. Thus, each artificial set of outbreaks would have identical row and column totals, as shown in Table 2. The resulting test would then be one of conditional association between outbreaks and extreme precipitation, controlling for variations across both regions and seasons.

Of the 548 waterborne disease outbreaks reported between 1948 and 1994, 133 (approximately 24%) were known to be from surface water contamination, 197 (approximately 36%) were known to be from groundwater contamination, and 218 (approximately 40%) had an unknown water contamination source. The outbreak data also included the etiologic agents involved in each outbreak. More than

TABLE 2—Waterborne Disease Outbreaks, by Hydrologic Region and Season: United States, 1948–1994

Region	Season				Total
	Winter	Spring	Summer	Fall	
1	2	8	17	11	38
2	14	27	63	29	133
3	4	5	12	8	29
4	6	2	18	8	34
5	6	9	18	6	39
6	1	1	2	3	7
7	2	12	10	3	27
8	1	1	5	2	9
9	1	0	1	1	3
10	5	5	24	7	41
11	6	9	16	8	39
12	0	3	4	2	9
13	0	1	5	1	7
14	6	6	7	4	23
15	1	3	3	1	8
16	0	1	3	0	4
17	6	17	34	8	65
18	9	6	14	4	33
Total	70	116	256	106	548

Note. Winter = December, January, February; Spring = March, April, May; Summer = June, July, August; Fall = September, October, November.

half the outbreaks were determined to be "acute gastrointestinal illness," about 13% were attributed to *Giardia*, and the remainder were caused by 35 other specific agents.

We used the Monte Carlo test presented above to test the significance of the overlaid information shown in Figure 1 and other associations between waterborne disease outbreaks and extreme precipitation, controlling for the possible confounding effects due to hydrologic region and season. Different scenarios were investigated by varying the preceding monthly lag time and level of extreme precipitation. Separate analyses were performed for outbreaks due to surface water contamination, outbreaks due to groundwater contamination, and the combined data, including outbreaks with an unknown water contamination source. The results, which are presented in Table 3, include for each scenario the observed percentage of outbreaks coincident with extreme precipitation events; an estimated expected percentage of coincident events, assuming no association; and the *P* value testing the significance of the observed percentage.

Results for the association depicted in Figure 1 (combined data, monthly lag 0, 1, 2, and 90th percentile extreme precipitation) indicate that after controlling for variations across regions and seasons, we would have expected 43.2% of the outbreaks to be coincident with extreme precipitation if there was no association between outbreaks and extreme precipitation. The observed percentage of outbreaks coincident with levels of extreme precipitation—51.0%—was highly significant ($P=.002$). *P* values of less than .001 in Table 3 indicate the strongest evidence of an association; they occurred when the random selection of watershed outbreaks, for the 1000 iterations performed in step 1 of the Monte Carlo algorithm, did not produce a percentage of outbreaks coincident with this level of extreme precipitation that was higher than the observed percentage.

The association between outbreaks and extreme precipitation remained statistically significant at the .05 level across all of the scenarios we considered for the combined data. The analysis stratified by water contamination source showed that outbreaks due to surface water contamination were most significant for extreme precipitation during the month of the outbreak. Outbreaks due to groundwater contamination, however, showed highest significance for extreme precipitation 2 months prior to the outbreak. This might be expected, considering the direct vs complex routes of exposure.

DISCUSSION

This study represents the first quantitative analysis of the relationship between extreme precipitation and waterborne disease outbreaks at the national level and over an extended period. Our findings show a statistically significant association between weather events and disease. However, we recognize that multiple factors are involved, which must occur simultaneously in time and space. Elements of an outbreak event include (1) a source of contamination (infected humans, domestic animals, or wildlife); (2) fate and transport of the contaminant from source to drinking water supplies; (3) inadequate treatment; and (4) detection and reporting of the outbreak.[18] Given the variability of these factors across the United States, the robustness of our findings demonstrates the important role of extreme wet-weather events in microbial fate and transport and as a contributing factor in US waterborne disease outbreaks.

Incorporating data on other causal components will be important in the development of better predictive models extending beyond this study's limitations. We have partially controlled for source of outbreak by conducting analyses at the watershed level. Watersheds might be expected to maintain some consistency in land use patterns; however, these patterns, inevitably, have changed over the 47 years analyzed. Several state-specific analyses that could include more detailed land use and treatment facility information would, therefore, be of benefit as a follow-up to this national-level study.

Our study is limited by the temporal resolution of the waterborne disease outbreak

TABLE 3—Monte Carlo Simulation Results for the Association Between Waterborne Disease Outbreaks and Extreme Precipitation: United States, 1948–1994

	Extreme Precipitation Percentile								
	Surface Water Contamination			Groundwater Contamination			Combined		
Monthly Lag	80th	90th	95th	80th	90th	95th	80th	90th	95th
Monthly lag 0									
Observed, %	39.1	28.9	22.7	31.2	21.4	13.5	33.3	22.8	16.8
Monte Carlo, %	26.9	17.4	11.7	28.8	18.6	12.4	27.7	17.9	12.0
P	.001	<.001	.001	.229	.173	.314	.001	<.001	.002
Monthly lag 0,1									
Observed, %	55.1	41.7	33.9	53.9	39.3	26.2	52.3	38.3	28.8
Monte Carlo, %	45.5	31.2	21.7	48.0	33.0	22.7	46.5	31.9	22.0
P	.022	.003	.002	.059	.039	.132	.003	.001	<.001
Monthly lag 0,1,2									
Observed, %	65.9	50.8	42.9	71.6	52.1	36.8	68.0	51.0	39.4
Monte Carlo, %	58.9	42.3	30.3	61.6	44.4	31.6	59.9	43.2	30.7
P	.063	.023	.001	.002	.021	.062	<.001	.002	<.001
Monthly lag 1									
Observed, %	34.6	22.8	18.1	33.2	22.8	14.5	31.6	20.3	14.9
Monte Carlo, %	26.8	17.4	11.6	28.7	18.5	12.3	27.5	17.7	11.8
P	.033	.060	.026	.083	.070	.183	.005	.047	.009
Monthly lag 1,2									
Observed, %	54.8	36.5	31.0	57.8	41.7	28.6	54.4	37.5	27.8
Monte Carlo, %	45.4	31.0	21.5	47.7	32.6	22.4	46.3	31.6	21.7
P	.023	.109	.003	.002	.009	.027	<.001	.001	<.001

Note. Shown are results for outbreaks known to be from surface water contamination, outbreaks known to be from groundwater contamination, and the combined data, including outbreaks with an unknown water contamination source. Listed for each monthly lag and extreme precipitation scenario are the observed percentage of outbreaks coincident with extreme precipitation, the Monte Carlo–expected percentage of coincident events, and the corresponding *P* value.

data. These data have been reported in the same way for approximately 50 years. Improved understanding and better prevention might be achieved if outbreak data included start and end dates rather than simply the month of occurrence.[18]

Reporting bias is a key component in the waterborne disease outbreak data. Experts estimate that we may be seeing only a small fraction of the actual outbreaks.[19] With such a bias, many of the cluster detection methods that focus primarily on geographic clustering of diseases would clearly be inappropriate. The method we applied, which is focused more on the clustering of outbreaks around extreme precipitation, is appropriate under the assumption that outbreak reporting is independent of surrounding monthly precipitation.

Although the United States is thought to have high-quality drinking water, the risk of contamination from leaking septic tanks or agricultural runoff remains. One pathogen, *Cryptosporidium*, a protozoan that completes its life cycle within the intestine of mammals, is shed in high numbers of infectious oocysts that are dispersed in feces. It is highly prevalent in ruminants and readily transmitted to humans.[20] In a cross-sectional analysis of 50 livestock farms sampled within the 100-year floodplain in Lancaster County, Pennsylvania, manure samples from 64% of the farms tested positive for *C parvum*.[21] Therefore, it is biologically plausible that increases in rainfall and runoff intensity would result in more contamination of source waters by this parasite.

Our results are also consistent with findings from other studies. For example, Atherholt et al. found that concentrations of *Cryptosporidium* oocysts and *Giardia* cysts in the Delaware River were positively correlated with rainfall.[22] In 1998, a drinking water outbreak of cryptosporidiosis that occurred in Brushy Creek, Tex, was linked to storms that led to sewage contamination of wells and creeks.[23] *Cryptosporidium* oocysts are very small (~5 microns) and are difficult to remove from water; a recent study found that 13% of finished water still contained *Cryptosporidium* oocysts,[24] indicating some passage of microorganisms from source to treated drinking water.

Municipal water systems, even today, can be overburdened by extreme rainfall events. For example, many communities still have combined sewer systems designed to carry both storm water and sanitary wastewater to a sewage treatment plant. During periods of heavy rainfall or snowmelt, the stormwater can exceed the capacity of the sewer system or treatment plant, and these systems are designed to discharge the excess wastewater directly into surface water bodies.[25,26] For northern latitudes and high-elevation regions, the addition of temperature values

could further enhance the analysis by addressing the contribution of snowmelt.

During the heavy rainfall that accompanied the very strong El Niño of 1997 and 1998, a survey of a southwest Florida estuary found higher concentrations of fecal indicator organisms than occurred throughout the rest of the year,[27,28] implicating heavy rainfall as a risk factor for waterborne or seafood-borne disease. In urban watersheds, more than 60% of the annual load of all contaminants is transported during storm events.[29] In general, turbidity increases during storm events, and studies have recently shown a correlation between increases in turbidity and illness in communities.[30,31]

In summary, there is mounting evidence that heavy precipitation and runoff events significantly contribute to the risk of waterborne disease outbreaks. In the future, incorporation of other site-specific parameters, particularly land use patterns and treatment facility specifications, may allow for the development of more localized predictive models that can benefit water managers and public health planners. Our findings provide further insight into the linkage between weather and human disease that can be applied to risk assessments of future climate change. ■

About the Authors

Frank C. Curriero is with the Department of Biostatistics and Jonathan A. Patz is with the Department of Environmental Health Sciences, The Johns Hopkins University, Baltimore, Md. Joan B. Rose is with the Department of Marine Sciences, University of South Florida, St. Petersburg. Subhash Lele is with the Department of Mathematical Sciences, University of Alberta, Edmonton.

Requests for reprints should be sent to Jonathan A. Patz, MD, MPH, Program on Health Effects of Global Environmental Change, Department of Environmental Health Sciences, The Johns Hopkins University, 615 N Wolfe St, Baltimore, MD 21205 (e-mail: jpatz@jhsph.edu).

This article was accepted January 1, 2001.

Contributors

F.C. Curriero developed the statistical methodology and performed all data analyses. J.A. Patz was the principal investigator for this study and conceived and led the overall design of this project. J.B. Rose obtained all the outbreak data and was responsible for plotting them, using a geographic information systems (GIS) format; provided information on the details of the database; and reviewed the article. S. Lele provided expert guidance on the statistical analyses and made revisions to the manuscript.

Acknowledgments

This study was supported by the US Environmental Protection Agency, STAR Grant R824995, "Integrated Assessment of the Public Health Effects of Climate Change for the United States."

We are grateful to Rebecca Calderon of the Office of Research and Development, US Environmental Protection Agency, for providing the waterborne disease outbreak data. We also thank Scott Daeschner, University of South Florida, and Timothy Shields, the Johns Hopkins University, for their assistance in processing the outbreak data and GIS support, and Drs Paul Jameson and Dave Easterling, National Climatic Data Center, for providing quality assurance pertaining to the climate data.

References

1. Patz JA, McGeehin MA, Bernard SM, et al. The potential health impacts of climate variability and change for the United States: executive summary of the report of the health sector of the US National Assessment. *Environ Health Perspect.* 2000;108:367–376.

2. Weniger BG, Blaser MJ, Gedrose J, Lippy EC, Juranek DD. An outbreak of waterborne giardiasis associated with heavy water runoff due to warm weather and volcanic ashfall. *Am J Public Health.* 1983;73:868–872.

3. Hoxie NJ, Davis JP, Vergeront JM, Nashold RD, Blair KA. Cryptosporidiosis-associated mortality following a massive waterborne outbreak in Milwaukee, Wisconsin. *Am J Public Health.* 1997;87:2032–2035.

4. MacKenzie WR, Hoxie NJ, Proctor ME, et al. Massive waterborne outbreak of *Cryptosporidium* infection associated with a filtered public water supply. *N Engl J Med.* 1994;331:161–167.

5. Kramer MH, Herwaldt BL, Craun GF, Calderon RL, Juranek DD. Surveillance for waterborne-disease outbreaks–United States, 1993–1994. *MMWR Morb Mortal Wkly Rep.* 1996;45(SS-1):1–33.

6. Karl TR, Knight RW, Easterling DR, Quayle RG. Indices of climate change for the United States. *Bull Am Meteorol Soc.* 1996;77:279–303.

7. Karl TR, Steurer PM. Increased cloudiness in the United States during the first half of the twentieth century: fact or fiction? *Geophys Res Lett.* 1990;17:1925–1928.

8. Groisman PY, Easterling DR. Variability and trends of precipitation and snowfall over the United States and Canada. *J Climate.* 1994;7:184–205.

9. Karl TR, Knight RW, Plummer N. Trends in high-frequency climate variability in the twentieth century. *Nature.* 1995;377:217–220.

10. Karl TR, Knight RW. Secular trends of precipitation amount, frequency, and intensity in the USA. *Bull Am Meteorol Soc.* 1998;79:231–241.

11. Fowler AM, Hennessey KJ. Potential impacts of global warming on the frequency and magnitude of heavy precipitation. *Natural Hazards.* 1995;11:283–303.

12. Mearns LO, Giorgi F, McDaniel L, Shields C. Analysis of daily variability of precipitation in a nested regional climate model: comparison with observations and doubled CO_2 results. *Global Planetary Change.* 1995;10:55–78.

13. Trenberth KE. Conceptual framework for changes of extremes of the hydrologic cycle with climate change. *Climatic Change.* 1999;42:327–339.

14. US Geological Survey. Available at http://water.usgs.gov. Accessed May 30, 2001.

15. National Climate Data Center. Available at http://www.ncdc.noaa.gov/ol/climate/climatedata.html. Accessed May 30, 2001.

16. *Stat Med.* 1996;15; nos. 7–9.

17. Agresti A. *An Introduction to Categorical Data Analysis.* New York, NY: John Wiley & Sons Inc; 1996.

18. Rose JB, Daeschner S, Easterling DR, Curriero FC, Lele S, Patz JA. Climate and waterborne outbreaks in the U.S.: a preliminary descriptive analysis. *J Am Water Works Assoc.* 2000;92(9):77–87.

19. Frost FJ, Craun GF, Calderon RL. Waterborne disease surveillance. *J Am Water Works Assoc.* 1996;88(9):66–75.

20. Fayer R, Speer CA, Dubey JP. The general biology of *Cryptosporidium.* In: Fayer R, ed. *Cryptosporidium and Cryptosporidiosis.* Boca Raton, Fla: CRC Press Inc; 1997:1–42.

21. Graczyk TK, Evans BM, Shiff CJ, Karreman HJ, Patz JA. Environmental and geographical factors contributing to contamination of watershed with *Cryptosporidium parvum* oocysts. *Environ Res.* 2000;82:263–271.

22. Atherholt TB, LeChevallier MW, Norton WD, Rosen JS. Effect of rainfall on *Giardia* and *Cryptosporidium. J Am Water Works Assoc.* 1998;90(9):66–80.

23. *CCN: Cryptosporidium Capsule Newsletter.* August 1998.

24. LeChevallier MS, Norton WD. *Giardia* and *Cryptosporidium* in raw and finished water. *J Am Water Works Assoc.* 1995;87(9):54–68.

25. Perciasepe R. *Combined Sewer Overflows: Where Are We Four Years After Adoption of the CSO Control Policy?* Washington, DC: Office of Wastewater Management, Environmental Protection Agency; 1998.

26. Rose JB, Simonds J. *King County Water Quality Assessment: Assessment of Public Health Impacts Associated With Pathogens and Combined Sewer Overflows.* Seattle, Wash: Water and Land Resources Division, Department of Natural Resources; 1998.

27. Harvell CD, Kim K, Burkholder JM, et al. Emerging marine diseases: climate links and anthropogenic factors. *Science.* 1999;285:1505–1510.

28. Lipp EK, Rose JB, Vincent R, Kurz RC, Rodriquez-Palacios C. *Assessment of the Microbiological Water Quality of Charlotte Harbor, Florida.* Tampa: Southwest Florida Water Management District; 1999.

29. Fisher GT, Katz BG. *Urban Stormwater Runoff: Selected Background Information and Techniques for Problem Assessment With a Baltimore, Maryland, Case Study.* Reston, Va: US Geological Survey; 1988.

30. Morris RD, Naumova EN, Levin R, Munasinghe RL. Temporal variation in drinking water turbidity and diagnosed gastroenteritis in Milwaukee. *Am J Public Health.* 1996;86:237–239.

31. Schwartz J, Levin R, Hodge K. Drinking water turbidity and pediatric hospital use for gastrointestinal illness in Philadelphia. *Epidemiology.* 1997;8:615–620.

ENSO and cholera: A nonstationary link related to climate change?

Xavier Rodó*, Mercedes Pascual[†‡], George Fuchs[§¶], and A. S. G. Faruque[§]

*Climate Research Group, Center of Meteorology and Climatology, Barcelona Science Park, University of Barcelona, c/Baldiri Reixach, 4-6, Catalunya, 08028 Barcelona, Spain; [†]Department of Ecology and Evolutionary Biology, University of Michigan, Ann Arbor, MI 48109; and [§]International Center for Diarrhoeal Disease Research, Dhaka 1000, Bangladesh

Edited by Simon A. Levin, Princeton University, Princeton, NJ, and approved July 8, 2002 (received for review April 5, 2002)

We present here quantitative evidence for an increased role of interannual climate variability on the temporal dynamics of an infectious disease. The evidence is based on time-series analyses of the relationship between El Niño/Southern Oscillation (ENSO) and cholera prevalence in Bangladesh (formerly Bengal) during two different time periods. A strong and consistent signature of ENSO is apparent in the last two decades (1980–2001), while it is weaker and eventually uncorrelated during the first parts of the last century (1893–1920 and 1920–1940, respectively). Concomitant with these changes, the Southern Oscillation Index (SOI) undergoes shifts in its frequency spectrum. These changes include an intensification of the approximately 4-yr cycle during the recent interval as a response to the well documented Pacific basin regime shift of 1976. This change in remote ENSO modulation alone can only partially serve to substantiate the differences observed in cholera. Regional or basin-wide changes possibly linked to global warming must be invoked that seem to facilitate ENSO transmission. For the recent cholera series and during specific time intervals corresponding to local maxima in ENSO, this climate phenomenon accounts for over 70% of disease variance. This strong association is discontinuous in time and can only be captured with a technique designed to isolate transient couplings.

A main issue at the center of the current debate on climate change is the impact that any anthropogenic-induced changes will have on human society (1, 2). Of considerable importance among these impacts are those affecting human health, particularly the spread and intensification of water-born (1, 3–7) and vector-born diseases (1, 8, 9). A central difficulty that precludes quantitative assessment of these impacts arises from the lack of studies comparing past and present dynamics of infectious diseases over sufficiently long time periods relevant to climate change. For endemic diseases with a long history, such as cholera in Bangladesh, the existence of historical records and on-going surveillance programs make such a comparison possible. Studies of climate and disease so far have been limited to two main areas: the exploration of links between temporal patterns of disease and the interannual variability of climate, mainly El Niño/Southern Oscillation (ENSO; e.g., ref. 7), and the building of scenarios for the geographical spread of disease with climate change (e.g., refs. 10 and 11). The former addresses only interannual variability; it does not address long-term change. Thus, for endemic diseases such as cholera, one key question has been overlooked. Has the interannual variability of climate become a stronger driver of disease dynamics in recent decades? Currently, there is considerable interest in the consequences of climate change for the interannual variability of climate itself, particularly for ENSO and associated phenomena (12). In this context, the question of a nonstationary link between climate variability and disease dynamics is central to address the effect of climate change.

We provide here evidence for a change in the association of cholera dynamics and ENSO from the first to the last decades of the 20th century. Previous results support a role of ENSO in cholera dynamics in the past 2 decades in the Indian subcontinent, specifically in Bangladesh (7). Historical data for cholera in former Bengal allow us to compare here past and present patterns of disease prevalence and their relationship to climate variability.

Methods and Data

We will use a variety of techniques to demonstrate a strong and consistent association between cholera levels and ENSO in the past 2 decades, which is initially more irregular in the earlier time period and then absent from the historical record. Singular spectrum analysis (SSA; *Appendix*) is first applied to isolate the main interannual variability in the data. To determine the frequencies present in these interannual patterns, the power spectra of the reconstructed time series are obtained with the maximum entropy method (MEM; ref. 13). Comparison of the dominant frequencies supports an intensification of the role of climate variability from past to present. The original time series are then analyzed to quantify the strength of the association between cholera and ENSO with a method specifically developed to identify transient couplings (ref. 14; *Appendix*). The strong recent coupling is discontinuous in time, occurring during intervals of local maxima in ENSO. Results are interpreted in light of the reported variation in regional climate in the past decades.

The data for the historical period (hereafter referred to as past) consist of monthly cholera mortality for the district of Dhaka in former Bengal from 1893 to 1940 (15, 16). The mortality data were normalized to a constant fraction of the population (mortality per thousand) based on population censuses for Bengal available every 10 yr (from 1891 to 1941), with population numbers between censuses interpolated linearly. The data for the recent period (hereafter referred as present) were obtained by the ICDDR (International Center for Diarrhoeal Disease Research, Bangladesh) in Dhaka from a systematic subsample of all patients visiting their hospital. The selection of patients for cholera testing, which includes both inpatients and outpatients, is carried out randomly and not on the basis of diarrhoeal symptoms. The percentage tested that is infected with cholera is reported monthly from 1980–2001 (see Fig. 1 and *Appendix*). The Southern Oscillation Index (SOI) series covers the same time intervals as for cholera (17, 18).

Results

SSA was applied to each of the four time series with seasonality removed to isolate the dominant interannual variation in the dynamics (19–21). Fig. 2 shows the temporal evolution of the resulting reconstructions (RCs) corresponding to the first four eigenvalues. A more prominent quasiquadrennial cycle (a period of

This paper was submitted directly (Track II) to the PNAS office.

Abbreviations: ENSO, El Niño/Southern Oscillation; SOI, Southern Oscillation Index; SSA, singular spectrum analysis; SDC, scale-dependent correlation.

See commentary on page 12506.

[‡]To whom reprint requests should be addressed at: Department of Ecology and Evolutionary Biology, University of Michigan, 830 North University Avenue, Ann Arbor, MI 48109-1048. E-mail: pascual@umich.edu.

[¶]Present address: Departments of Pediatrics, and Maternal and Child Health, University of Arkansas for Medical Sciences, Little Rock, AR 72205.

NMED - PATZ
REBUTTAL EXHIBIT 6

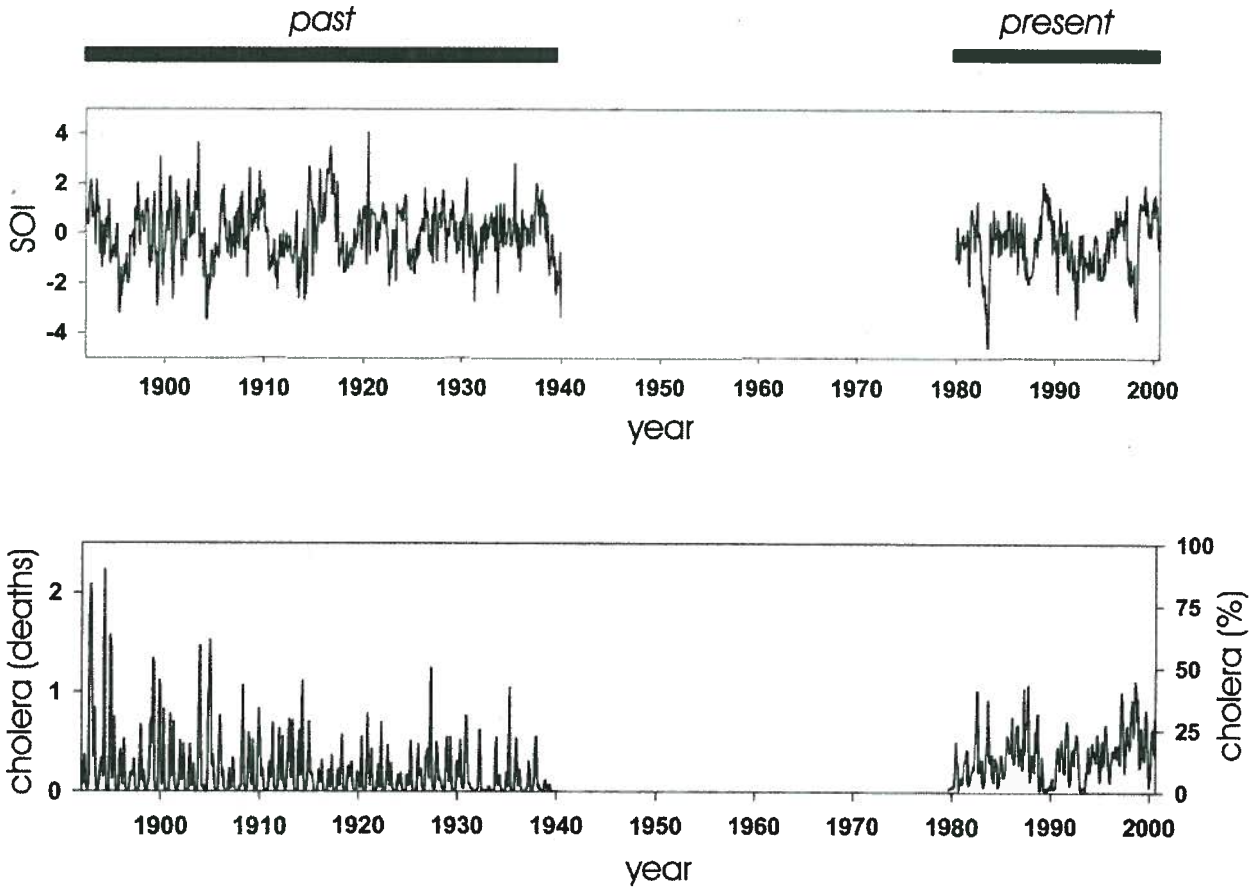

Fig. 1. (*Upper*) Standardized SOI series for the past (1893–1940) and present (1980–2001) periods. Values between 1940 and 1980 are not shown in accordance with the period with no cholera data. (*Lower*) Total cholera deaths (mortality) in Dhaka (Bangladesh) for the historical period 1893–1940, and percentage of cholera cases (cholera morbidity) in the same region for the present period (1980–2001). Scale at left is in mortality per 1,000 individuals and scale at right refers to percentages (see *Methods and Data*).

between 4 and 5 yr) seems to dominate the present portion of both records (Fig. 2; and see also Fig. 4) with a striking correspondence of maxima of cholera to minima of SOI. The past reconstructed dynamics for both cholera and ENSO seem to change in amplitude and in dominant frequencies around 1915–20. Concomitant cycles of opposite phase are not apparent in the past, particularly after

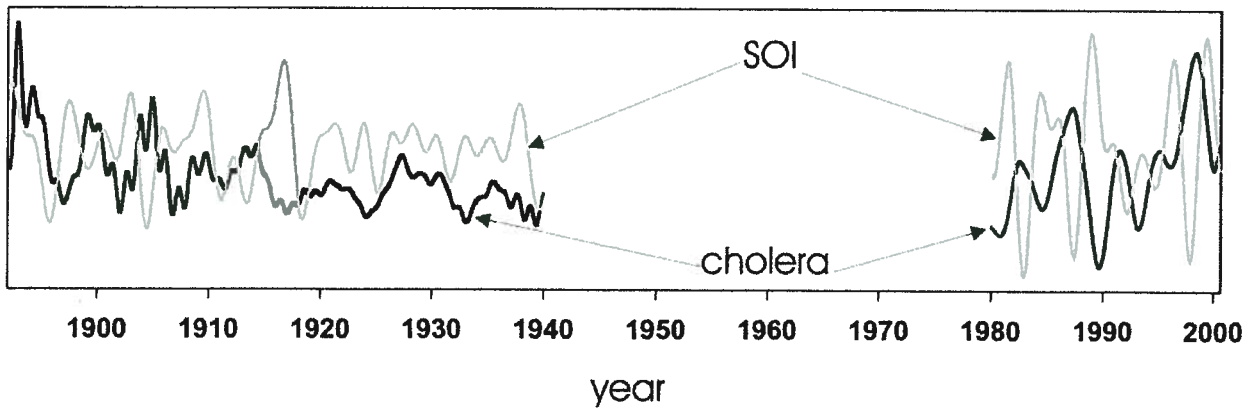

Fig. 2. Reconstructions of the first cluster of eigenvalues detected by SSA (refs. 19 and 20, and *Appendix*) of the cholera and SOI series in Fig. 1. The reconstruction of principal components (PCs) 1 to 4 for cholera is plotted in black, whereas that of PCs 1 to 4 for SOI is shown in gray. In all cases, a window length of 60 months was used for the reconstructions to capture periods of ≈2 and 4 yr (the quasibiennial and quasiquadrennial components, respectively) in both ENSO and cholera.

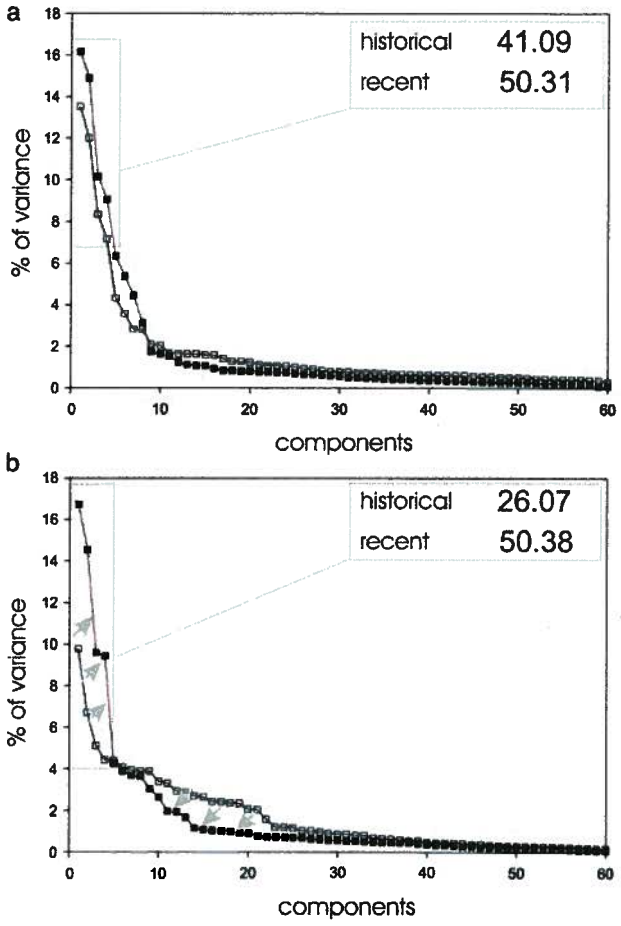

Fig. 3. Variance spectra for the series in Fig. 1. (*a*) SOI. (*b*) Cholera. White and black squares refer to past and present intervals, respectively. The relative variance accounted for by the four reconstructed components of Fig. 2 is shown separately for the historical and present periods in *Inset*. Gray arrows in *b* indicate the changes occurring in the different portions of the spectra. For all analyses, a window length of 60 months was selected to be able to isolate the typical temporal scales of El Niño.

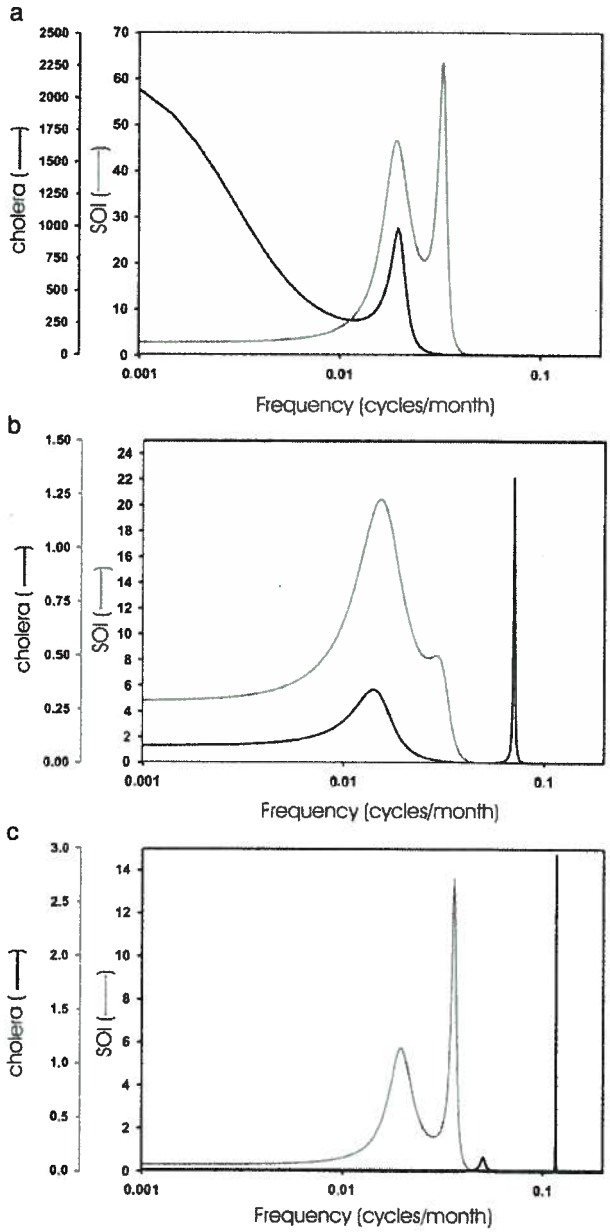

Fig. 4. Frequency spectra computed for the reconstructed time series of cholera and SOI of Fig. 2, for the present (*a*) and past divided into two periods, 1893–1920 (*b*) and 1920–1940 (*c*). The frequency spectra were obtained with the MEM. During the last 2 decades, a quasiquadrennial cycle is present for both ENSO and cholera which closely matches in frequency (*a*). This correspondence is also seen for the first part of the historical record (*b*: main period at 6.5 yr) but disappears with no clear dominant frequency in the interannual variability of cholera in the later part (*c*). The spectrum of SOI for the present shows a more important contribution of the 4–5 yr range. This part of the spectrum weakens around 1920 (*c*). (For consistency, results were crosschecked with those from the multitaper method spectrum analysis).

1915–1920 with a few exceptions in the earlier part of the record around 1899 and 1905, and perhaps also 1912. Examination of the variance spectrum for the SSA decomposition and of the frequency spectrum for the reconstructed time series allow us to examine these observations quantitatively.

Comparison of the SSA variance spectra between past and present shows a substantial increase in the relative weight of the four eigenvalues accounting for the dominant interannual variability of cholera (from 26% to 50%, Fig. 3*b*). There is also an increase for SOI in the contribution of the dominant eigenvalues, although it is a more moderate one (from 41% to 50%, Fig. 3*a*). As typically observed for nonlinear signals, three different portions in the variance spectrum can be consistently isolated: (*i*) a group of dominant and significant eigenvalues; (*ii*) an intermediate slope; and finally (*iii*) a noise floor (Fig. 3*b*). These regions are interpreted as corresponding to (*i*) the deterministic variability generated by internal processes and/or extrinsic forcing, which contains the main oscillatory components; (*ii*) the nonlinear interactions between the former; and finally (*iii*) the unpredictable part of the signal undistinguishable from noise (22). For cholera, there is both a substantial increase in the relative importance of the first part of the spectrum as well as a noticeable decrease in the contribution of the middle region, from past to present (Fig. 3*b*). Based on the comparison below of the dominant frequencies present in the reconstructed time series, we interpret these changes as the result of a more prominent role of climate forcing by ENSO in the present.

Fig. 4 shows the frequency spectra for the reconstructed time

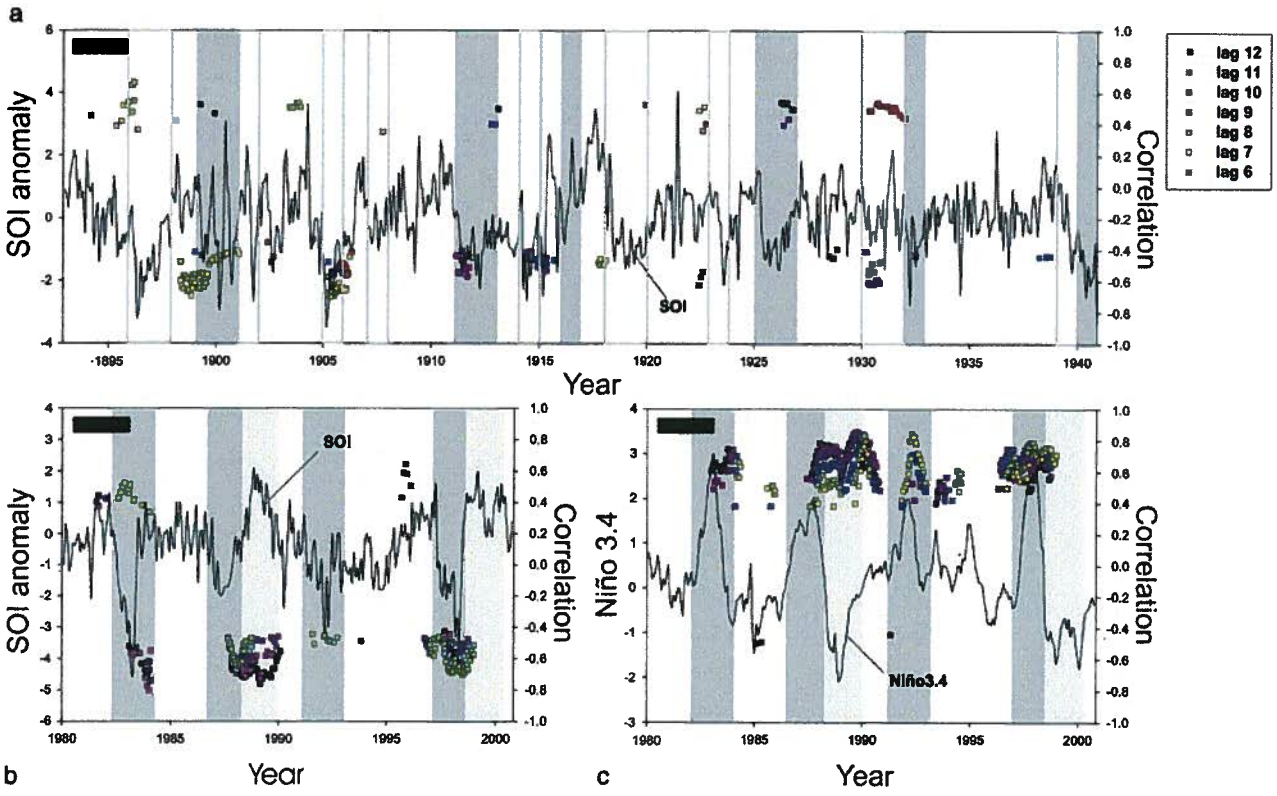

Fig. 5. Results of the SDC analysis (14) for both the historical or past period (*a*) and the present interval (*b* and *c*). SDC analysis computes all possible correlations between fragments of a given size for all locations in the two series. Several window sizes were inspected in intermediate plots (not shown) for each analysis, namely S = 200, S = 100, and S = 25. The window S = 25 was chosen as a scale that produces the highest local correlations. This fragment size appears as a black bar in the top-left corner of each graph. Significant correlations are represented by points anchored in the central value of the fragment size (S) that has been used to calculate correlations. In this figure, the ENSO time series (SOI or Niño 3.4) is used as the reference data set to display the location of significant correlations. The colors of the dots correspond to different time lags for the location of the respective fragment in the cholera data set, with cholera lagging SOI in *b* or Niño 3.4 in *c*. Significance levels are $P < 0.01$ for all points in the graph, and $P < 0.00001$ for the overall SDC pattern (14). Boxes refer to strong–very strong El Niño (dark boxes), strong–very strong La Niña (light-gray boxes), and moderate ENSO episodes (white boxes). Episodes were classified according to standardized terminology, both for the historical ENSO period (39) and for the recent interval (40). The analysis identifies isolated episodes of covariation and quantifies the corresponding local contribution to the overall variance. Local correlations in the four EN episodes attain values up to a maximum of $r(-8 \text{ months})_{xy} = 0.84$ ($P < 0.0001$) in the EN of 1991. The highest values for the La Niña of 1988 are $r(-11 \text{ months})_{xy} = 0.86$ ($P < 0.0001$). Thus, ENSO accounts for over 70% of total variability in the recent cholera series during transient intervals of association. These intervals overlap with the timing of the highest cholera cases. Outside these intervals, the two dynamics decouple, with correlation values close to zero. Comparison among results obtained with both SOI and Niño 3.4 indicate the superior utility of oceanic conditions in the tropical Pacific as remote predictors for cholera (*c*). Values attained are slightly higher for Niño 3.4, and the clusters associated to each episode are formed by many more correlations than when calculated with the SOI. Because of the quality of historical SST records in the Niño region, only sea-level pressures (or SOI) were considered for that period. Correlations with Niño 3.4 are able to capture peaks in cholera for the complex 1991–1994 episode, an episode otherwise insensitive to SOI analyses. An ENSO signature clearly dominates the recent cholera series, whereas it is more inconsistent and then largely absent from first and second parts of the historical record, respectively. (See *Appendix* and ref. 14 for further details on the method).

series. Dominant frequencies correspond to peaks in these spectra. For both variables, the frequency spectra show changes over time but demonstrate that the interannual variability of present cholera, a cycle of ≈4- to 5-yr periodicity, matches clearly the dominant frequency of SOI (Fig. 4*a*). For the past, the data were analyzed both for the whole time series and for the first and second parts separately to examine possible changes before and after 1915–1920. Results show that, for the first part of the historical record, a peak of ≈6.5 yr is present for both cholera and SOI (Fig. 4*b*). This correspondence breaks down, however, when for SOI, the contribution of this component weakens in the second part of the record (Fig. 4*c*). These changes in the frequency spectrum of SOI are consistent with those described for ENSO in the literature (23). These results support a nonstationary relationship between cholera in Dhaka and ENSO, with climate variability acting as a strong driver of disease dynamics in recent times.

To examine this possibility further, we analyzed the original data with a method that specifically quantifies the strength of the association between variables and does so locally in time. This property of scale-dependent correlation (SDC) analysis (14) is important because reported linear correlations between disease dynamics and climate variability, which average over the whole record, are typically low (7). Two possible reasons arise: either climatic variables are weak drivers and the dynamics of disease are influenced by myriad other factors, or they are strong drivers but in a nonlinear fashion acting only during specific intervals of time corresponding to extreme events. The latter implies a discontinuous association between variables that is not properly addressed by standard statistical techniques but is detected by SDC analysis, a time series method specifically developed to isolate transient signals (14).

Fig. 5 shows the results of the analysis applied to past and present intervals. These results show again sharp contrasts between past and present, with evidence for a stronger and more consistent association between variables in recent times. SDC analysis essen-

tially obtains correlation values locally in time by computing and determining the significance of correlation coefficients in windows of a given size along the two records and for a given time lag between the variables (14). In Fig. 5, only local correlation values significant at the 0.01 level are reported and shown with respect to the position of the time window for the ENSO index. For the historical records, the pattern of significant correlations is sparse and highly irregular, with few correlations significant at $P < 0.01$. The distributions of these correlations in time show no consistent regular aggregation with respect to SOI maxima or minima. Only in the first part of the historical data, small clusters of negative correlations barely comparable to present ones are apparent for two of these clusters and weaker otherwise (Fig. 5*a*). In the present, significant and typically higher correlations (often as high as 0.9, with a maximum for the La Niña of 1988–89) are obtained for the recent records, but they are discontinuous in time (Fig. 5 *b* and *c*). The times of such high correlations cluster and coincide with both warm and cold phases of ENSO, as shown by superimposing on the figure an alternating banded pattern for the reported El Niño and La Niña episodes identified since 1980. A delay ranging from +7 to +12 months between the peaks (whether positive or negative) in ENSO and the maximum correlation with cholera is apparent from Fig. 5 *b* and *c*). In addition, all groups of correlations are of the same sign, negative for SOI (Fig. 5*b*) and positive for Niño 3.4 (Fig. 5*c*), indicating an increase/decrease in cholera after warm/cold ENSO events, respectively. In the present, however, no association persists between cholera and ENSO for intervals among peaks. The coupling between cholera and ENSO is, therefore, strong but transient, occurring only during specific intervals of time corresponding to extreme events (Fig. 5 *b* and *c*). This on–off relationship may result from a threshold above which the influence of climate on disease dynamics is activated. This finding explains the low and uninformative value of the linear correlation between variables that is obtained by averaging over periods of coupling and decoupling (a maximum of $r = +0.29$ at a lag of 10 months for the present record).

Discussion

An intensification of the role of ENSO in cholera dynamics must be interpreted in light of the known changes of ENSO itself in the past decades and ultimately tied to variation in regional climate to provide a mechanistic explanation. The ENSO system is the primary driver of interannual variability in global climate, but its long-term behavior is poorly understood. Instrumental observations reveal a shift in 1976, unique in this past century, toward an intensified hydrologic cycle under doubled CO_2 scenarios (24) and warmer and wetter conditions in the tropical Pacific, with widespread climatic and ecological consequences. It is further recognized that the recent changes in the influence of El Niño in the subtropics are closely related to this shift in ENSO, with a tendency toward warmer events since the late 1970s and the appearance of occasional episodes of prolonged warm anomalies such as the one in the early 1990s. From the 1980s onwards, there has been a noticeable increase in the variance of ENSO, with a strong amplification in its quasiquadrennial component (Fig. 2) relative to other periods in the record for which the quasibiennial component is dominant (25).

At a regional level, it has been documented that changes in the ENSO quasiquadrennial component of the last 3 decades occur in coincidence with a southeastward shift in the Walker circulation anomalies (26). This period also coincides with record high global mean temperatures (27). From both observations and model simulations, these changes in ENSO are also qualitatively consistent with those expected from increased greenhouse gases in the atmosphere (28), although this subject remains controversial (29–31). Resulting conditions have favored through the local Hadley cell a reduced subsidence over the Indian region and an increase in surface air temperature (SAT; refs. 25 and 32). An additional increase in SAT in Eurasia linked to the global warming trend seems also to contribute to a much greater warming of the Indian subcontinent compared with the adjacent tropical oceans (33). Both ENSO and these global warming effects have contributed to winter (December, January, and February) temperature increases in the Indian region, of between 2 and 3° C in 1981–1997 with regard to 1871–1980 (26). Maxima in temperatures centered over the Tibetan Plateau and more inland areas also could strongly affect the snowpack dynamics in the Himalayas, ultimately altering its interannual retreat–recovery dynamics and affecting the monsoonal flow and the river flood discharge over the lowlands in coastal Bangladesh.

Warming over land in the Indian subcontinent may have noticeable effects on the temperature of water bodies that serve as an environmental habitat and as a vehicle of transmission for the bacterium. Water temperature is known to affect the proliferation of the bacterium (34). Regional correlation maps have shown a significant association of temperature with the recent cholera data for Dhaka (7). Enhanced warming also can affect disease transmission by changing human behavior, with a possible increase in the contact with contaminated water sources under warm conditions immediately before and during the spring, when the first seasonal peak in cholera is typically observed in Dhaka. The effect of more extreme ENSO and global warming conditions of drought and flood, which remain to be examined but are consistent with future global and regional scenarios (35), also might impact sanitation conditions critical to cholera transmission.

Individually or in combination, any of these factors could now underlie a more effective role of climate variability in the dynamics of cholera. A higher mean in the climatology also could facilitate the more frequent attainment of a threshold that, when surpassed, activates an identifiable effect in cholera.

Most observational and modeling evidence points so far to an increase in both the amplitude and variability of ENSO in the years to come under a global warming scenario (36) or, alternatively, as the result of natural variability on decadal or longer time scales (37). The consequences for infectious diseases are only now beginning to be foreseen. Our results support a sustained, and possibly intensified, future role of ENSO in the interannual variability of cholera.

Appendix: Methods and Data

SSA. SSA provides a decomposition of the signal into its significant and noisy parts (19–21). Specifically, SSA decomposes the dynamics of a time series into a (nonlinear) trend, oscillatory components, including those with anharmonic shapes, and noise. Based on principal component analysis, the method yields a set of eigenvalues and eigenvectors from a symmetric covariance matrix. This matrix contains in column j and row i the covariance of the data at lag i-j. It is obtained by first augmenting the time series of interest, say n(t), into a multivariate time series $N(t) = [n(t + 1), n(t + 2), \ldots, n(t + M)]$ where M is called the window length or embedding dimension. The eigenvalues of the covariance matrix quantify the variance associated with each eigenvector and are plotted in decreasing order in the SSA variance spectrum (Fig. 3). The corresponding eigenvectors are known as empirical orthogonal functions or EOFs. Projection of the signal onto the EOFs gives the principal components (PCs). To reconstruct the time series, the EOFs associated with the first group of significant eigenvalues are chosen, and the associated PCs are combined. The reconstructions (RCs) preserve the phase of the time series and produce no loss of information, in the sense that the sum of all individual reconstructed components gives the original time series. SSA has been shown to be well suited for the analysis of short and noisy time series from nonlinear systems (21).

Here, several realizations of SSA were performed for each time series, with varying window length M, to check for consistency in the decomposition obtained. The shape of the eigenspectrum is roughly independent of M in the four cases (for

both cholera and SOI in the past and present intervals), except for historical cholera, which presents slight variations because of its nonstationary character. Monte Carlo tests for red and white noise were used in all cases to assess the significance of the components analyzed with respect to noise realizations (38). The two empirical orthogonal functions (EOFs) in each one of the two leading pairs (EOFs 1 and 2 and EOFs 3 and 4) are in phase quadrature and correspond to a pair of eigenvalues that are approximately equal and have overlapping error bars. Such pairs provide evidence for oscillatory components (32).

SDC Analysis. In SDC analysis (14), correlations are calculated among fragments of a given size (S = length of fragment or window) between the two series and at all locations in both series. The analysis is repeated for different window sizes to identify the intermediate spatial scale that yields the highest correlation values. Local correlations in SDC approach the values of the traditional linear-lag correlation when fragments are comparable in length to the whole series. As S decreases, local patches of higher correlation values typically develop, identifying intervals of stronger association. As S drops below the temporal scale of coupling, local correlations decrease and the patches fragment into random patterns. For a given window size, the significance of specific correlation values between two fragments is evaluated with a randomization test. Surrogate series (random rearrangements of the original data) are first produced by random rearrangements of the original data. SDC uses both an exact randomization procedure, in which all possible rearrangements without repetition are enumerated, and a random sampling of all these possible rearrangements. Specifically, for a given number of data points s, if the required number of permutations (m) is larger than the possible number of surrogates ($m > s!$), SDC generates all of the rearrangements; otherwise, it switches to a sampled randomization test. The null hypothesis of the test states that the observed correlation between two fragments at a given scale is due to chance alone (H_O: $r_O = 0$). Under these conditions, any correlation calculated after a random rearrangement of the elements of one of the segments will be an expected result of H_O. SDC performs m random permutations inside the fragments of the first series ($X_{[i,i+s]}$) and then correlates each rearranged segment with the second series ($Y_{[j,j+s]}$) to yield the reference distribution under the null hypothesis. This distribution is then used to calculate the probability of the observed correlation, $P(r_O)$. Because we are interested in all of the significant correlations, SDC performs different one-tailed tests depending on the sign. When r_O is significant [with $P(r_O) < \alpha$ for the selected significance threshold α], SDC adds a dot in the graph (e.g., Fig. 5). Significance is also evaluated for the overall pattern of correlations for all possible locations of fragments in a two-dimensional graph whose pattern is tested against the expectation of a binomial-based null model. In this graph, each point represents the location and intensity of a significant correlation above a threshold value.

Cholera Data. Cholera percentages are used, rather than cholera cases, for the recent period because in the surveillance program, the total number of people tested varied over time (as this number is a fixed percentage of the population visiting the clinic). Thus, percent cases is a better surrogate for real cholera cases in the population at large. However, cholera cases and percent cholera cases are highly correlated ($r_{xy} = +0.93$, $P < 0.001$; Fig. 6, which is published as supporting information on the PNAS web site, www.pnas.org), and the choice of variable does not alter our results. For the past, cholera mortality provides another surrogate for cholera cases, as a large fraction of infected persons died of the disease (16). Our analyses and conclusions are based largely on the temporal patterns of variation (frequencies and timing of events) and covariation within time periods. They do not rely on the direct comparison of absolute values and variances of the cholera data. This observation justifies the use of two different measurements (deaths and percent cases) for cholera levels.

We thank M. A. Rodríguez-Arias and J. A. Morguí for useful discussions, M. J. Bouma for the historical data, and A. P. Dobson for comments on an earlier version of the manuscript. This work was supported by a National Oceanic and Atmospheric Administration grant (Joint Program on Climate Variability and Human Health, with Electric Power Research Institute–National Science Foundation–Environmental Protection Agency–National Aeronautics and Space Administration) and a James S. McDonnell Foundation Centennial fellowship (to M.P.) and by Ramon y Cajal Contract MCYT (to X.R.).

1. Watson, R. T., Zinyowera, M. C. & Moss, R. H. (1998) in *IPCC Special Report on The Regional Impacts of Climate Change: An Assessment of Vulnerability* (Cambridge Univ. Press, Cambridge, U.K.).
2. Huq, S. S. (2001) *Science* **294,** 1617.
3. Colwell, R. R. (1996) *Science* **274,** 2025–2031.
4. World Health Organization (1996) in *Regional Health Report 1996* (W.H.O., Geneva).
5. Brandling-Bennett, A. D. & Pinheiro, F. (1996) *Emerging Infectious Diseases* **2,** 59–61.
6. McCarthy, M. (2001) *Lancet* **357,** 1183.
7. Pascual, M., Rodó, X., Ellner, S., Colwell, R. & Bouma, M. (2000) *Science* **289,** 1766–1769.
8. Martens, W. J., Niessen, L. W., Rotmans, J., Jetten, T. H. & McMichael, A. (1995) *Environ. Health Perspect.* **103,** 458–464.
9. World Health Organization (1996) in *Climate Change and Human Health*, eds. McMichael, A., Haines, A., Slooff, R. & Kovats, S. (W.H.O., Geneva).
10. Jetten, T. H. & Focks, D. A. (1997) *Am. J. Trop. Med. Hyg.* **57,** 285–297.
11. Martens, W. J., Jetten, T. H., Rotmans, J. & Niessen, L. W. (1995) *Global Environ. Change* **5,** 195–209.
12. Hartmann, D. L. (2002) *Science* **295,** 811–812.
13. Childers, D. G., ed. (1978) *Modern Spectrum Analysis* (IEEE, New York).
14. Rodó, X. (2001) *Clim. Dyn.* **18,** 203–217.
15. Sanitary Commissioner for Bengal Reports (yearly) *Bengal Public Health Reports, 1891–1942* (Bengal Secretariat, Calcutta and Bengal Government, Alipore).
16. Bouma, M. J. & Pascual, M. (2001) *Hydrobiologia* **460,** 147–156.
17. Ropelewski, C. F. & Jones, P. D. (1987) *Mon. Wea. Rev.* **115,** 2161–2165.
18. Allan, R. J., Nicholls, N., Jones, P. D. & Butterworth, I. J. (1991) *J. Clim.* **4,** 743–749.
19. Broomhead, D. S. & King, G. (1986) *Physica D* **20,** 217–236.
20. Vautard, R. & Ghil, M. (1989) *Physica D* **35,** 395–424.
21. Vautard, R., Yiou, P. & Ghil, M. (1992) *Physica D* **58,** 95–126.
22. Yiou, P., Ghil, M., Jouzel, J., Paillard, D. & Vautard, R. (1994) *Clim. Dyn.* **9,** 371–389.
23. Torrence, C. & Compo, G. P. (1998) *Bull. Am. Met. Soc.* **79,** 61–78.
24. Graham, N. E. (1994) *Simulation of Recent Global Temperature Trends* (Scripps Institute for Oceanography), No. 9425.
25. Webster, P. J., Magana, V. O., Palmer, T. N., Shukla, J., Tomas, R. A., Yanai, M. & Yasunari, T. (1998) *J. Geophys. Res.* **103,** 14451–14510.
26. Kumar, K. K., Rajagopalan, B. & Cane, M. A. (1999) *Science* **284,** 2156–2159.
27. Shrestha, A. B., Wake, C., Dibb, J. & Mayewski, P. (2000) *Int. J. Clim.* **20,** 317–327.
28. Dai, A., Trenberth, K. & Karl, T. (1998) *Geophys. Res. Lett.* **25,** 3367–3370.
29. Urban, F. E., Cole, J. & Overpeck, J. (2000) *Nature (London)* **407,** 989–993.
30. Trenberth, K. & Hoar, T. (1996) *Geophys. Res. Lett.* **23,** 57–60.
31. Knutson, T. R. & Manabe, S. (1998) *J. Clim.* **11,** 2273–2296.
32. Klein, S. A., Soden, B. J. & Lau, N.-C. (1999) *J. Clim.* **12,** 917–932.
33. Meehl, G. A. & Washington, W. M. (1996) *Nature (London)* **382,** 56–60.
34. Singleton, F. L., Atwell, R. W., Jangi, M. S. & Colwell, R. R. (1984) *Appl. Environ. Microbiol.* **44,** 1047–1058.
35. Houghton, J. T., Ding, Y., Griggs, D. J., Noguer, M., van der Linden, P. J. & Xiaosu, D., eds. (2001) *Climate Change 2001: The Scientific Basis* (Cambridge Univ. Press, Cambridge, U.K.).
36. Timmermann, A. (1999) *Nature (London)* **398,** 694–697.
37. Chen, J., Carlson, B. E. & DelGenio, A. D. (2002) *Science* **295,** 838–841.
38. Dettinger, M. D., Ghil, M., Strong, C. M., Weibel, W. & Yiou, P. (1995) *EOS Trans. Am. Geophys. Union* **76,** 12–21.
39. Quinn, W. H., Neal, V. & Mayolo, S. E. (1987) *J. Geophys. Res.* **92,** 14.449–14.461.
40. Smith, C. A. & Sardeshmukh, P. (2000) *Int. J. Clim.* **20,** 1543–1557.

Climate Change and Waterborne Disease Risk in the Great Lakes Region of the U.S.

Jonathan A. Patz, MD, MPH, Stephen J. Vavrus, PhD, Christopher K. Uejio, MA, Sandra L. McLellan, PhD

Abstract: Extremes of the hydrologic cycle will accompany global warming, causing precipitation intensity to increase, particularly in middle and high latitudes. During the twentieth century, the frequency of major storms has already increased, and the total precipitation increase over this time period has primarily come from the greater number of heavy events. The Great Lakes region is projected to experience a rise these extreme precipitation events.

For southern Wisconsin, the precipitation rate of the 10 wettest days was simulated using a suite of seven global climate models from the UN Intergovernmental Panel on Climate Change (IPCC) Fourth Assessment Report. For each ranking, the precipitation rate of these very heavy events increases in the future. Overall, the models project that extreme precipitation events will become 10% to 40% stronger in southern Wisconsin, resulting in greater potential for flooding, and for the waterborne diseases that often accompany high discharge into Lake Michigan.

Using 6.4 cm (2.5 in) of daily precipitation as the threshold for initiating combined sewer overflow into Lake Michigan, the frequency of these events is expected to rise by 50% to 120% by the end of this century. The combination of future thermal and hydrologic changes may affect the usability of recreational beaches. Chicago beach closures are dependent on the magnitude of recent precipitation (within the past 24 hours), lake temperature, and lake stage. Projected increases in heavy rainfall, warmer lake waters, and lowered lake levels would all be expected to contribute to beach contamination in the future.

The Great Lakes serve as a drinking water source for more than 40 million people. Ongoing studies and past events illustrate a strong connection between rain events and the amount of pollutants entering the Great Lakes. Extreme precipitation under global warming projections may overwhelm the combined sewer systems and lead to overflow events that can threaten both human health and recreation in the region.
(Am J Prev Med 2008;35(5):451–458) © 2008 American Journal of Preventive Medicine

Background

Climate Change and Hydrologic Extremes

Global climate change is expected to cause warming temperatures, sea-level rise, and a change in frequency of extremes of the hydrologic cycle (more floods and droughts). This study focuses on the health implications of heavy precipitation, with an in-depth look at related health risks in the U.S. Such heavy precipitation events often result in substantial societal impacts, including an increased risk of waterborne disease outbreaks. Heavy precipitation can lead to stormwater discharge of contaminants into water bodies if the volume exceeds the containment capacity. The seasonal contamination of surface water in early spring in North America and Europe may explain some of the seasonality in sporadic cases of many types of waterborne diseases. According to the North American chapter of the most recent IPCC report,[1] heavy precipitation events are expected to increase under climate change scenarios (Figure 1).

Rainfall Projections for the Great Lakes Region

For the Great Lakes region of the U.S., contamination events typically occur when daily rainfall levels exceed a threshold of about 5–6 cm (2–2.5 in).[2,3] Given that rainfall extremes are expressions of climate, there is heightened concern as to how this type of event might change in a warmer future climate.

From the Center for Sustainability and the Global Environment (SAGE), Department of Population Health Sciences, University of Wisconsin-Madison, Madison, Wisconsin

Address correspondence and reprint requests to: Jonathan Patz, MD, MPH, Center for Sustainability and the Global Environment, University of Wisconsin-Madison, 1710 University Avenue, Room 258, Madison WI 53726. E-mail: patz@wisc.edu.

NMED - PATZ
REBUTTAL EXHIBIT 7

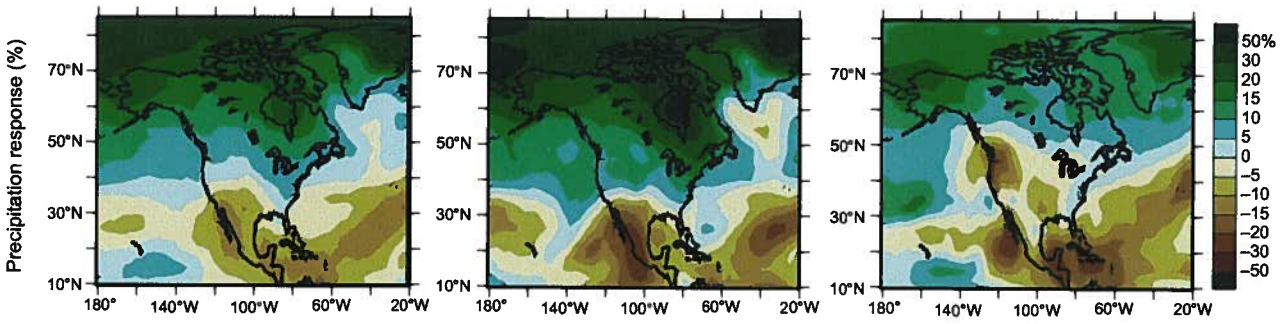

Figure 1. Projected changes in total precipitation from the late twentieth to the late twenty-first centuries, based on middle-of-the-road increases in greenhouse gases: annual (left), winter (center), and summer (right). Source: IPCC, 2007[1]

Meteorologic theory indicates that the intensity of a precipitation event is regulated primarily by the local amount of moisture in the atmosphere during a storm and that the moisture-holding capacity of the atmosphere increases exponentially with temperature.[4] Consequently, expectations are high that more intense precipitation will accompany global warming. This possibility is supported by many modeling studies that have simulated the climatic response to increasing concentrations of greenhouse gases.[5–8] Precipitation intensity (total precipitation divided by the number of wet days) is projected to increase almost everywhere, particularly in middle and high latitudes where average precipitation is also expected to increase.[9] Most of the Great Lakes region is projected to experience a rise in both average and extreme precipitation events.[1,10]

These anticipated future changes are consistent with recent trends over the U.S., including the Great Lakes area. Major storms have been occurring with greater frequency during the twentieth century, and the total precipitation increase over this period has resulted disproportionately from the increase in heavy events.[11–13] This trend has been accentuated by the increase in heavy events toward the end of the century, the time of most pronounced global warming.[14,15]

These large-scale findings were tailored to the Wisconsin–Chicago region, where we are conducting research on the health impacts of extreme events. In one example, the recent and future simulated precipitation rate of the 10 wettest days were computed for the Madison WI area from seven global climate models (GCMs) used in the UN Intergovernmental Panel on Climate Change (IPCC) Fourth Assessment Report[1] (Figure 2). For each ranking (tenth wettest day to the wettest day), the precipitation rate of these very heavy events increases in the future, and the enhancements are most pronounced for the most extreme events (wettest and second wettest days). Overall, the models project that these extremely heavy precipitation events will become 10% to 40% stronger in southern Wisconsin, resulting in greater potential for flooding and for the waterborne diseases that often accompany high discharge into Lake Michigan.[3]

A somewhat different approach was used to estimate future changes in extreme precipitation over Chicago. For this application, the GCM output from two representative models, the geophysical fluid dynamics laboratory (GFDL) model and the parallel climate model (PCM) was statistically downscaled to provide higher-resolution information. Statistical downscaling uses historical observational data to tailor projections from a global model to a local scale. A statistical relationship is first established between a location's measured precipitation and the corresponding climate model output during a prior time interval, typically around 30 years. This historical relationship—between climate model output at the relatively coarse scale of the GCM and the daily precipitation values recorded on the local scale—is then used to downscale future model projections to the same local scale. This method assumes that

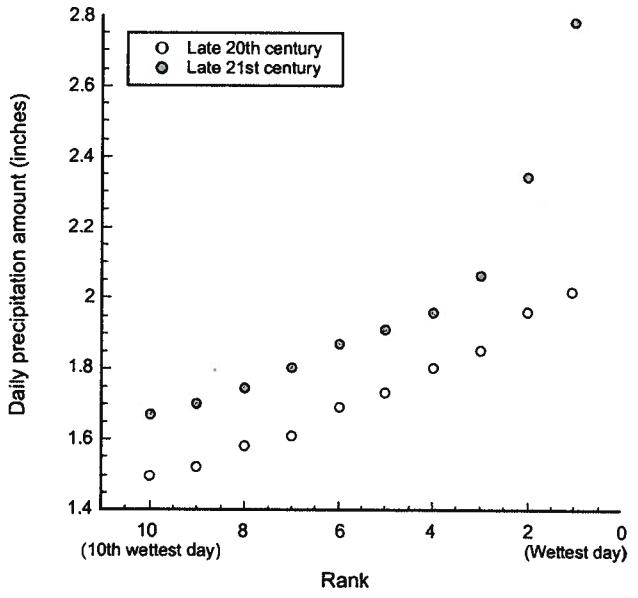

Figure 2. GCM-simulated precipitation amounts in southern Wisconsin for the 10 wettest days in the late twentieth and late twenty-first centuries (10 days total for each century), based on middle-of-the-road projected increases in greenhouse gases.
GCM, global climate model

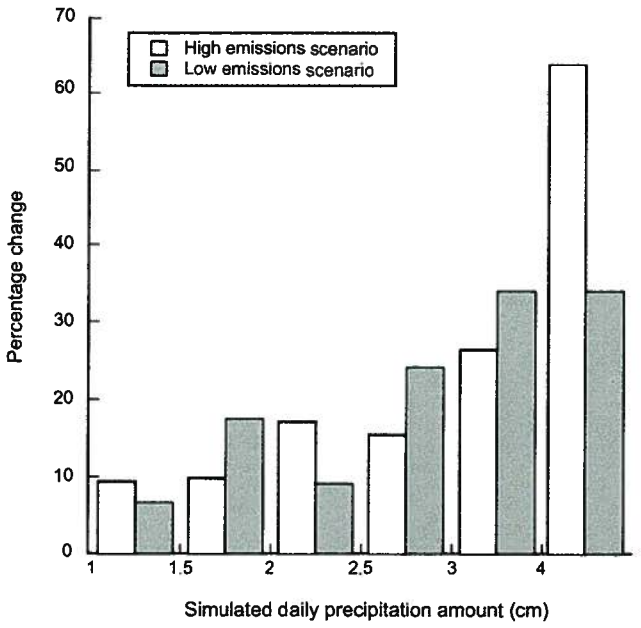

Figure 3. Projected change in the frequency of heavy precipitation in Chicago by the late twenty-first century, based on downscaled climate model output for high-end and low-end greenhouse gas emissions scenarios from two global climate models used in the Chicago Climate Impact Assessment. Source: Hayhoe and Wuebbles[2]

the relationships between large- and small-scale processes remain the same over time.

The change was analyzed in the frequency of heavy daily precipitation events, ranging from 1 to 5 cm (0.4–2.0 in), between the late twentieth and late twenty-first centuries (Figure 3). Although the precise changes are dependent on the assumed greenhouse gas emissions scenario, the results clearly indicate more frequent extreme events, ranging from ≤10% increases for 1–1.5 cm (0.4–0.6 in) events to >60% for the heaviest storms (≥4 cm [≥1.6 in]) in the high-emissions scenario. Using 6.35 cm (2.5 in) of daily precipitation as the threshold for initiating combined sewer overflow into Lake Michigan,[2] the frequency of these events is expected to rise by 50%–120% by the end of this century. This translates into an expected occurrence of about one event every other year in the recent past to approximately one event every year (low-emissions scenario) to 1.2 events every year (high-emissions scenario) by the end of this century.[2]

The expected changes in the hydrologic cycle, including increases in extreme precipitation events, should have a direct bearing on waterborne diseases in the Great Lakes. For example, the 1993 *Cryptosporidium* outbreak in Milwaukee was preceded by the heaviest rainfall in 50 years in the associated watersheds.[16] Summertime bacteria concentrations in an inland lake in Wisconsin (Lake Geneva) exhibit positive, significant correlations not only with mean summertime rainfall but also with the duration between rainfall events, a variable that is expected to increase in the future.[17] The combination of future thermal and hydrologic changes may affect the usability of recreational beaches. Chicago beach closures are dependent on the magnitude of recent precipitation (within the past 24 hours), lake temperature, and lake stage (i.e., height of the water surface above an established level).[18] Projected increases in heavy rainfall, warmer lake waters, and lowered lake levels[19] would all be expected to enhance beach contamination in the future. Although more extreme rainfalls would seem to contradict the projection of lower lake levels, the latter expectation stems from a large anticipated increase in evaporation at the lake surface (which can offset the precipitation gain) and a higher proportion of future precipitation falling as heavy events, even if the total precipitation amount does not rise.

Vulnerability Factors

Even today, many of our community water systems can be overburdened by extreme rainfall events. Heavy rainfall or snow melt can exceed the capacity of the sewer system or treatment plant, which are designed to discharge the excess wastewater directly into surface water bodies.[20,21] In urban watersheds, more than 60% of the annual loads of all contaminants are transported during storm events.[22] In general, turbidity increases during storm events, and studies have recently shown a correlation between increases in turbidity and illness in communities.[23,24] Also, higher winter temperatures could further enhance flooding from the contribution of snow melt.

Combined Sewage Overflows and Aging Water Infrastructure

Older cities around the nation have combined sewer systems, which are designed to capture both sanitary sewage and stormwater and convey these flows to a wastewater treatment plant. Large rain events can overwhelm these systems, causing untreated sewage mixed with stormwater to be released directly into receiving waters. The U.S. Environmental Protection Agency (EPA) has estimated that 770 communities release more than 3.2 trillion liters (850 billion gallons) of combined sewage to the nation's waterways annually.[25] As infrastructure improvements to sewer system capacity are made, the number of combined sewer overflows can be decreased. For example, the construction of an inline storage system in Milwaukee reduced the number of combined sewer overflows from 40–60 per year to 0–4 per year (with the average approximating 1.5 per year over the past 10 years). However, it remains difficult to capture the most extreme events. Changing weather patterns that bring

more extreme storms to some regions may outpace the infrastructure improvements.

Case Study

Climate and water quality in Milwaukee. The urban environment presents unique risks of water contamination. Runoff from impervious surfaces contains metals, pesticides, pathogens, and fecal indicator bacteria. It has been linked to adverse public health effects.[26–28] In most municipal areas, urban stormwater is conveyed in separated sewer systems and discharged directly into receiving waters. Aging infrastructure may cause sanitary sewage to infiltrate into stormwater pipes, where it is essentially discharged with no treatment. Beaches are often located in urbanized areas and highly susceptible to stormwater impacts.[29–31] Accelerating development of urban coastal areas and changing storm patterns may synergistically increase the amounts of urban stormwater released into coastal systems.

The Milwaukee River Basin consists of 1440 km^2 (556 miles^2) of rural, agricultural, suburban, and urban land use. The basin's watersheds drain to three major rivers that converge in downtown Milwaukee and discharge through a 140 m (0.09 mile) channel leading to Lake Michigan. Following storm events, the fecal indicator bacteria *Escherichia coli* can be detected in the channel at levels as high as 2000–7000 colony forming units (CFU)/100 ml. These levels are 10 times higher than the EPA-recommended limit for recreational waters.[32] The presence of *E. coli* demonstrates that fecal pollution is present; however, given the complexity of this system, the bacteria may come from agricultural runoff, urban stormwater, or sanitary sewage. Human viruses have been detected at this same site following storm events with no reported sewage overflows, providing evidence that sanitary sewage may be continually released into the basins tributaries. Storm events of >3 inches of rainfall within 24 hours may overwhelm the combined sewer systems and lead to an overflow. In this case, the levels of *E. coli* detected in the channel leading to Lake Michigan can be up to 10 times higher (e.g., 20,000–50,000 CFU/100 ml) than when there are no sewage overflows.[3] These events generally occur less than three times per year, and do not occur at all in dry years (Figure 4).

Milwaukee is not unique in terms of its impact on the lake; many cities around the Great Lakes are situated near major rivers that come from a complex mixture of watershed sources. The Great Lakes, which serve as a drinking water source for more than 40 million people, are particularly susceptible to fecal pollution and can become reservoirs for waterborne diseases. Ongoing studies and past events illustrate a strong connection between rain events and the amount of pollutants entering the Great Lakes. The 1993 *Cryptosporidium* outbreak in Milwaukee, which sickened more than

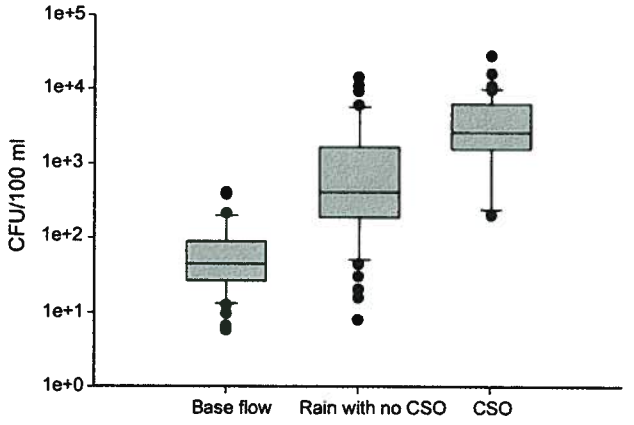

Figure 4. Levels of *E. coli* in the Milwaukee estuary, which discharges to Lake Michigan, 2001–2007, during base flow (n=46); following rain events with no CSO (n=70); and following CSO events (n=54). Boxes indicate 75% of values, with median values drawn in each. Whiskers are 95% of values and outliers are shown as closed circles. There were significant differences in *E. coli* levels following rainfall and CSOs compared to base flow ($p \leq 0.05$).
CFU, colony forming units; CSO, combined sewer overflow

400,000 people, coincided with record high flows in the Milwaukee River, a reflection of the amount of rainfall in the watershed.[16]

Land-Use Patterns

Land cover conversion to impervious surfaces (such as roadways and parking lots) increases both the volume and velocity of stormwater runoff, while also reducing groundwater infiltration.[33] The percentage of impervious surface within a watershed, for example, explains most of the variability for indicator bacteria across watersheds.[34] Bacteria levels also tend to be elevated in agricultural catchments with higher levels of grazing cattle and sheep.[35] Zoning and development policies can be a strong influence on the amount of impervious surface within each municipality.[36]

Pathways of Human Exposure

Drinking Water

Waterborne disease outbreaks stemming from drinking water source contamination require a combination of determining factors. The requirements include: contamination of the source water, transport of the contaminant to the water intake or well of the drinking water system, insufficient treatment to reduce the level of contamination, and exposure to the contaminant.

Recontamination of treated water may also occur at the public or homeowner's distribution system level.[37]

Waterborne disease outbreaks from all causes in the U.S. are distinctly seasonal, clustered in key watersheds, and associated with heavy precipitation.[16] In Walkerton, Ontario, in May 2000, heavy precipitation com-

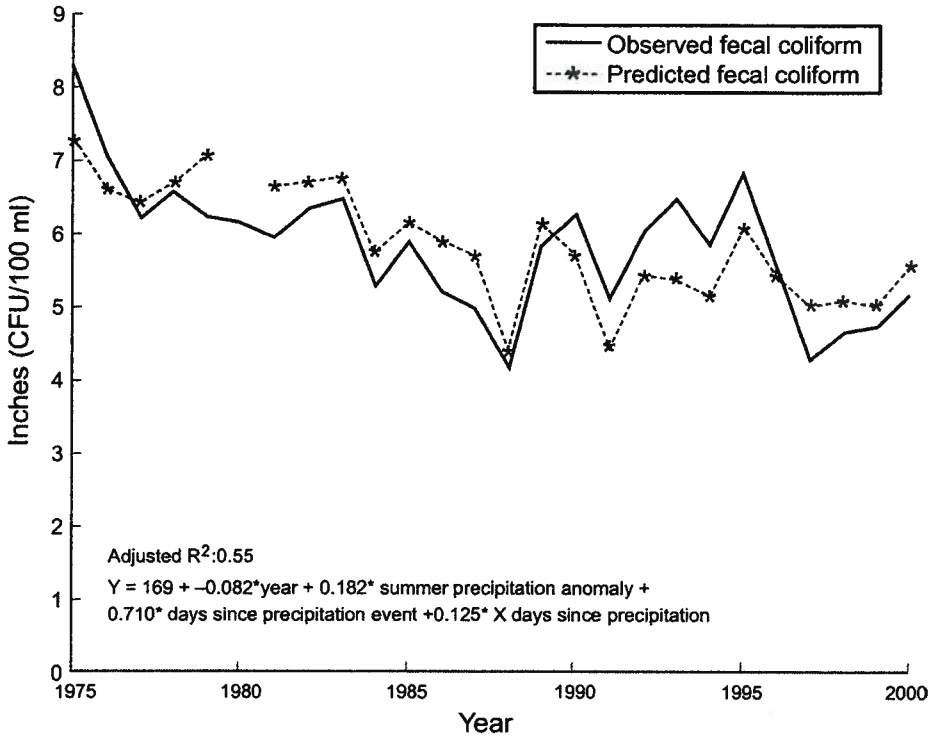

Figure 5. Relationship between rainfall and beach contamination, Lake Geneva, Wisconsin
CFU, colony-forming units

bined with failing infrastructure contaminated drinking water with *E. coli* 0157:H7 and *Campylobacter jejuni*, resulting in an estimated 2300 illnesses and seven deaths.[38]

Recreational Water and Stormwater Issues

Heavy runoff after severe rainfall can also contaminate recreational waters and increase the risk of human illness[39] through higher bacterial counts. This association is strongest at beaches closest to rivers.[40] Ear, nose, and throat; respiratory; and gastrointestinal illnesses are commonly associated with recreational swimming in fresh and oceanic waters. Less abundant and potentially more severe waterborne diseases such as hepatitis, giardiasis, cryptosporidiosis, and toxic algal blooms pose serious health threats to vulnerable human populations and local wildlife. Swimmers have an elevated risk of contracting gastrointestinal illnesses versus nonswimmers, and this risk generally increases with prolonged exposure.[41] Frequent water users, such as lifeguards or recreational enthusiasts, are at risk for waterborne disease, and young children, the elderly, pregnant women, and the immunocompromised have the greatest risk of suffering serious complications.[41,42] Macrodemographic trends toward an older and more immunocompromised U.S. population suggest that vulnerability to waterborne pathogens will continue to increase.

Precipitation events and subsequent runoff may flush pathogens and indicator bacteria directly into water bodies and overwhelm or decrease the efficiency of the sewage disposal infrastructure. Although pathogens tend to co-occur with indicator bacteria, indicators are prone to false positive readings. Indicator bacteria may survive in soil sediments or beach sand, become re-suspended during a precipitation event, and confound estimates of waterborne disease risk.[30,43,44] The periodicity and amplitude of contamination events are likely affected by processes that re-suspend or transport pathogens.[45,46] Indicator bacteria are influenced by precipitation events up to a week prior to sample collection although recent precipitation (0–3 days) tends to exhibit the strongest relationships with their numbers.[16] Interval time between rainfall events can increase pollutant accumulation and subsequent loading into water bodies.[18,47] A disproportionately large pollutant mass similarly may be transported with the first precipitation event following the dry season in mid-latitude locations.[48,49] Figure 5 shows an example of rainfall and contamination levels for Lake Geneva WI. Unseasonably high precipitation typically increases indicator bacteria loading into water bodies.[50] Earth system processes like the El Niño Southern Oscillation (ENSO) strongly influence interannual precipitation and therefore must be taken into account, especially for contamination events between September and March.[50–52]

Resulting Waterborne Illnesses

Agents of disease. More than 100 different types of pathogenic bacteria, viruses, and protozoa can be found in contaminated water.[53–55] Many of these have been implicated in a variety of illnesses transmitted by food or water.

Waterborne and foodborne diseases continue to cause significant morbidity in the U.S. In 2002, there were 1330 water-related disease outbreaks,[56] 34 from recreational water and 30 from drinking water.[57,58] In recreational water, bacteria accounted for 32% of outbreaks, parasites (primarily *Cryptosporidium*) for 24%, and viruses for 10%.[57] Bacteria were the most com-

monly identified agent in drinking water (29%, primarily *Campylobacter*) followed by parasites and viruses (each 5%).[58] Gastroenteritis continues to be the primary disease associated with food and water exposure. In 2003 and 2004, gastroenteritis was noted in 48% and 68% of reported recreational and drinking water outbreaks, respectively.[57,58]

Surveillance

Variability of indicator bacteria is controlled by the physical dynamics of each water body, and quality can be inferred from water's chemical and biologic qualities. Prevailing wind direction, toward or away from the beach, modulates biophysical environment and indicator bacteria relationships in large water bodies.[46] Tidal cycles in large water bodies enhance indicator bacteria exchange from subsurface and soil reservoirs.[59,60] Elevated nitrate, ammonium, and caffeine in water quality measurements suggest recent cross-contamination with sewage-like materials.[61,62] Recent advances in molecular detection techniques have developed alternative indicators that are human-specific (e.g., demonstrating sewage inputs) such as human-specific *Bacteroides* spp., *Methanobrevibacter smithii*, and the surface protein gene present in enterococcus (*esp*).[63–65] Precipitation and subsequent runoff events increase nutrient loading into water bodies, potentially enhancing floral productivity and water chlorophyll levels.[46] Indicator bacteria survival is inversely related to water salinity and survival exponentially decreases with the duration and magnitude of solar radiation exposure.[66] Surface water runoff also disturbs and re-suspends sediments, increases water turbidity, decreases solar radiation, and proportionally increases indicator bacteria loading into water bodies.[46]

Conclusion and Recommendations

A broad range of improvements can be made toward attaining safe water quality in the U.S. These include such activities as data collection/surveillance, infrastructure improvements, land use planning, education, and research. Ultimately, better assessment of water quality and risk to the drinking water system from the watershed to the tap, as well as recreational water exposures, will allow for better prevention and controls to limit the impact of contamination events.

Data Collection

Based on the current state of surveillance, better indicators of fecal pollution are required. Public health officials and water managers need especially to be informed about the source of contamination, which could be from farm runoff, stormwater, or sanitary sewage.[67] Progress has been made in the field of microbial source tracking in terms of identifying source-specific alternative indicators, and molecular approaches offer a broader range of target organisms because they are not dependent on culture (for reviews, see Santo Domingo et al.[68] and Savichtcheva and Okabe[69]). These have been used successfully in field studies.[70–72] However, widespread implementation will require extensive validation (including geographic differences), further assay development to reduce cost and complexity of new assay procedures, and standardization for use in public health laboratories.

One of the disadvantages of the current system is that the outbreaks are detected after the fact—that is, after the contamination event and after individuals have become ill. The disease surveillance system is incapable of detecting outbreaks when diagnosed cases are not reported to health departments, such as when mild symptoms are attributed to other causes or when health problems cannot be treated medically. In addition, delays exist in detecting outbreaks because of the time necessary for laboratory testing and reporting of findings. Predictive forecasts of swimming-related health risk currently support beach management decisions at some U.S. coastal oceanic and Great Lakes beaches.[46,73,74] Near-term forecast models require knowledge of the relationships between beach-specific environments and swimming health risks, collected and refined over multiple years of observations. Forecast models tend to have high sensitivity but relatively lower specificity and are therefore prone to false positive predictions of unsafe swimming conditions. Future research should investigate the extent to which dynamic environmental conditions can augment alternative human-specific pathogen indicators.

Infrastructure Improvements

This article has given specific examples of shortcomings in our current water systems. Upgrading sewage/stormwater infrastructure will obviously decrease the incidence of waterborne pathogen pollution.[59,75] For example, ≤20% of childhood bacterial or viral diarrheal illnesses can be attributed to the density of holding tanks and other septic tanks.[76] Improperly managed holding septic tanks discharge untreated sewage and contaminate surface water. Improving infrastructure may further reduce risks of contamination from extreme weather events.

Land use/watershed protection. Watershed protection will continue to be an extremely important factor influencing water quality.[67] Watershed water quality has a direct impact on source water and processed water quality as well as on recreational sites and coastal waters. Better farming practices (to capture and treat agricultural wastes) and surrounding vegetation buffers, along with improved city disposal systems to capture and treat wastes, would reduce the runoff of nutrients, toxic chemicals, trace elements, and micro-

organisms flowing into reservoirs, groundwater, lakes, rivers, estuaries, and coastal zones.

Education and research. According to Rose and others,[67] coordinated monitoring of physical, chemical, and biologic parameters should go toward building databases and integrated models that include environmental, ecologic, and social conditions, consequences, and costs. Collaborative, multidisciplinary training and research—involving health and veterinary professionals, biologists, ecologists, physical scientists, database specialists, modelers, and economists—is required to carry out comprehensive assessments and management plans. Interagency agreements will be needed to coordinate and support this initiative. Testing models and hypotheses based on observed temporal and spatial co-occurrences may help focus research policies. It is essential to better delineate—in time and location—the occurrence of disease and to maintain standardized health databases.

Waterborne diseases remain a major public health problem in the U.S. and around the world. Enhanced understanding of the weather-sensitivity of many waterborne diseases is necessary along with improved surveillance, watershed/source water protection, and educational programs to improve the safety of our water. Scenarios of future global warming accompanied by climatic extremes only increase the importance of these improvements.

The research conducted by Jonathan Patz, Stephen Vavrus, and Christopher Uejio is supported under a grant from the U.S. EPA STAR grants program, grant # R 832752010 entitled Health Risks from Climate Variability and Change in the Upper Midwest: a Place-based Assessment of Climate-related Morbidity. Contributions by Sandra McLellan are supported by NOAA Oceans and Human Health Initiative extramural grant NA05NOS4781243.

No financial disclosures were reported by the authors of this paper.

References

1. Intergovernmental Panel on Climate Change. Climate change 2007: impacts, adaptation and vulnerability. Contribution of Working Group II to the Fourth Assessment Report of the Intergovernmental Panel on Climate Change. Parry ML, Canziani OF, Palutikof JP, van der Linden PJ, Hanson CE, eds. Cambridge UK: Cambridge University Press, 2007. www.ipcc.ch/ipccreports/ar4-wg2.htm.
2. Hayhoe K, Hellmann J, Lesht B, Nadelhoffer K, Wuebbles D. 2008: Climate change and Chicago: projections and potential impacts. An Assessment Prepared for the City of Chicago. In press.
3. McLellan SL, Hollis EJ, Depas MM, Van Dyke M, Harris J, Scopel CO. Distribution and fate of Escherichia coli in Lake Michigan following contamination with urban stormwater and combined sewer overflows. J Great Lakes Res 2007;33:566–80.
4. Trenberth KE. Conceptual framework for changes of extremes of the hydrological cycle with climate change. Clim Change 1999;42:327–39.
5. Barnett DN, Brown SJ, Murphy JM, Sexton DMH, Webb MJ. Quantifying uncertainty in changes in extreme event frequency in response to doubled CO_2 using a large ensemble of GCM simulations. Clim Dynamics 2006;26:489–511.
6. Kharin VV, Zwiers FW. Estimating extremes in transient climate change simulations. J Clim 2005;18:1156–73.
7. Meehl GA, Arblaster JM, Tebaldi C. Understanding future patterns of increased precipitation intensity in climate model simulations. Geophys Res Lett 2005;32:doi:10.1029/2005GL023680.
8. Wilby RL, Wigley TML. Future changes in the distribution of daily precipitation totals across North America. Geophys Res Lett 2002;29: doi:10.1029/2001GL013048.
9. Tebaldi C, Hayhoe K, Arblaster JM, Meehl GA. Going to the extremes. Clim Change 2006;79(3–4):185–211.
10. Diffenbaugh NS, Pal JS, Trapp RJ, Giorgi F. Fine-scale processes regulate the response of extreme events to global climate change. Proc Natl Acad Sci 2005;102:15774–8.
11. Changnon SA, Kunkel KE. Climate-related fluctuations in Midwestern floods during 1921–1985. J Water Resources Plann Manage 1995;121: 326–34.
12. Karl TR, Knight RW. Secular trends of precipitation amount, frequency, and intensity in the United States. Bull Am Meteor Soc 1998;79:231–41.
13. Karl TR, Knight RW, Plummer N. Trends in high-frequency climate variability in the 20th-century. Nature 1995;377:217–20.
14. Groisman PY, Knight RW, Karl TR, Easterling DR, Sun BM, Lawrimore JH. Contemporary changes of the hydrological cycle over the contiguous United States: trends derived from in situ observations. J Hydrometeorology 2004;5:64–85.
15. Kunkel KE, Easterling DR, Redmond K, Hubbard K. Temporal variations of extreme precipitation events in the United States: 1895–2000. Geophys Res Lett 2003;30:doi:10.1029/2003GL018052.
16. Curriero FC, Patz JA, Rose JB, Lele S. The association between extreme precipitation and waterborne disease outbreaks in the United States, 1948–1994. Am J Public Health 2001;91:1194–9.
17. Allen MR, Ingram WJ. Constraints on future changes in climate and the hydrologic cycle. Nature 2002;419:224–32.
18. Olyphant GA, Whitman RL. Elements of a predictive model for determining beach closures on a real time basis: the case of 63rd Street Beach Chicago. Environ Monit Assess 2004;98(1–3):175–90.
19. Kunkel R, Wendland F, Hannappel S, Voigt HJ, Wolter R. The influence of diffuse pollution on groundwater content patterns for the groundwater bodies of Germany. Water Sci Technol 2007;55:97–105.
20. Perciasepe R. Combined sewer overflows: where are we four years after adoption of the CSO control policy? Washington DC: EPA Office of Wastewater Management, 1998.
21. Rose JB, Simonds J. King County water quality assessment: assessment of public health impacts associated with pathogens and combined sewer overflows. Seattle WA: Report for Water and Land Resources Division, Dept of Natural Resources, 1998.
22. Fisher GT, Katz BG. Urban stormwater runoff: selected background information and techniques for problem assessment with a Baltimore Maryland case study. Baltimore MD: U.S. Geological Survey Water-Supply Paper 2347, 1988.
23. Morris RD, Naumova EN, Levin R, Munasinghe RL. Temporal variation in drinking water turbidity and diagnosed gastroenteritis in Milwaukee. Am J Public Health 1996;86:237–9.
24. Schwartz J, Levin R, Hodge K. Drinking water turbidity and pediatric hospital use for gastrointestinal illness in Philadelphia. Epidemiology 1997;8:615–20.
25. U.S. Environmental Protection Agency. Impacts and control of CSOs and SSOs. Washington DC: U.S. Environmental Protection Agency Office of Water, 2004. Report No.: EPA 833-R-04-001.
26. Bannerman RT, Owens DW, Dodds RB, Hornewer NJ. Sources of pollutants in Wisconsin stormwater. Water Sci Technol 1993;28(3–5):241–59.
27. Gaffield SJ, Goo RL, Richards LA, Jackson RJ. Public health effects of inadequately managed stormwater runoff. Am J Public Health 2003;93: 1527–33.
28. Haile RW, Witte JS, Gold M, et al. The health effects of swimming in ocean water contaminated by storm drain runoff. Epidemiology 1999;10:355–63.
29. Scopel CO, Harris J, McLellan SL. Influence of nearshore water dynamics and pollution sources on beach monitoring outcomes at two adjacent Lake Michigan beaches. J Great Lakes Res 2006;32:543–52.
30. Whitman RL, Nevers MB. Foreshore sand as a source of Escherichia coli in nearshore water of a Lake Michigan beach. Appl Environ Microbiol 2003;69:5555–62.
31. Yamahara KM, Layton BA, Santoro AE, Boehm AB. Beach sands along the California coast are diffuse sources of fecal bacteria to coastal waters. Environ Sci Technol 2007;41:4515–21.

32. US Environmental Protection Agency. Improved enumeration methods for recreational water quality indicators: Enterococci and Escherichia coli. Washington DC: US Environmental Protection Agency Office of Water, Office of Science and Technology, 2000. Report No: EPA 821/R-97/004.
33. Arnold CL, Gibbons JC. Impervious surface coverage. J Am Plann Assoc 1996;62:243–58.
34. Mallin MA, Williams KE, Esham EC, Lowe RP. Effect of human development on bacteriological water quality in coastal watersheds. Ecol Appl 2000;10:1047–56.
35. Crowther J, Kay D, Wyer MD. Faecal-indicator concentrations in waters draining lowland pastoral catchments in the UK: relationships with land use and farming practices. Water Res 2002;36:1725–34.
36. Stone B, Bullen JL. Urban form and watershed management: how zoning influences residential stormwater volumes. Environ Plann B Plann Des 2006;33:21–37.
37. Anonymous. Cryptosporidium in water supplies. London: Department of the Environment, Department of Health, 1990.
38. Hrudey SE, Payment P, Huck PM, Gillham RW, Hrudey EJ. A fatal waterborne disease epidemic in Walkerton Ontario: comparison with other waterborne outbreaks in the developed world. Water Sci Technol 2003;47:7–14.
39. Schuster CJ, Ellis A, Robertson WJ, Charron DF, Aramini JJ, Marshall B, Medeiros DT. Infectious disease outbreaks related to drinking water in Canada, 1974–2001. Can J Public Health 2005;96:254–8.
40. Dwight RH, Semenza JC, Baker DB, Olson BH. Association of urban runoff with coastal water quality in Orange County California. Water Environ Res 2002;74:82–90.
41. Wade TJ, Pai N, Eisenberg JN, Colford JM, Jr. Do U.S. Environmental Protection Agency water quality guidelines for recreational waters prevent gastrointestinal illness? A systematic review and meta-analysis. Environ Health Perspect 2003;111:1102–9.
42. Gerba C, Rose J, Haas C, Crabtree K. Waterborne rotavirus: a risk assessment. Water Res 1996;30:2929–40.
43. Colford JM Jr, Wade TJ, Schiff KC, Wright CC, Griffith JF, Sandhu SK, et al. Water quality indicators and the risk of illness at beaches with nonpoint sources of fecal contamination. Epidemiology 2007;18:27–35.
44. McLellan SL, Salmore AK. Evidence for localized bacterial loading as the cause of chronic beach closings in a freshwater marina. Water Res 2003;37:2700–8.
45. Kim JH, Grant SB, McGee CD, Sanders BF, Largier JL. Locating sources of surf zone pollution: a mass budget analysis of fecal indicator bacteria at Huntington Beach California. Environ Sci Technol 2004;38:2626–36.
46. Nevers MB, Whitman RL. Nowcast modeling of Escherichia coli concentrations at multiple urban beaches of southern Lake Michigan. Water Res 2005;39:5250–60.
47. Ackerman D, Weisberg SB. Relationship between rainfall and beach bacterial concentrations on Santa Monica Bay beaches. J Water Health 2003;1:85–9.
48. Bertrand-Krajewski J, Chebbo G, Saget A. Distribution of pollutant mass vs volume in stormwater discharges and the first flush phenomenon. Water Res 1998;32:2341–56.
49. Krometis LA, Characklis GW, Simmons OD, 3rd, Dilts MJ, Likirdopulos CA, Sobsey MD. Intra-storm variability in microbial partitioning and microbial loading rates. Water Res 2007;41:506–16.
50. Lipp EK, Kurz R, Vincent R, Rodriguez-Palacios C, Farrah SR, Rose JB. The effect of seasonal variability and weather on microbial fecal pollution and enteric pathogens in a subtropical estuary. Estuaries 2001;24:266–76.
51. Chigbu P, Gordon S, Strange T. Influence of inter-annual variations in climatic factors on fecal coliform levels in Mississippi Sound. Water Res 2004;38:4341–52.
52. Emiliani F. Effects of hydroclimatic anomalies on bacteriological quality of the Middle Parana River (Santa Fe Argentina). Rev Argent Microbiol 2004;36:193–201.
53. Asai S, Krzanowski JJ, Anderson WH, et al. Effects of toxin of red tide, Ptychodiscus brevis, on canine tracheal smooth muscle: a possible new asthma-triggering mechanism. J Allergy Clin Immunol 1982;69:418–28.
54. American Society for Microbiology. Microbial pollutants in our nation's water: environmental and public health issues. Washington DC: American Society for Microbiology, Office of Public Affairs, 1998.
55. American Water Works Association. Protecting public health. Boston: AWWA, 1996.
56. Lynch M, Painter J, Woodruff R, Braden C. Surveillance for foodborne-disease outbreaks—United States, 1998–2002. MMWR Surveill Summ 2006;55:1–42.
57. Dziuban EJ, Liang JL, Craun GF, et al. Surveillance for waterborne disease and outbreaks associated with recreational water—United States, 2003–2004. MMWR Surveill Summ 2006;55:1–30.
58. Liang JL, Dziuban EJ, Craun GF, et al. Surveillance for waterborne disease and outbreaks associated with drinking water and water not intended for drinking—United States, 2003–2004. MMWR Surveill Summ 2006;55: 31–65.
59. Boehm AB, Grant SB, Kim JH, et al. Decadal and shorter period variability of surf zone water quality at Huntington Beach, California. Environ Sci Technol 2002;36:3885–92.
60. Boehm AB, Weisberg SB. Tidal forcing of enterococci at marine recreational beaches at fortnightly and semidiurnal frequencies. Environ Sci Technol 2005;39:5575–83.
61. Olyphant GA, Thomas J, Whitman RL, Harper D. Characterization and statistical modeling of bacterial (Escherichia coli) outflows from watersheds that discharge into southern Lake Michigan. Environ Monit Assess 2003;81(1–3):289–300.
62. Scott TM, Rose JB, Jenkins TM, Farrah SR, Lukasik J. Microbial source tracking: current methodology and future directions. Appl Environ Microbiol 2002;68:5796–803.
63. Bernhard AE, Field KG. Identification of nonpoint sources of fecal pollution in coastal waters by using host-specific 16S ribosomal DNA genetic markers from fecal anaerobes. Appl Environ Microbiol 2000;66:1587–94.
64. Scott TM, Jenkins TM, Lukasik J, Rose JB. Potential use of a host associated molecular marker in Enterococcus faecium as an index of human fecal pollution. Environ Sci Technol 2005;39:283–7.
65. Ufnar JA, Wang SY, Christiansen JM, Yampara-Iquise H, Carson CA, Ellender RD. Detection of the nifH gene of Methanobrevibacter smithii: a potential tool to identify sewage pollution in recreational waters. J Appl Microbiol 2006;101:44–52.
66. Whitman RL, Nevers MB, Korinek GC, Byappanahalli MN. Solar and temporal effects on Escherichia coli concentration at a Lake Michigan swimming beach. Appl Environ Microbiol 2004;70:4276–85.
67. Rose JB, Epstein PR, Lipp EK, Sherman BH, Bernard SM, Patz JA. Climate variability and change in the United States: potential impacts on water- and foodborne diseases caused by microbiologic agents. Environ Health Perspect 2001;109:S:211–21.
68. Santo Domingo JW, Bambic DG, Edge TA, Wuertz S. Quo vadis source tracking? Towards a strategic framework for environmental monitoring of fecal pollution. Water Res 2007;41:3539–52.
69. Savichtcheva O, Okabe S. Alternative indicators of fecal pollution: relations with pathogens and conventional indicators, current methodologies for direct pathogen monitoring and future application perspectives. Water Res 2006;40:2463–76.
70. Bower PA, Scopel CO, Jensen ET, Depas MM, McLellan SL. Detection of genetic markers of fecal indicator bacteria in Lake Michigan and determination of their relationship to Escherichia coli densities using standard microbiological methods. Appl Environ Microbiol 2005;71:8305–13.
71. Brownell MJ, Harwood VJ, Kurz RC, McQuaig SM, Lukasik J, Scott TM. Confirmation of putative stormwater impact on water quality at a Florida beach by microbial source tracking methods and structure of indicator organism populations. Water Res 2007;41:3747–57.
72. Santoro AE, Boehm AB. Frequent occurrence of the human-specific Bacteroides fecal marker at an open coast marine beach: relationship to waves, tides and traditional indicators. Environ Microbiol 2007;9:2038–49.
73. Bruesch ME, Biedrzycki PA. Preliminary comparative analysis of two models used to predict E. coli levels in recreational water in Milwaukee. Great Lakes Beach Conference, Oct 3, 2002.
74. Kuntz JE, Murray R. Non-point source of bacteria at the beach. Stamford CT: Laboratory HD, 1996.
75. Nevers MB, Whitman RL, Frick WE, Ge Z. Interaction and influence of two creeks on Escherichia coli concentrations of nearby beaches: exploration of predictability and mechanisms. J Environ Qual 2007;36:1338–45.
76. Crowther J, Kay D, Wyer MD. Relationships between microbial water quality and environmental conditions in coastal recreational waters: the Fylde coast UK. Water Res 2001;35:4029–38.

An adaptability limit to climate change due to heat stress

Steven C. Sherwood[a,1] **and Matthew Huber**[b]

[a]Climate Change Research Centre, University of New South Wales, Sydney, New South Wales 2052, Australia; and [b]Purdue Climate Change Research Center, Purdue University, West Lafayette, IN 47907

Edited by Kerry A. Emanuel, Massachusetts Institute of Technology, Cambridge, MA, and approved March 24, 2010 (received for review November 19, 2009)

Despite the uncertainty in future climate-change impacts, it is often assumed that humans would be able to adapt to any possible warming. Here we argue that heat stress imposes a robust upper limit to such adaptation. Peak heat stress, quantified by the wet-bulb temperature T_W, is surprisingly similar across diverse climates today. T_W never exceeds 31 °C. Any exceedence of 35 °C for extended periods should induce hyperthermia in humans and other mammals, as dissipation of metabolic heat becomes impossible. While this never happens now, it would begin to occur with global-mean warming of about 7 °C, calling the habitability of some regions into question. With 11–12 °C warming, such regions would spread to encompass the majority of the human population as currently distributed. Eventual warmings of 12 °C are possible from fossil fuel burning. One implication is that recent estimates of the costs of unmitigated climate change are too low unless the range of possible warming can somehow be narrowed. Heat stress also may help explain trends in the mammalian fossil record.

climate impacts | global warming | mammalian physiology | paleoclimate

Recent studies have highlighted the possibility of large global warmings in the absence of strong mitigation measures, for example the possibility of over 7 °C of warming this century alone (1). Warming will not stop in 2100 if emissions continue. Each doubling of carbon dioxide is expected to produce 1.9–4.5 °C of warming at equilibrium, but this is poorly constrained on the high side (2, 3) and according to one new estimate has a 5% chance of exceeding 7.1 °C per doubling (4). Because combustion of all available fossil fuels could produce 2.75 doublings of CO_2 by 2300 (5), even a 4.5 °C sensitivity could eventually produce 12 °C of warming. Degassing of various natural stores of methane and/or CO_2 in a warmer climate (6, 7, 8) could increase warming further. Thus while central estimates of business-as-usual warming by 2100 are 3–4 °C, eventual warmings of 10 °C are quite feasible and even 20 °C is theoretically possible (9).

Such worst-case scenarios (along with possible surprise impacts) may be an important or even dominant factor in evaluating the risk of carbon emissions, analogous to situations in which people buy insurance (9). It is widely agreed that warmings of over 6 °C would have disastrous consequences for humankind, but it is very hard to pin down rigorously what the consequences would be, let alone quantify their costs. Thresholds have been proposed for ice sheet and rainforest collapse, for example, but predicting the timing or societal impacts of such events is challenging (10). Economic costs of warming are generally extrapolated from present-day data, but this is clearly unsatisfactory for climates so different from any in human experience. Inability to specify consequences of very large warmings is therefore a hurdle to rational decision-making on climate mitigation.

We propose that a somewhat neglected aspect of global warming, the direct impact on humans and other mammals in the form of heat stress, may provide a climate impacts benchmark that is relatively well-constrained by physical laws. We find a tolerance limit that is well above other oft-cited thresholds, such as the 2 °C target now adopted by many nations, but still reachable if things go badly, therefore an important linchpin for risk estimates.

Heat stress is already a leading cause of fatalities from natural phenomena (11, 12). While fatalities appear associated with warm nights (13), hot days alter the lifestyles and work productivity of those living at low latitudes (14). Both impacts will clearly worsen in warmer climates (15, 16), but most believe humans will simply adapt, reasoning that humans already tolerate a very wide range of climates today. But when measured in terms of peak heat stress—including humidity—this turns out to be untrue. We show that even modest global warming could therefore expose large fractions of the population to unprecedented heat stress, and that with severe warming this would become intolerable.

A resting human body generates ~100 W of metabolic heat that (in addition to any absorbed solar heating) must be carried away via a combination of heat conduction, evaporative cooling, and net infrared radiative cooling. Net conductive and evaporative cooling can occur only if an object is warmer than the environmental wet-bulb temperature T_W, measured by covering a standard thermometer bulb with a wetted cloth and fully ventilating it. The second law of thermodynamics does not allow an object to lose heat to an environment whose T_W exceeds the object's temperature, no matter how wet or well-ventilated. Infrared radiation under conditions of interest here will usually produce a small additional heating; we err on the side of underestimating stress by neglecting this and assuming that solar heating will be avoided during peak heat stress.

While empirical heat indices such as "wet bulb globe temperature" (WBGT) are typically used to quantify heat stress, tolerance of a given index value varies significantly according to clothing, activity, and acclimatization (14). We consider T_W instead because, unlike other indices, it establishes a clear thermodynamic limit on heat transfer that cannot be overcome by such adaptations.

Humans maintain a core body temperature near 37 °C that varies slightly among individuals but does not adapt to local climate. Human skin temperature is strongly regulated at 35 °C or below under normal conditions, because the skin must be cooler than body core in order for metabolic heat to be conducted to the skin (17). Sustained skin temperatures above 35 °C imply elevated core body temperatures (hyperthermia), which reach lethal values (42–43 °C) for skin temperatures of 37–38 °C even for acclimated and fit individuals (18, 19, 20, 21). We would thus expect sufficiently long periods of $T_W > 35$ °C to be intolerable.

Results

Fig. 1*A* shows area-weighted histograms of three quantities estimated from recent observations over land areas (excluding high latitudes): near-surface air temperature T sampled at all

Author contributions: S.C.S. designed research; S.C.S. and M.H. performed research; S.C.S. analyzed data; M.H. contributed new reagents/analytic tools; and S.C.S. and M.H. wrote the paper.

The authors declare no conflict of interest.

This article is a PNAS Direct Submission.

See Commentary on page 9483.

[1]To whom correspondence should be addressed. E-mail: s.sherwood@unsw.edu.au.

This article contains supporting information online at www.pnas.org/lookup/suppl/doi:10.1073/pnas.0913352107/-/DCSupplemental.

NMED - PATZ
REBUTTAL EXHIBIT 8

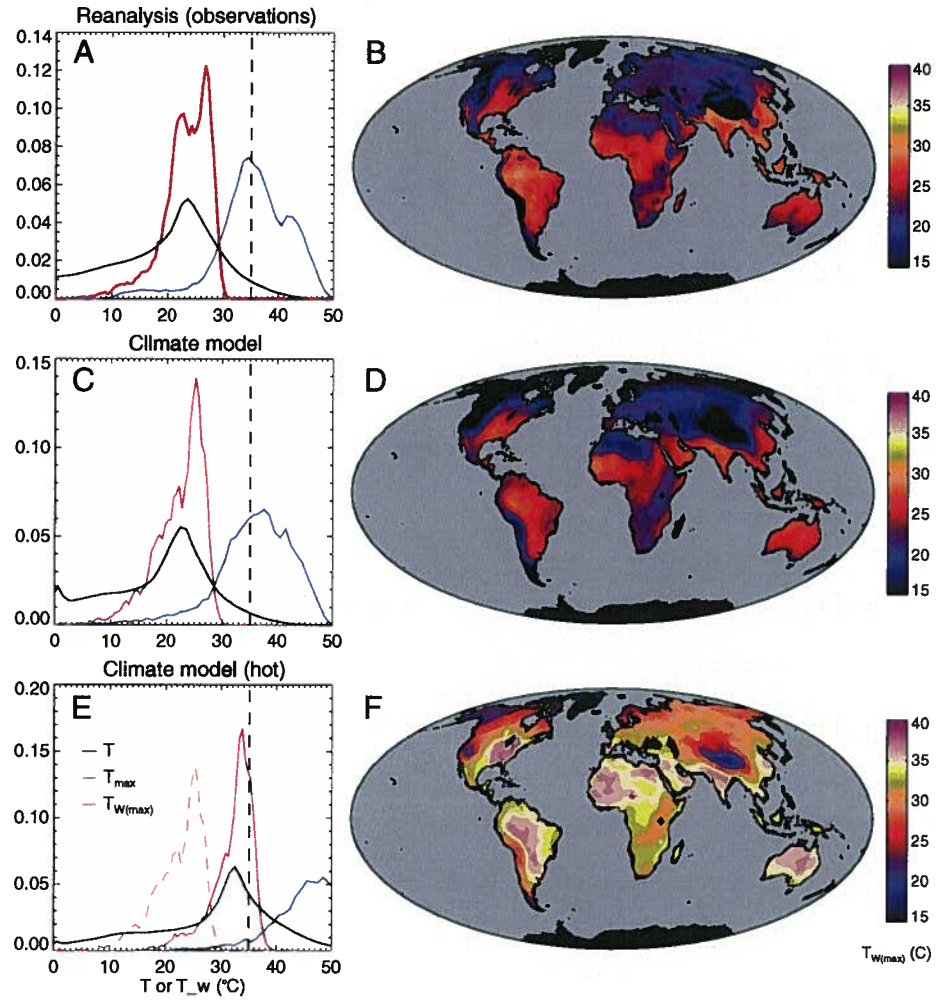

Fig. 1. (*A*) Histograms of 2-meter T (*Black*), T_{max} (*Blue*), and $T_{W(max)}$ (*Red*) on land from 60S–60N during the last decade (1999–2008). "Max" histograms are annual maxima accumulated over location and year, while the T histogram is accumulated over location and reanalysis time. Data are from the ERA-Interim reanalysis 4xdaily product (similar results are found for the 50m level from the NCEP reanalysis, see *SI Text*). (*B*) Map of $T_{W(max)}$. (*C* and *D*) Same as *A* and *B* but from a slab-ocean version of the CAM3 climate model that produces global-mean surface temperature close to modern values. (*E* and *F*) Same as *C* and *D* but from a high-CO_2 model run that produces a global-mean T 12 °C warmer; accounting for GCM bias, the $T_{W(max)}$ distributions are roughly what would be expected with 10 °C of global-mean warming relative to the last decade (see text). Dashed line in *E* is $T_{W(max)}$ reproduced from *C*. White land areas in *F* exceed 35 °C.

locations and times, the annual maximum T_{max} of this sampled in all locations and years, and annual maximum wet-bulb $T_{W(max)}$. The distribution of T is broad, with a most-common value near 25 °C and a thin tail reaching to 50 °C (albeit with very few points above 40 °C). The distribution of T_{max} shows that a large majority of locations reaches 30 °C at some point during a typical year, and a few reach close to the 50 °C global record. Shifting either of these curves warmer by a few degrees would only move a tiny fraction of their area into uncharted territory (above 50 °C).

By constrast, the highest instantaneous T_W anywhere on Earth today is about 30 °C (with a tiny fraction of values reaching 31 °C). The most-common $T_{W(max)}$ is 26–27 °C, only a few degrees lower. Thus, peak potential heat stress is surprisingly similar across many regions on Earth. Even though the hottest temperatures occur in subtropical deserts, relative humidity there is so low that $T_{W(max)}$ is no higher than in the deep tropics (Fig. 1*B*). Likewise, humid midlatitude regions such as the Eastern United States, China, southern Brazil, and Argentina experience $T_{W(max)}$ during summer heat waves comparable to tropical ones, even though annual mean temperatures are significantly lower. The highest values of T in any given region also tend to coincide with low relative humidity. Maxima of $T_{W(max)}$ over the decade are higher than those shown by nearly 1 °C in most tropical regions and up to 2 °C in midlatitudes (though still never exceeding 31 °C), so our focus on annual events may underestimate the danger. Also, we use six-hourly data, which has a similar but smaller effect.

The likely reason for the apparent ceiling on T_W is a convective instability mechanism. We find essentially identical results for quantities near or 50 m above the surface (see *SI Text*). The equivalent potential temperature θ_e, a measure of air buoyancy and atmospheric stability, is a monotonic function of T_W and air pressure. Values that exceed a threshold determined by temperatures aloft will produce storm activity that cools air near the surface, limiting θ_e (22). The corresponding ceiling on T_W increases with pressure, explaining why $T_{W(max)}$ is positively correlated with this ($r = 0.71$), and why equator-ward of 45 N/S, most locations where $T_{W(max)} < 26$ °C are above 650 m elevation. Most other locations are in areas of very low storm activity and rainfall. Because $T_{W(max)}$ and human population are both larger at low elevations and in rainy regions, 58% of the world's population in 2005 resided where $T_{W(max)} \geq 26$ °C (population data obtained from Columbia University, sedac.ciesin.columbia.edu/gpw).

The simplest prediction of global warming's effect on $T_{W(max)}$ is to assume a uniform upward shift of the T_W distribution. A 4 °C

increase in T_W would then subject over half the world's population annually to unprecedented values and cut the "safety buffer" that now exists between the highest $T_{W(\mathrm{Max})}$ and 35 °C to roughly a quarter. A shift of 5 °C would allow $T_{W(\mathrm{max})}$ to exceed 35 °C in some locations, and a shift of 8.5 °C would bring the most-common value to 35 °C. It has been similarly pointed out that a few degrees of warming will produce unprecedented temperature and agricultural stresses in the tropics (23).

The shift ratio of the $T_{W(\mathrm{max})}$ distribution per °C of global-mean T might be different from unity, however, or the shape of the distribution might change—due either to changes in relative humidity [though unlikely a priori and not observed with recent warming (24)], dynamics, or spatially inhomogeneous warming. To investigate, we ran the Community Atmospheric Model version 3.1 coupled to a mixed-layer ocean model, with a variety of CO_2 levels (see *SI Text*). Fig. 1 *C* and *D* shows the same quantities as in Fig. 1 *A* and *B*, from a simulation having a global-mean surface temperature close to observed. The simulated and observed distributions have similar shape. $T_{W(\mathrm{max})}$ is biased 1–2 °C too low (due to a low bias in humidity during heat extremes), whereas $T_{W(\mathrm{max})}$ is too high in some midlatitude regions, but the simulation seems sufficient for the intended purpose.

Comparison of the peak in $T_{W(\mathrm{max})}$ vs. global temperature among different model simulations (Fig. 2) shows that $T_{W(\mathrm{max})}$ near the surface consistently tracks tropical surface temperature. The rise rate is then only 0.75 °C per 1 °C increase in global-mean temperature, because the tropics warms more slowly than higher latitudes. One example simulation, globally warmer than the one in Fig. 1 *C* and *D* by about 12 °C, is shown in Fig. 1 *E* and *F*. The $T_{W(\mathrm{max})}$ distribution is slightly narrower but not greatly changed in this simulation except for an upward shift of 9 °C, or about 7 °C above observations. Its $T_{W(\mathrm{max})}$ distribution is therefore what we might expect with a global-mean warming of approximately 10 °C. In this simulation, several regions experience 35 °C wet-bulb values each year, and even Siberia reaches values exceeding anything in the present-day tropics.

The ability of climate models to represent extremes or the details of Fig. 1*F* is arguable. However, the link of $T_{W(\mathrm{max})}$ to tropical temperatures is a plausible consequence of the dynamical links between air in the tropics and aloft in midlatitudes (25), and the polar amplification of warming predicted here compares reasonably to that observed over the twentieth century. Thus, the 0.75 factor obtained here should not be too far off.

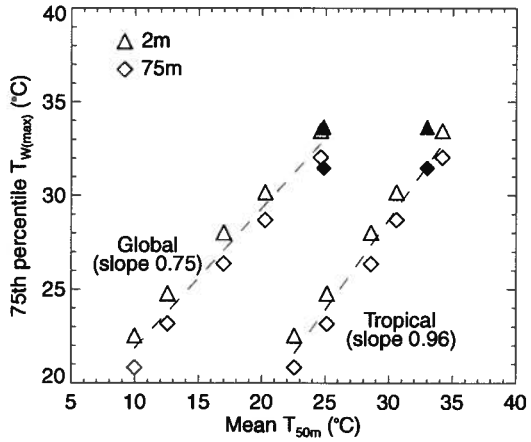

Fig. 2. The 75th percentile value of $T_{W(\mathrm{max})}$ (a measure of the peak occurrence value) at two or 75 meters above ground vs. global or tropical mean 75-m temperature in CAM3 simulations. Solid symbols are for a simulation representing possible Eocene conditions. Dashed lines show best linear fits, with slopes given (Eocene run not included in fit).

Discussion

Could humans survive $T_W > 35$ °C? Periods of net heat storage can be endured, though only for a few hours (see *SI Text*) and with ample time needed for recovery. Unfortunately, observed extreme-T_W events ($T_W > 26$ °C) are long-lived: Adjacent nighttime minima of T_W are typically within 2–3 °C of the daytime peak, and adjacent daily maxima are typically within 1 °C. Conditions would thus prove intolerable if the peak T_W exceeded, by more than 1–2 °C, the highest value that could be sustained for at least a full day. Furthermore, heat dissipation would be very inefficient unless T_W were at least 1–2 °C below skin temperature (see *SI Text*), so to sustain heat loss without dangerously elevated body temperature would require T_w of 34 °C or lower. Taking both of these factors into account, we estimate that the survivability limit for peak six-hourly T_W is probably close to 35 °C for humans, though this could be a degree or two off. Similar limits would apply to other mammals but at various thresholds depending on their core body temperature and mass.

Mammals have survived past warm climates; does this contradict our conclusions? The last time temperatures approached values considered here is the Paleogene, when global-mean temperature was perhaps 10 °C (26) and tropical temperature perhaps 5–6 °C warmer than modern (27, 28), implying T_W of up to 36 °C with a most-common $T_{W(\mathrm{Max})}$ of 32–33 °C. This would still leave room for the survival of mammals in most locations, especially if their core body temperatures were near the high end of those of today's mammals (near 39 °C). Transient temperature spikes, such as during the PETM or Paleocene-Eocene Thermal Maximum (26), might imply intolerable conditions over much broader areas, but tropical terrestrial mammalian records are too sparse to directly test this. We thus find no inconsistency with our conclusions, but this should be revisited when more evidence is available.

On evolutionary time scales we might expect taxa stressed by heat to undergo adaptive increases in surface-area-to-mass ratio to aid heat dissipation relative to metabolic rate. While data from the tropics are sparse, the major mammalian taxa heavier than 1 kg—carnivora, artiodactyls, and perissodactyls—were indeed about a factor of 10 less massive on average during the early Eocene than during cooler, later periods (29, 30), part of a growth trend known as "Cope's law" (31). Similarly, "transient dwarfing" of midlatitude mammals occurred during the PETM (32). Both phenomena have been attributed to changes in food supply but could also be explained as an adaptation to changing heat stress.

In principle humans can devise protections against the unprecedented heat such as much wider adoption of air conditioning, so one cannot be certain that $T_{W(\mathrm{Max})} = 35$ °C would be uninhabitable. But the power requirements of air conditioning would soar; it would surely remain unaffordable for billions in the third world and for protection of most livestock; it would not help the biosphere or protect outside workers; it would regularly imprison people in their homes; and power failures would become life-threatening. Thus it seems improbable that such protections would be satisfying, affordable, and effective for most of humanity.

We conclude that a global-mean warming of roughly 7 °C would create small zones where metabolic heat dissipation would for the first time become impossible, calling into question their suitability for human habitation. A warming of 11–12 °C would expand these zones to encompass most of today's human population. This likely overestimates what could practically be tolerated: Our limit applies to a person out of the sun, in gale-force winds, doused with water, wearing no clothing, and not working. A global-mean warming of only 3–4 °C would in some locations halve the margin of safety (difference between $T_{W\,\mathrm{max}}$ and 35 °C) that now leaves room for additional burdens or limitations to cooling. Considering the impacts of heat stress that occur already, this would certainly be unpleasant and costly if not debilitating. More

detailed heat stress studies incorporating physiological response characteristics and adaptations would be necessary to investigate this.

If warmings of 10 °C were really to occur in next three centuries, the area of land likely rendered uninhabitable by heat stress would dwarf that affected by rising sea level. Heat stress thus deserves more attention as a climate-change impact.

The onset of $T_{W\max} > 35$ °C represents a well-defined reference point where devastating impacts on society seem assured even with adaptation efforts. This reference point constrasts with assumptions now used in integrated assessment models. Warmings of 10 °C and above already occur in these models for some realizations of the future (33). The damages caused by 10 °C of warming are typically reckoned at 10–30% of world GDP (33, 34), roughly equivalent to a recession to economic conditions of roughly two decades earlier in time. While undesirable, this is hardly on par with a likely near-halving of habitable land, indicating that current assessments are underestimating the seriousness of climate change.

Methods

The observational estimates of wet-bulb and dry-bulb temperature extremes were derived from six-hourly 2-meter temperature, humidity, and pressure data from the ERA-Interim dataset. Results from this dataset were corroborated by similar results from the NCEP-DOE reanalysis II dataset. Simulations of present-day and hot climates were performed using the NCAR (National Center for Atmospheric Research) Community Atmosphere Model with varying levels of carbon dioxide. Quantities were computed from the model using the same variables and formula as for the reanalysis data.

A more detailed explanation and justification of data and methods is given in the *SI Text*. Further discussions can also be found there to support claims as to the limits of tolerable heat stress.

ACKNOWLEDGMENTS. S.C.S. completed part of this work while at Yale University; he thanks G. Havenith and T. Kjellstrom for useful discussions. We acknowledge the Columbia University CIESIN, the United Nations FAO, and the CIAT for providing population data, and the ECMWF and NCEP/NCAR/NCDC for making the reanalysis datasets available. M.H. thanks the Institute of Geological and Nuclear Sciences in New Zealand for providing a conducive work environment while he was on a sabbatical from Purdue University and the National Science Foundation for providing funding for research under Grants 090278-ATM and 0902882-OCE.

1. Sokolov AP, et al. (2009) Probabilistic forecast for 21st century climate based on uncertainties in emissions (without policy) and climate parameters. *J Climate* 22:5175–5204.
2. Roe GH, Baker MB (2007) Why is climate sensitivity so unpredictable?. *Science* 318:629–632.
3. Knutti R, Hegerl GC (2008) The equilibrium sensitivity of the earth's temperature to radiation changes. *Nat Geosci* 1:735–742.
4. Meinshausen M, et al. (2009) Greenhouse-gas emission targets for limiting global warming to 2 degrees c. *Nature* 458:1158–U96.
5. Montenegro A, Brovkin V, Eby M, Archer D, Weaver AJ (2007) Long term fate of anthropogenic carbon. *Geophys. Res. Lett.* 34:L19707.
6. Friedlingstein P, et al. (2006) Climate-carbon cycle feedback analysis: Results from the C4MIP model intercomparison. *J Climate* 19:3337–3353.
7. Williams JW, Jackson ST, Kutzbacht JE (2007) Projected distributions of novel and disappearing climates by 2100 AD. *Proc Natl Acad Sci USA* 104:5738–5742.
8. Ise T, Dunn AL, Wofsy SC, Moorcroft PR (2008) High sensitivity of peat decomposition to climate change through water-table feedback. *Nat Geosci* 1:763–766.
9. Weitzman ML (2009) On modeling and interpreting the economics of catastrophic climate change. *Rev Econ Stat* 91:1–19.
10. Alley RB, et al. (2003) Abrupt climate change. *Science* 299:2005–2010.
11. Kovats RS, Hajat S (2008) Heat stress and public health: A critical review. *Annu Rev Publ Health* 29:41–55.
12. Borden KA, Cutter SL (2008) Spatial patterns of natural hazards mortality in the United States. *Int J Health Geogr* 7 Art. No. 64.
13. Karl TR, et al. (1993) A new perspective on recent global warming-asymmetric trends of daily maximum and minimum temperatures. *B Am Meteorol Soc* 74:1007–1023.
14. Kjellstrom T, Kovats RS, Lloyd SJ, Hold T, Tol RSJ (2008) The direct impact of climate change on regional labour productivity. (ESRI). Working paper 260 27 pp.
15. Delworth TL, Mahlman JD, Knutson TR (1999) Changes in heat index associated with CO_2-induced global warming. *Climatic Change* 43:369–386.
16. Diffenbaugh NS, Giorgi F, Pal JS (2008) Climate change hotspots in the United States. *Geophys Res Lett* 35:L16709.
17. McNab BK (2002) *The Physiological Ecology of Vertebrates: A View from Energetics* (Cornell Univ Press, Ithaca, NY) p 525.
18. Pandolf KB, Goldman RF (1978) Convergence of skin and rectal temperatures as a criterion for heat tolerance. *Aviat Space Environ Med* 49:1095–1101.
19. Bynum GD, et al. (1978) Induced hyperthermia in sedated humans and the concept of critical thermal maximum. *Am J Physiol Regulatory Integrative Comp Physiol* 235:228–236.
20. Bouchama A, et al. (2005) Inammatory, hemostatic, and clinical changes in a baboon experimental model for heatstroke. *J Appl Physiol* 98:697–705.
21. Mehnert P, et al. (2000) Prediction of the average skin temperature in warm and hot environments. *Eur J Appl Physiol* 82:52–60.
22. Emanuel KA, Neelin JD, Bretherton CS (1994) On large-scale circulations in convecting atmospheres. *Q J Roy Meteor Soc* 120:1111–1143.
23. Battisti DS, Naylor RL (2009) Historical warnings of future food insecurity with unprecedented seasonal heat. *Science* 323:240–244.
24. Willett KM, Gillett NP, Jones PD, Thorne PW (2007) Attribution of observed surface humidity changes to human influence. *Nature* 449:710–U6.
25. Pauluis O, Czaja A, Korty R (2008) The global atmospheric circulation on moist isentropes. *Science* 321:1075–1078.
26. Zachos JC, Pagani M, Sloan L, Thomas E, Billups K (2001) Trends, rhythms, and aberrations in global climate 65 ma to present. *Science* 292:686–93.
27. Pearson PN, et al. (2007) Stable warm tropical climate through the Eocene epoch. *Geology* 35:211–214.
28. Head JJ, et al. (2009) Giant boid snake from the Palaeocene neotropics reveals hotter past equatorial temperatures. *Nature* 457:715–U4.
29. Smith FA, et al. (2004) Similarity of mammalian body size across the taxonomic hierarchy and across space and time. *Am Nat* 163:672–691.
30. Alroy J, Koch PL, Zachos JC (2000) Global climate change and North American mammalian evolution. *Paleobiology* 26:259–288.
31. Alroy J (1998) Cope's rule and the dynamics of body mass evolution in North American fossil mammals. *Science* 280:731–734.
32. Gingerich P (2006) Environment and evolution through the paleocene-eocene thermal maximum. *Trends Ecol Evol* 21:246–253.
33. Hope C (2006) The marginal impact of CO_2 from PAGE2002: An integrated assessment model incorporating the IPCC's five reasons for concern. *Integ Assessment J* 6:19–56.
34. Nordhaus W, Boyer J (2000) *Warming the World: Economics Models of Global Warming* (MIT Press, Cambridge, MA).

Intensification of hot extremes in the United States

Noah S. Diffenbaugh[1,2] and Moetasim Ashfaq[1,2,3]

Received 5 May 2010; revised 24 June 2010; accepted 28 June 2010; published 6 August 2010.

[1] Governments are currently considering policies that will limit greenhouse gas concentrations, including negotiation of an international treaty to replace the expiring Kyoto Protocol. Existing mitigation targets have arisen primarily from political negotiations, and the ability of such policies to avoid dangerous impacts is still uncertain. Using a large suite of climate model experiments, we find that substantial intensification of hot extremes could occur within the next 3 decades, below the 2°C global warming target currently being considered by policy makers. We also find that the intensification of hot extremes is associated with a shift towards more anticyclonic atmospheric circulation during the warm season, along with warm-season drying over much of the U.S. The possibility that intensification of hot extremes could result from relatively small increases in greenhouse gas concentrations suggests that constraining global warming to 2°C may not be sufficient to avoid dangerous climate change. **Citation:** Diffenbaugh, N. S., and M. Ashfaq (2010), Intensification of hot extremes in the United States, *Geophys. Res. Lett.*, *37*, L15701, doi:10.1029/2010GL043888.

1. Introduction

[2] World governments are currently considering mitigation policies that will limit greenhouse gas (GHG) concentrations, including an international treaty to replace the expiring Kyoto Protocol [*United Nations Framework Convention on Climate Change* (*UNFCCC*), 2009]. Key questions include the level of GHG forcing that should be targeted and the urgency with which that target should be achieved, with considerable discussion oriented around trade-offs between avoiding policy-induced economic damage and GHG-induced climate damage [e.g., *Mastrandrea and Schneider*, 2004]. However, existing mitigation targets – such as the target of 2°C global warming above pre-industrial conditions set by world governments as part of the recent Copenhagen Accord [*UNFCCC*, 2009] – have arisen primarily from political negotiations. Although substantial scientific work has focused on the climate system response to varying GHG concentrations [*Mastrandrea and Schneider*, 2004; *Meehl et al.*, 2007b], there remains uncertainty as to whether "dangerous" climate change impacts could emerge below the target GHG envelope currently being considered by policy makers.

[3] Hot extremes, which are an important source of potential climate change impacts [e.g., *Battisti and Naylor*, 2009; *Poumadere et al.*, 2005; *Schlenker and Roberts*, 2009], can result from both large- and fine-scale climate processes. For instance, the 2003 European heat wave was associated with large-scale anticyclonic atmospheric anomalies [*Meehl and Tebaldi*, 2004], with local and regional land coupling both enhancing the large-scale circulation anomalies and accounting for more than half of the hot-day occurrence over much of the region [*Fischer et al.*, 2007b]. Likewise, the 20th-century Sahel drought has been attributed to a combination of large-scale ocean-atmosphere teleconnections and fine-scale land-atmosphere feedbacks [*Christensen et al.*, 2007]. Further, the response of hot extremes to high levels of GHG forcing appears sensitive to both large-scale atmospheric circulation and fine-scale surface-atmosphere interactions [*Diffenbaugh et al.*, 2005; *Meehl and Tebaldi*, 2004; *Seneviratne et al.*, 2006]. Quantification of the potential for near-term intensification of hot extremes therefore requires a climate modeling framework that can capture the uncertainties associated with both large- and fine-scale climate processes.

2. Methods

[4] We employ the RegCM3 nested climate model [*Pal et al.*, 2007], using the grid of *Diffenbaugh et al.* [2005], which covers the continental U.S. at 25-km horizontal resolution and 18 levels in the vertical. Our transient experiment includes five members simulating the period from 1950 to 2039 in the A1B emissions scenario [*Nackicenovic et al.*, 2000]. The first year (1950) is discarded to account for model equilibration. Each RegCM3 ensemble member uses the same parameterization options (as by *Diffenbaugh et al.* [2005]), with only the large-scale input varying between the members.

[5] Large-scale boundary conditions are provided by the NCAR CCSM3 [*Collins et al.*, 2006]. We use five of the CCSM3 simulations archived as part of the CMIP3 intercomparison [*Meehl et al.*, 2007a]. (These CCSM3 ensemble members are identified by NCAR as c, e, bES, fES, and gES.) In order to generate the necessary sub-daily, 3-dimensional atmospheric variables, we re-run the atmospheric component (CAM3) from 1948 to 2039, using the original CCSM3-generated SSTs and sea ice as boundary conditions for the global atmosphere [see *Trapp et al.*, 2009]. These CAM3 simulations use the same resolution as in the original CCSM3 simulations (T85 spectral truncation with 26 levels in the vertical). We also analyze GCM output from the CMIP3 climate model archive [*Meehl et al.*, 2007a], selecting the

[1]Woods Institute for the Environment and Department of Environmental Earth System Science, Stanford University, Stanford, California, USA.
[2]Purdue Climate Change Research Center and Department of Earth and Atmospheric Sciences, Purdue University, West Lafayette, Indiana, USA.
[3]Now at Oak Ridge National Laboratory, Oak Ridge, Tennessee, USA.

Copyright 2010 by the American Geophysical Union.
0094-8276/10/2010GL043888

NMED - PATZ
REBUTTAL EXHIBIT 9

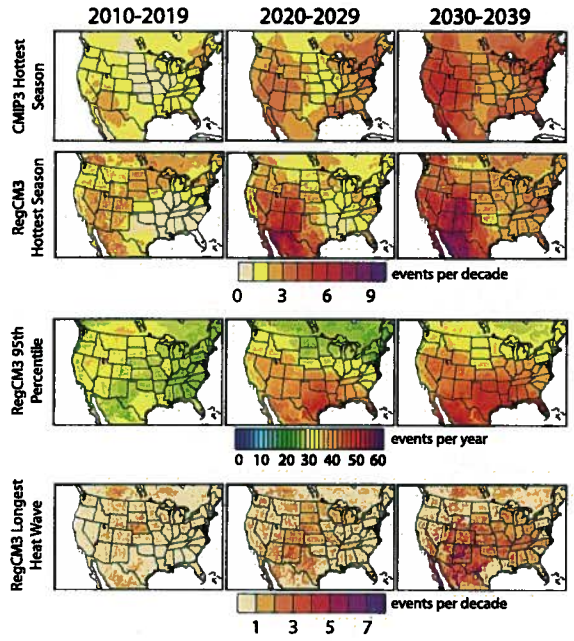

Figure 1. Projected changes in heat extremes in the coming decades. The top two rows show the decadal occurrence of the 1951–1999 hottest-season threshold in the CMIP3 and RegCM3 ensembles. The third and fourth rows show the decadal occurrence of the 95th -percentile daily maximum threshold (T95) and the historical hottest-heat-wave threshold for the RegCM3 ensemble.

output from "run 1" of each of the 22 GCMs that archived monthly surface air temperature results for the A1B scenario.

[6] We first calculate the hottest season of the 1951–1999 period at each grid point. Both the CMIP3 and RegCM3 ensembles are able to capture the observed magnitude and pattern of hottest-season and mean-summer temperature in the U.S. (Figure S1 of the auxiliary material).[1] The simulation of interannual variance of summer temperature is less accurate, with over-estimation of variance in the central U.S. (Figure S1). (*Walker and Diffenbaugh* [2009] diagnose the RegCM3 warm-season temperature biases over the U.S., including biases in the atmospheric circulation and moisture.) For each 21st century model realization, we calculate the number of exceedences of the hottest season of the respective 1951–1999 period. We then calculate the ensemble mean and standard deviation across the respective ensemble members.

[7] In addition, because of the availability of sub-daily output from the RegCM3 realizations, we are also able to calculate the occurrence of the annual-scale 95th -percentile daily maximum temperature (T95), and of the longest historical heat wave. For the former, which quantifies the frequency of exceedence of the present tail of the daily temperature distribution, we follow *Diffenbaugh et al.* [2005], using the 1980–1999 period as a baseline. In this approach, the T95 threshold at each grid point is calculated as the mean of the daily maximum temperature values from the 18th hottest day of each year in the baseline period. For the latter, we apply the heat wave duration index of *Frich et al.* [2002] to find the longest heat wave of the 1951–1999 period, along with the 21st century occurrence of heat waves that are at least as long as this historical maximum. As with the historical hottest season exceedence, we calculate the baseline and exceedence values at each grid point, and for each decade of the 2010–2039 period.

3. Results

[8] We find that the exceedence of the historical hottest-season threshold increases over the next three decades in the A1B scenario (Figure 1). The intensification of hot extremes emerges quickly in the RegCM3 simulations, with 3 to 4 exceedences per decade over large areas of the U.S. in the 2010–2019 period (Figure 1) (with an intra-ensemble standard deviation (S.D.) of 2 to 3 exceedences per decade over most of the U.S. (Figure S2)). This emergence intensifies in the 2020–2029 period, with up to 8 exceedences per decade over the western U.S. (S.D. of 3 to 4), and up to 4 exceedences per decade over much of the eastern U.S (S.D. of 2 to 3). Further, in the 2030–2039 period, most areas of Utah, Colorado, Arizona and New Mexico experience at least 7 exceedences per decade (S.D. of 3 to 4), and much of the rest of the U.S. experiences at least 4 exceedences per decade (S.D. of 2 to 5 over most areas). The summer warming in the RegCM3 ensemble is not uniform, with greater increases in the mean in the eastern U.S. than the western U.S. (Figure S3), along with increased variance in the northcentral U.S., increased skewness in the southwestern and southeastern U.S., and decreased kurtosis throughout most of the continental U.S. (Figure S3). The intensification of hottest-season exceedence is similar in the CMIP3 ensemble (compared with the RegCM3 ensemble), including up to 6 exceedences per decade over the western and northeastern U.S. in the 2030–2039 period, and up to 8 exceedences per decade over parts of the southeastern U.S. (with S.D. of 4 over most of the western and eastern U.S., and 3 over most of the central U.S.). However, the intensification of seasonal hot extremes emerges more quickly and strongly in the RegCM3 ensemble, particularly over the western U.S., where the higher-resolution topographic boundary condition leads to a more accurate representation of extreme seasonal temperature values (Figure S1).

[9] The annual occurrence of the T95 threshold exceeds 30 days per year over much of the U.S. during the 2020–2029 period (Figure 1) (S.D. of 2 to 12 (Figure S2)), with peak occurrence of up to 52 days per year over Texas and Florida (S.D. of 10 to 24). T95 occurrence exceeds 38 days per year over much of the U.S. in the 2030–2039 period (S.D. of 4 to 16), with the area exceeding 46 days per year expanding to include most of the southern Great Plains and much of the Gulf Coast region (S.D. of 10 to 24). Likewise, the area experiencing at least one exceedence of the historical heat wave threshold per decade covers most of the U.S. in the 2020–2029 period, including up to 5 exceedences per decade over areas of the western and central U.S. (Figure 1) (S.D. of 1 to 5 over most of the U.S. (Figure S2)). Occurrence of the longest historical heat wave further intensifies in the 2030–2039 period, including greater than 5 occurrences per decade over much of the western U.S., and

[1] Auxiliary materials are available in the HTML. doi:10.1029/2010GL043888.

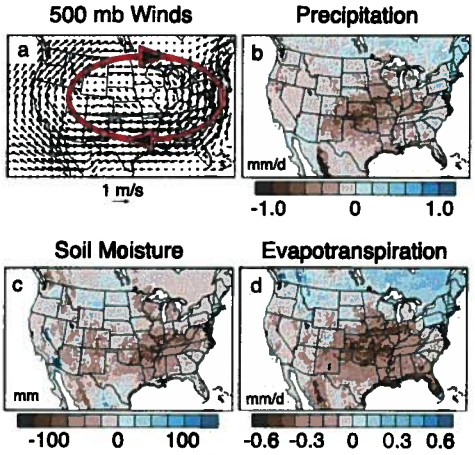

Figure 2. Changes in summer (a) 500 mb winds, (b) precipitation, (c) total soil moisture, and (d) evapotranspiration in the RegCM3 ensemble. Changes are calculated as 2030–2039 minus 1980–1999 for June-July-August. The ellipse and large arrows in Figure 2a are added for emphasis.

greater than 3 exceedences per decade over much of the eastern U.S. (S.D. of 3 to 7 over most of the U.S.).

4. Discussion

[10] The intensification of hot extremes in the RegCM3 ensemble is associated with warm-season drying over much of the U.S. (Figure 2). By the 2030–2039 period, a summer anticyclonic circulation anomaly develops aloft (at 500 mb) over most of the continental U.S. Associated with this anticyclonic anomaly are decreases (2030–2039 minus 1980–1999) in precipitation (exceeding −1.0 mm/day), total soil moisture (exceeding −125 mm), and evapotranspiration (exceeding −0.6 mm/day). Although the ensemble-mean large-scale circulation anomalies are very similar between the driving CAM3 and nested RegCM3 ensembles in the autumn, winter and spring, the summer anticyclonic anomaly is more widespread in RegCM3 than CAM3 (Figure S4).

[11] We find that the coupling of changes in summer temperature, precipitation and soil moisture is robust across the model realizations. For the 2030–2039 period, all five RegCM3 members exhibit a negative correlation between changes in summer total soil moisture and changes in summer temperature, and a positive correlation between changes in summer total soil moisture and changes in summer precipitation (Figure 3). (The ensemble mean correlation is −0.35 for change in temperature and 0.37 for change in precipitation.) We also find that all five RegCM3 members exhibit a decrease in summer total soil moisture across the domain. (The ensemble mean fractional change in total soil moisture is −0.02.) For the CMIP3 ensemble, we find that 89% of the realizations show a negative (positive) correlation between changes in summer soil moisture and changes in summer temperature (precipitation). (The ensemble mean correlation is −0.28 for change in temperature and 0.30 for change in precipitation.) We also find that 78% of the GCM realizations show a decrease in summer total soil moisture across the domain for the 2030–2039 period. (The ensemble mean fractional change in total soil moisture is −0.03.)

[12] Surface drying associated with anticyclonic circulation anomalies is thought to have amplified severe hot and dry events such as the 1988 event in the U.S. [*Chen and Newman*, 1998] and the 2003 event in Europe [*Fischer et al.*, 2007b], and has been identified as a key regulator of changes in climate variability in response to elevated GHG forcing [*Seneviratne et al.*, 2006]. The fact that most of the GCM realizations simulate soil-moisture/temperature/precipitation relationships of the same sign as the RegCM3 ensemble suggests that the coupling is likely to be robust over the U.S., a result that supports previous work [e.g., *Fischer et al.*, 2007a; *Lorenz et al.*, 2010; *Seneviratne et al.*, 2006]. However, although we have identified correlations between changes in temperature, precipitation, and soil moisture that are robust across a large suite of climate model experiments, it is not clear from the analysis of these experiments alone whether the surface drying is the cause of the intensified hot extremes. For instance, the decreases in soil moisture could be a product of decreases in precipitation (Figure 2) and/or increases in net surface radiation (Figure S5) associated with the changes in large-scale circulation (Figure 2). Targeted experiments that physically isolate moisture fluxes, radiation fluxes, and atmospheric circulation (as by *Seneviratne et al.* [2006]) are necessary in order to fully determine causation.

[13] The spread within the CMIP3 ensemble (in which multiple GCMs are included) is greater than the spread within the RegCM3 ensemble (in which only one GCM-RCM combination is included) (Figures S2 and 3). Earlier work using an RCM nested within an atmosphere-only GCM suggests that some of the spread in our nested

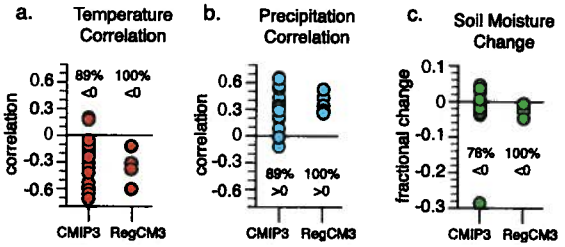

Figure 3. Simulated relationships between summer temperature, precipitation, and soil moisture in the RegCM3 and CMIP3 ensembles. (a) Correlation between the change in summer temperature and the change in summer soil moisture for the 2030–2039 period. (b) Correlation between the change in summer precipitation and the change in summer soil moisture for the 2030–2039 period. (c) Change in summer soil moisture for the 2030–2039 period. Each circle represents one model realization. We first calculate the change in mean summer temperature, precipitation and soil moisture for the 2030–2039 period (relative to the 1980–1999 period, with the change in total soil moisture calculated as a fraction of the 1980–1999 summer mean). We then calculate the correlation between the change in temperature (precipitation) and the change in soil moisture across the land grid points that encompass the RegCM3 domain. The CMIP3 ensemble uses "run 1" from the 18 CMIP3 GCMs archiving total soil moisture.

ensemble could be generated by internal atmospheric variability [*Dutton and Barron*, 2000]. The fact that our high-resolution ensemble is nested within an ensemble of coupled AOGCM experiments further enhances the effects of internal variability on the ensemble simulation. This atmosphere-ocean internal variability dominates the near-term "uncertainty" in the CMIP3 ensemble [*Hawkins and Sutton*, 2009]. However, by the mid-century, structural uncertainty from different model formulations is greater than that from internal variability [*Hawkins and Sutton*, 2009], suggesting that multiple GCM-RCM combinations could yield greater spread than is seen in our nested simulations.

[14] Our results suggest that near-term increases in GHG forcing could result in warm-season drying and intensification of hot extremes throughout much of the U.S. Indeed, all of the individual RegCM3 ensemble members exhibit at least 6 hottest-season occurrences in the 2030–2039 period over much of the western U.S. (Figure S6). However, the members vary in the level of hot event intensification in the eastern U.S., with three of the members showing substantial intensification in the 2030–2039 period, and two of the members showing very little intensification (Figure S6). (For reference, the RegCM3 f-member shows the greatest summer warming over the continental U.S. in the 2030–2039 period, while the g-member shows the least.) The variation seen within the physically-uniform RegCM3 ensemble (Figures S2, S3, and 3) suggests a strong influence of internal variability on decadal-scale changes in regional- and local-scale hot extremes.

5. Conclusions

[15] Because of the known sensitivity of natural and human systems, intensification of hot extremes could carry substantial impacts. At the end of the 2030–2039 period, the expected global mean temperature change relative to the late 20th century ranges from 1.0 to 1.7°C in the CMIP3 A1B scenario [*Meehl et al.*, 2007b], and from 1.1 to 1.3°C in the CCSM3 ensemble [*Meehl et al.*, 2006]. Given the IPCC calculation of approximately 0.8°C of global warming from the mid-19th century to the late 20th century [*Trenberth et al.*, 2007], the CMIP3 ensemble warming above pre-industrial conditions is approximately 1.8 to 2.5°C by the year 2040, while the CCSM3 ensemble is approximately 1.9 to 2.1°C. Further, given that global warming is likely to continue for decades after stabilization of GHG concentrations [*Meehl*, 2005], and that the late-21st century warming in the A1B scenario ranges from 2.25 to 4.25°C above the late 20th century [*Meehl et al.*, 2007b], the response to a given GHG stabilization target is likely to be greater than to the equivalent concentrations within the transient trajectory tested here. Although accurate decadal-scale climate prediction represents a significant challenge [e.g., *Meehl et al.*, 2009], the intensification of hot extremes reported here suggests that constraining global warming to 2°C above pre-industrial conditions may not be sufficient to avoid dangerous climate change.

[16] **Acknowledgments.** We thank two anonymous reviewers for their insightful comments. We thank Purdue's Rosen Center for Advanced Computing for providing computing resources for the CAM and RegCM simulations. We acknowledge the modeling groups, PCMDI, the WCRP's WGCM, and the U.S. DOE for their roles in making the CMIP3 dataset available. Our work was supported by NSF awards 0541491 and 0756624, and DOE awards DE-FG02-08ER64649 and DE-SC0001483.

References

Battisti, D. S., and R. L. Naylor (2009), Historical warnings of future food insecurity with unprecedented seasonal heat, *Science*, *323*(5911), 240–244, doi:10.1126/science.1164363.

Chen, P., and M. Newman (1998), Rossby wave propogation and the rapid development of upper-level anomalous anticyclones during the 1988 U.S. drought, *J. Clim.*, *112*4912504doi:10.1175/1520-0442(1998)011<2491:RWPATR>2.0.CO;2.

Christensen, J. H., et al. (2007), Regional climate projections, in *Climate Change 2007: The Physical Science Basis. Contribution of Working Group I to the Fourth Assessment Report of the Intergovernmental Panel on Climate Change*, edited by S. Solomon et al., pp. 847–940, Cambridge Univ. Press, Cambridge, U. K.

Collins, W. D., et al. (2006), The Community Climate System Model version 3 (CCSM3), *J. Clim.*, *19*, 2122–2143, doi:10.1175/JCLI3761.1.

Diffenbaugh, N. S., et al. (2005), Fine-cale processes regulate the response of extreme events to global climate change, *Proc. Natl. Acad. Sci. U. S. A.*, *102*(44), 15,774–15,778, doi:10.1073/pnas.0506042102.

Dutton, J. F., and E. J. Barron (2000), Intra-annual and interannual ensemble forcing of a regional climate model, *J. Geophys. Res.*, *105*(D24), 29,523–29,538, doi:10.1029/2000JD900467.

Fischer, E. M., S. I. Seneviratne, D. Lüthi, and C. Schär (2007a), Contribution of land-atmosphere coupling to recent European summer heat waves, *Geophys. Res. Lett.*, *34*, L06707, doi:10.1029/2006GL029068.

Fischer, E. M., et al. (2007b), Soil moisture—Atmosphere interactions during the 2003 European summer heat wave, *J. Clim.*, *20*, 5081–5099, doi:10.1175/JCLI4288.1.

Frich, P., et al. (2002), Observed coherent changes in climate extremes during the second half of the twentieth century, *Clim. Res.*, *19*, 193–212, doi:10.3354/cr019193.

Hawkins, E., and R. Sutton (2009), The potential to narrow uncertainty in regional climate predictions, *Bull. Am. Meteorol. Soc.*, *90*(8), 1095–1107, doi:10.1175/2009BAMS2607.1.

Lorenz, R., E. B. Jaeger, and S. I. Seneviratne (2010), Persistence of heat waves and its link to soil moisture memory, *Geophys. Res. Lett.*, *37*, L09703, doi:10.1029/2010GL042764.

Mastrandrea, M. D., and S. H. Schneider (2004), Probabilistic integrated assessment of "dangerous" climate change, *Science*, *304*(5670), 571–575, doi:10.1126/science.1094147.

Meehl, G. A. (2005), Climate change commitment in the twenty-first and twenty-second centuries, *Bull. Am. Meteorol. Soc.*, *86*(3), 326–327.

Meehl, G. A., and C. Tebaldi (2004), More intense, more frequent, and longer lasting heat waves in the 21st century, *Science*, *305*(5686), 994–997, doi:10.1126/science.1098704.

Meehl, G. A., et al. (2006), Climate change projections for the twenty-first century and climate change commitment in the CCSM3, *J. Clim.*, *19*, 2597–2616, doi:10.1175/JCLI3746.1.

Meehl, G. A., et al. (2007a), The WCRP CMIP3 multimodel dataset: A new era in climate change research, *Bull. Am. Meteorol. Soc.*, *88*(9), 1383–1394, doi:10.1175/BAMS-88-9-1383.

Meehl, G. A., et al. (2007b), Global climate projections, in *Climate Change 2007: The Physical Science Basis. Contribution of Working Group I to the Fourth Assessment Report of the Intergovernmental Panel on Climate Change*, edited by S. Solomon et al., pp. 747–845, Cambridge Univ. Press, Cambridge, U. K.

Meehl, G. A., et al. (2009), Decadal prediction, *Bull. Am. Meteorol. Soc.*, *90*(10), 1467–1485, doi:10.1175/2009BAMS2778.1.

Nackicenovic, N., et al. (2000), Special Report on Emissions Scenarios, 570 pp., Cambridge Univ. Press, Cambridge, U. K.

Pal, J. S., et al. (2007), Regional climate modeling for the developing world: The ICTP RegCM3 and RegCNET, *Bull. Am. Meteorol. Soc.*, *88*(9), 1395–1409, doi:10.1175/BAMS-88-9-1395.

Poumadere, M., et al. (2005), The 2003 heat wave in France: Dangerous climate change here and now, *Risk Anal.*, *25*(6), 1483–1494, doi:10.1111/j.1539-6924.2005.00694.x.

Seneviratne, S. I., et al. (2006), Land-atmosphere coupling and climate change in Europe, *Nature*, *443*(7108), 205–209, doi:10.1038/nature05095.

Schlenker, W., and M. J. Roberts (2009), Nonlinear temperature effects indicate severe damages to US crop yields under climate change, Proceedings of the National Academy of Sciences of the United States of America, *106*(37), 15,594–15,598.

Trapp, R. J., N. S. Diffenbaugh, and A. Gluhovsky (2009), Transient response of severe thunderstorm forcing to elevated greenhouse gas concentrations, *Geophys. Res. Lett.*, *36*, L01703, doi:10.1029/2008GL036203.

Trenberth, K. E., et al. (2007), Observations: Surface and atmospheric climate change, in *Climate Change 2007: The Physical Science Basis.*

Contribution of Working Group I to the Fourth Assessment Report of the Intergovernmental Panel on Climate Change, edited by S. Solomon et al., pp. 235–336, Cambridge Univ. Press, Cambridge, U. K.

United Nations Framework Convention on Climate Change (UNFCCC) (2009), The Copenhagen Accord, 5 pp., U. N., Geneva, Switzerland

Walker, M. D., and N. S. Diffenbaugh (2009), Evaluation of high-resolution simulations of daily-scale temperature and precipitation over the United States, *Clim. Dyn.*, *33*, 1131–1147, doi:10.1007/s00382-009-0603-y.

M. Ashfaq and N. S. Diffenbaugh, Woods Institute for the Environment and Department of Environmental Earth System Science, Stanford University, 473 Via Ortega, Stanford, CA 94305-4216, USA. (diffenbaugh@stanford.edu)

Emissions pathways, climate change, and impacts on California

Katharine Hayhoe[a,b], Daniel Cayan[c], Christopher B. Field[d], Peter C. Frumhoff[e], Edwin P. Maurer[f], Norman L. Miller[g], Susanne C. Moser[h], Stephen H. Schneider[i], Kimberly Nicholas Cahill[d], Elsa E. Cleland[d], Larry Dale[g], Ray Drapek[j], R. Michael Hanemann[k], Laurence S. Kalkstein[l], James Lenihan[j], Claire K. Lunch[d], Ronald P. Neilson[j], Scott C. Sheridan[m], and Julia H. Verville[e]

[a]ATMOS Research and Consulting, 809 West Colfax Avenue, South Bend, IN 46601; [c]Climate Research Division, The Scripps Institution of Oceanography, and Water Resources Division, U.S. Geological Survey, 9500 Gilman Drive, La Jolla, CA 92093-0224; [d]Department of Global Ecology, Carnegie Institution of Washington, 260 Panama Street, Stanford, CA 94305; [e]Union of Concerned Scientists, Two Brattle Square, Cambridge, MA 02238; [f]Civil Engineering Department, Santa Clara University, Santa Clara, CA 95053; [g]Atmosphere and Ocean Sciences Group, Earth Sciences Division, Lawrence Berkeley National Laboratory, 1 Cyclotron Road, Berkeley, CA 94720; [h]Environmental and Societal Impacts Group, National Center for Atmospheric Research, P.O. Box 3000, Boulder, CO 80307; [i]Department of Biological Sciences and Institute for International Studies, Stanford University, Stanford, CA 94305; [j]Corvallis Forestry Sciences Laboratory, U.S. Department of Agriculture Forest Service, 3200 SW Jefferson Way, Corvallis, OR 97331; [k]Department of Agricultural and Resource Economics, University of California, Berkeley, CA 94720; [l]Center for Climatic Research, Department of Geography, University of Delaware, Newark, DE 19716; and [m]Department of Geography, Kent State University, Kent, OH 44242

Contributed by Christopher B. Field, June 23, 2004

The magnitude of future climate change depends substantially on the greenhouse gas emission pathways we choose. Here we explore the implications of the highest and lowest Intergovernmental Panel on Climate Change emissions pathways for climate change and associated impacts in California. Based on climate projections from two state-of-the-art climate models with low and medium sensitivity (Parallel Climate Model and Hadley Centre Climate Model, version 3, respectively), we find that annual temperature increases nearly double from the lower B1 to the higher A1fi emissions scenario before 2100. Three of four simulations also show greater increases in summer temperatures as compared with winter. Extreme heat and the associated impacts on a range of temperature-sensitive sectors are substantially greater under the higher emissions scenario, with some interscenario differences apparent before midcentury. By the end of the century under the B1 scenario, heatwaves and extreme heat in Los Angeles quadruple in frequency while heat-related mortality increases two to three times; alpine/subalpine forests are reduced by 50–75%; and Sierra snowpack is reduced 30–70%. Under A1fi, heatwaves in Los Angeles are six to eight times more frequent, with heat-related excess mortality increasing five to seven times; alpine/subalpine forests are reduced by 75–90%; and snowpack declines 73–90%, with cascading impacts on runoff and streamflow that, combined with projected modest declines in winter precipitation, could fundamentally disrupt California's water rights system. Although interscenario differences in climate impacts and costs of adaptation emerge mainly in the second half of the century, they are strongly dependent on emissions from preceding decades.

California, with its diverse range of climate zones, limited water supply, and economic dependence on climate-sensitive industries such as agriculture, provides a challenging test case to evaluate impacts of regional-scale climate change under alternative emissions pathways. As characterized by the Intergovernmental Panel on Climate Change, demographic, socioeconomic, and technological assumptions underlying long-term emissions scenarios vary widely (1). Previous studies have not systematically examined the difference between projected regional-scale changes in climate and associated impacts across scenarios. Nevertheless, such information is essential to evaluate the potential for and costs of adaptation associated with alternative emissions futures and to inform mitigation policies (2).

Here, we examine a range of potential climate futures that represent uncertainties in both the physical sensitivity of current climate models and divergent greenhouse gas emissions pathways. Two global climate models, the low-sensitivity National Center for Atmospheric Research/Department of Energy Parallel Climate Model (PCM) (3) and the medium-sensitivity U.K. Met Office Hadley Centre Climate Model, version 3 (HadCM3), model (4, 5) are used to calculate climate change resulting from the SRES (Special Report on Emission Scenarios) B1 (lower) and A1fi (higher) emissions scenarios (1). These scenarios bracket a large part of the range of Intergovernmental Panel on Climate Change nonintervention emissions futures with atmospheric concentrations of CO_2 reaching ≈550 ppm (B1) and ≈970 ppm (A1fi) by 2100 (see *Emissions Scenarios* in *Supporting Text*, which is published as supporting information on the PNAS web site). Although the SRES scenarios do not explicitly assume any specific climate mitigation policies, they do serve as useful proxies for assessing the outcome of emissions pathways that could result from different emissions reduction policies. The scenarios at the lower end of the SRES family are comparable to emissions pathways that could be achieved by relatively aggressive emissions reduction policies, whereas those at the higher end are comparable to emissions pathways that would be more likely to occur in the absence of such policies.

Climate Projections

Downscaling Methods. For hydrological and agricultural analyses, HadCM3 and PCM output was statistically downscaled to a 1/8° grid (≈150 km^2) (6) and to individual weather stations (7) for analyses of temperature and precipitation extremes and health impacts. Downscaling to the 1/8° grid used an empirical statistical technique that maps the probability density functions for modelled monthly precipitation and temperature for the climatological period (1961–1990) onto those of gridded historical observed data, so the mean and variability of observations are reproduced by the climate model data. The bias correction and spatial disaggregation technique is one originally developed for adjusting General Circulation Model output for long-range streamflow forecasting (6), later adapted for use in studies examining the hydrologic impacts of climate change (8), and compares favorably to different statistical and dynamic downscaling techniques (9) in the context of hydrologic impact studies.

Station-level downscaling for analyses of temperature and precipitation extremes and health impacts used a deterministic method in which grid-cell values of temperatures and precipi-

Freely available online through the PNAS open access option.

Abbreviations: DJF, December, January, February; HadCM3, Hadley Centre Climate Model, version 3; JJA, June, July, August; PCM, Parallel Climate Model; SRES, Special Report on Emission Scenarios; SWE, snow water equivalent.

[b]To whom correspondence should be addressed. E-mail: hayhoe@atmosresearch.com.

© 2004 by The National Academy of Sciences of the USA

www.pnas.org/cgi/doi/10.1073/pnas.0404500101

NMED - PATZ
REBUTTAL EXHIBIT 10

Table 1. Summary of midcentury (2020–2049) and end-of-century (2070–2099) climate and impact projections for the HadCM3 and PCM B1 and A1fi scenarios

			2020–2049				2070–2099			
			PCM		HadCM3		PCM		HadCM3	
	Units	1961–1990	B1	A1fi	B1	A1fi	B1	A1fi	B1	A1fi
Change in statewide avg temperatures										
Annual	°C	15.0	1.35	1.5	1.6	2.0	2.3	3.8	3.3	5.8
Summer (JJA)	°C	22.8	1.2	1.4	2.2	3.1	2.15	4.1	4.6	8.3
Winter (DJF)	°C	7.6	1.3	1.2	1.4	1.45	2.15	3.0	2.3	4.0
Change in statewide avg precipitation										
Annual	mm	544	−37	−51	+6	−70	+38	−91	−117	−157
Summer (JJA)	mm	20	−3	+2	−1	−7	+4	−46	−5	−1
Winter (DJF)	mm	269	−45	−55	+4	−44	+13	−13	−79	−92
Sea level rise	cm	—	8.7	9.5	11.6	12.7	19.2	28.8	26.8	40.9
Heatwave days										
Los Angeles	Days	12	28	35	24	36	44	76	47	95
Sacramento	Days	58	91	101	93	104	109	134	115	138
Fresno	Days	92	113	120	111	116	126	147	126	149
El Centro	Days	162	185	185	176	180	191	213	197	218
Length of heatwave season*	Days	115	135	142	132	141	149	178	162	204
Excess mortality for Los Angeles†										
Without acclimatization	avg no. of deaths/yr	—	—	—	—	—	394	948	667	1,429
With acclimatization	avg no. of deaths/yr	165	—	—	—	—	319	790	551	1,182
Change in April 1 snowpack SWE										
1,000–2,000 m elevation	%	3.6 km³	−60	−56	−58	−66	−65	−95	−87	−97
2,000–3,000 m elevation	%	6.5 km³	−34	−34	−24	−36	−22	−73	−75	−93
3,000–4,000 m elevation	%	2.3 km³	−11	−15	4	−16	15	−33	−48	−68
All elevations	%	12.4 km³	−38	−37	−26	−40	−29	−73	−72	−89
Change in annual reservoir inflow‡										
Total	%	21.7 km³	−18	−22	5	−10	12	−29	−24	−30
Northern Sierra	%	15.2 km³	−19	−22	3	−9	9	−29	−20	−24
Southern Sierra	%	6.5 km³	−16	−23	10	−14	17	−30	−33	−43
Change in April–June reservoir inflow‡										
Total	%	9.1 km³	−20	−24	−11	−19	−1	−46	−41	−54
Northern Sierra	%	5.5 km³	−21	−24	−16	−19	−6	−45	−34	−47
Southern Sierra	%	3.6 km³	−18	−24	−2	−19	5	−47	−52	−65
Change water year flow centroid‡										
Total	Days	03/26	0	2	−15	−7	−7	−14	−23	−32
Northern Sierra	Days	03/13	0	3	−16	−5	−3	−11	−18	−24
Southern Sierra	Days	05/01	−10	−7	−19	−12	−22	−34	−34	−43

avg, average; JJA, June, July, August; DJF, December, January, February; SWE, snow water equivalent.

*The number of days between the beginning of the year's first and end of the year's last heatwave.

†Reference period is 1990–1999, and projections are for the period 2090–2099.

‡Results are for inflows to seven major dams and reservoirs in the Sacramento/San Joaquin water system, including three in the Northern Sierra (Shasta, Oroville, and Folsom) and four in the Southern Sierra (New Melones, New Don Pedro, Lake McClure, and Pine Flat).

tation from the reference period were rescaled by simple monthly regression relations to ensure that the overall probability distributions of the simulated daily values closely approximated the observed probability distributions at selected long-term weather stations (7). The same regression relations were then applied to future simulations, such that rescaled values share the weather statistics observed at the selected stations. At the daily scales addressed by this method, the need to extrapolate beyond the range of the historically observed parts of the probability distributions was rare even in the future simulations (typically <1% of the future days) because most of the climate changes involve more frequent warm days than actual truly warmer-than-ever-observed days (7).

Except where otherwise noted, we present projected climate anomalies and impacts averaged over 2020–2049 (with a midpoint of 2035) and 2070–2099 (here designated as end-of-century, with a midpoint of 2085), relative to a 1961–1990 reference period.

Temperature. All simulations show increases in annual average temperature before midcentury that are slightly greater under the higher A1fi emissions scenario (see Fig. 4, which is published as supporting information on the PNAS web site). By end-of-century, projected temperature increases under A1fi are nearly twice those under B1, with the more sensitive HadCM3 model producing larger absolute changes (Table 1). Downscaled seasonal mean temperature projections (10) show consistent spatial patterns across California, with lesser warming along the southwest coast and increasing warming to the north and northeast (Fig. 1). Statewide, the range in projected average temperature increases is higher than previously reported (11–14), particularly for summer temperature increases that are equal to or greater than increases in winter temperatures.

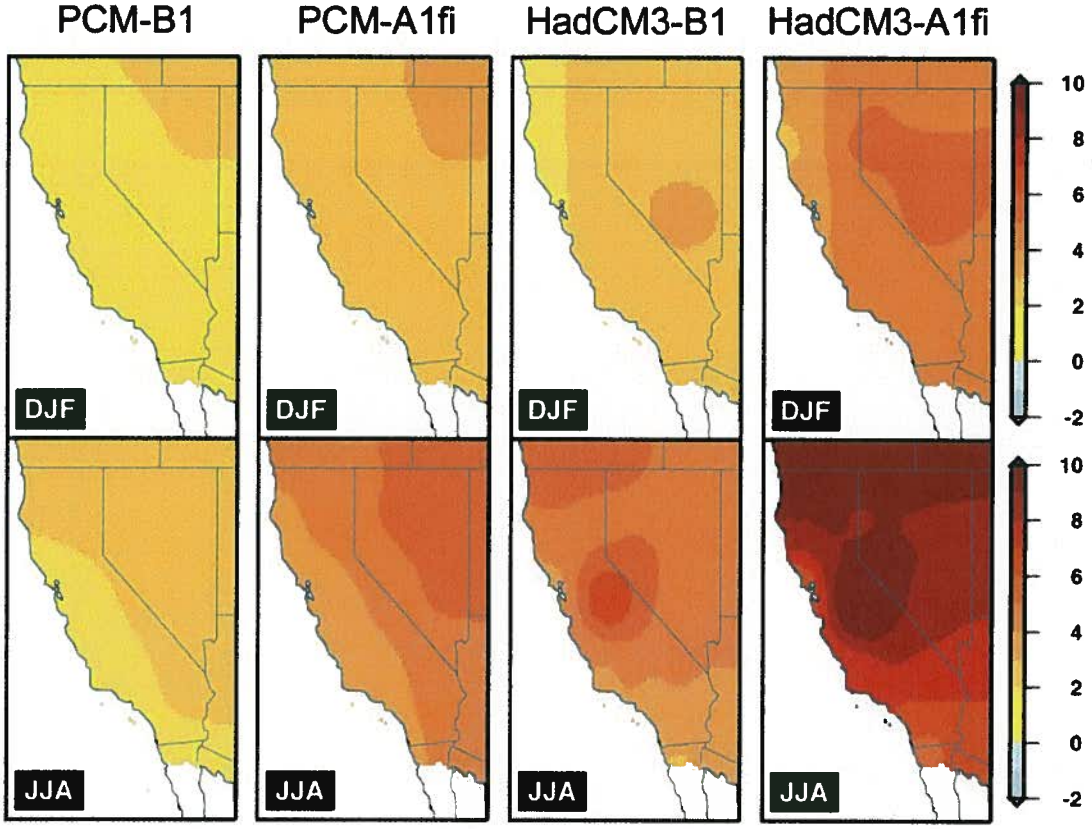

Fig. 1. Downscaled winter (DJF) and summer (JJA) temperature change (°C) for 2070–2099, relative to 1961–1990 for a 1/8° grid. Statewide, SRES B1 to A1fi winter temperature projections for the end of the century are 2.2–3°C and 2.3–4°C for PCM and HadCM3, respectively, compared with previous projections of 1.2–2.5°C and 3–3.5°C for PCM and HadCM2, respectively. End-of-century B1 to A1fi summer temperature projections are 2.2–4°C and 4.6–8.3°C for PCM and HadCM3, respectively, compared with previous projections of 1.3–3°C and 3–4°C for PCM and HadCM2, respectively (11–14).

Precipitation. Precipitation shows a tendency toward slight decreases in the second half of the century with no obvious interscenario differences in magnitude or frequency (see Figs. 5–10, which are published as supporting information on the PNAS web site). Three of four simulations project winter decreases of −15% to −30%, with reductions concentrated in the Central Valley and along the north Pacific Coast. Only PCM B1 projects slight increases (≈7%) by the end of the century (Table 1). These results differ from previous projections showing precipitation increases of 75–200% by 2100 (11–13), but they are consistent with recent PCM-based midrange projections (14, 15). The larger-scale pattern of rainfall over North America is more uniform across scenarios, showing an area of decreased (or lesser increase in) precipitation over California that contrasts with increases further up the coast (see Fig. 11, which is published as supporting information on the PNAS web site). Because interdecadal variability often dominates precipitation over California, projected changes in climate and impacts associated with the direct effects of temperature should be considered more robust than those determined by interactions between temperature and precipitation or precipitation alone.

Extreme Heat and Heat-Related Mortality

Temperature extremes increase in both frequency and magnitude under all simulations, with the most dramatic increases occurring under the A1fi scenario. Changes in local temperature extremes were evaluated based on exceedance probability analyses, by using the distribution of daily maximum temperatures downscaled to representative locations (16). Exceedance probabilities define a given temperature for which the probability exists that X% of days throughout the year will fall below that temperature (i.e., if the 35°C exceedance probability averages 95% for the period 2070–2099, this means that an average of 95% or ≈347 days per year are likely to lie below 35°C). For the four locations examined for extreme heat occurrence (Los Angeles, Sacramento, Fresno, and Shasta Dam), mean and maximum temperatures occurring 50% and 5% of the year increase by 1.5–5°C under B1 and 3.5–9°C under A1fi by the end of the century. Extreme temperatures experienced an average of 5% of the year during the historical period are also projected to increase in frequency, accounting for 12–19% (B1) and 20–30% (A1fi) of days annually by 2070–2099 (see Fig. 12, which is published as supporting information on the PNAS web site).

The annual number of days classified as heatwave conditions (3 or more consecutive days with temperature above 32°C) increases under all simulations, with more heatwave days under A1fi before midcentury (see Fig. 13, which is published as supporting information on the PNAS web site). Among the four locations analyzed, increases and interscenario differences are proportionally greatest for Los Angeles, a location that currently experiences relatively few heatwaves. By the end of the century, the number of heatwave days in Los Angeles increases four times under B1, and six to eight times under A1fi. Statewide, the length of the heatwave season increases by 5–7 weeks under B1 and by 9–13 weeks under A1fi by the end of this century, with interscenario differences emerging by midcentury (Table 1; see also Fig. 14, which is published information on the PNAS web site).

The connection between extreme heat and summer excess mortality is well established (17). Heat-related mortality estimates for the Los Angeles metropolitan area were determined

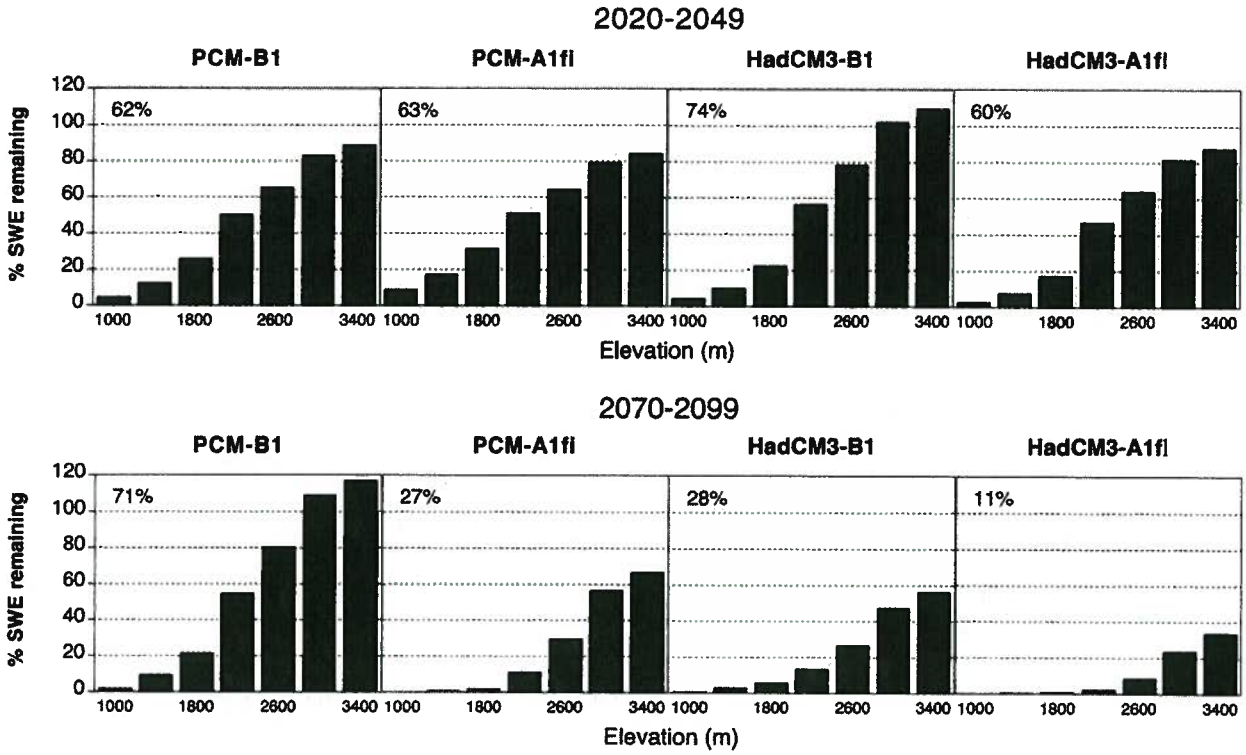

Fig. 2. Average snowpack SWE for 2020–2049 and 2070–2099 expressed as a percent of the average for the reference period 1961–1990 for the Sierra Nevada region draining into the Sacramento–San Joaquin river system. Total SWE losses by the end of the century range from 29–72% for the B1 scenario to 73–89% for the A1fi scenario. Losses are greatest at elevations below 3,000 m, ranging from 37–79% for B1 to 81–94% for A1fi by the end of the century. Increases in high elevation SWE for midcentury HadCM3 B1 and end-of-century PCM B1 runs result from increased winter precipitation in these simulations.

by threshold meteorological conditions beyond which mortality tends to increase. An algorithm was developed to determine the primary environmental factors (including maximum apparent temperature, number of consecutive days above the threshold apparent temperature, and time of year) that explain variability in excess mortality for all days with apparent maximum temperatures at or above the derived daily threshold apparent temperature (18) value of 34°C (see *Heat-Related Mortality* in *Supporting Text*). Estimates do not account for changes in population or demographic structure.

From a baseline of ≈165 excess deaths during the 1990s, heat-related mortality in Los Angeles is projected to increase by about two to three times under B1 and five to seven times under A1fi by the 2090s if acclimatization is taken into account (see *Heat-Related Mortality* in *Supporting Text*). Without acclimatization, these estimates are about 20–25% higher (Table 1). Actual impacts may be greater or lesser depending in part on demographic changes and societal decisions affecting preparedness, health care, and urban design. Individuals likely to be most affected include elderly, children, the economically disadvantaged, and those who are already ill (19, 20).

Impacts on Snowpack, Runoff, and Water Supply

Rising temperatures, exacerbated in some simulations by decreasing winter precipitation, produce substantial reductions in snowpack in the Sierra Nevada Mountains, with cascading impacts on California winter recreation, streamflow, and water storage and supply. Snowpack SWE was estimated by using daily, bias-corrected and spatially downscaled temperature and precipitation to drive the Variable Infiltration Capacity distributed land surface hydrology model. The Variable Infiltration Capacity model, using the resolution and parameterization also implemented in this study, has been shown to reproduce observed streamflows when driven by observed meteorology (10) and has been applied to simulate climate change (8) in this region. April 1 SWE decreases substantially in all simulations before midcentury (see Fig. 15, which is published as supporting information on the PNAS web site). Reductions are most pronounced at elevations below 3,000 m, where 80% of snowpack storage currently occurs (Table 1 and Fig. 2). Interscenario differences emerge before midcentury for HadCM3 and by the end of the century for both models. These changes will delay the onset of and shorten the ski season in California (see *Impact of Decreasing Snowpack on California's Ski Industry* in *Supporting Text*).

Water stored in snowpack is a major natural reservoir for California. Differences in SWE between the B1 and A1fi scenarios represent ≈1.7 km^3 of water storage by midcentury and 2.1 km^3 by the end of the century for HadCM3. For PCM, overall SWE losses are smaller, but the difference between the A1fi and B1 scenarios is larger by the end of the century, representing >4 km^3 of storage. Reductions for all simulations except PCM under the lower B1 emission scenario are greater than previous projections of diminishing snowpack for the end of the century (8, 21). By 2020–2049 the SWE loss is comparable to that previously projected for 2060 (22).

Warmer temperatures and more precipitation falling as rain instead of snow also causes snowmelt runoff to shift earlier under all simulations (Table 1), which is consistent with earlier studies (23). The magnitude of the shift is greater in the higher-elevation Southern basins and under the higher A1fi scenario. Stream inflows to major reservoirs decline because of diminished snowpack and increased evaporation before midcentury, except where winter precipitation increases (Table 1). The greater reductions in inflows seen under A1fi are driven by both higher temperatures and lower average precipitation as compared with B1.

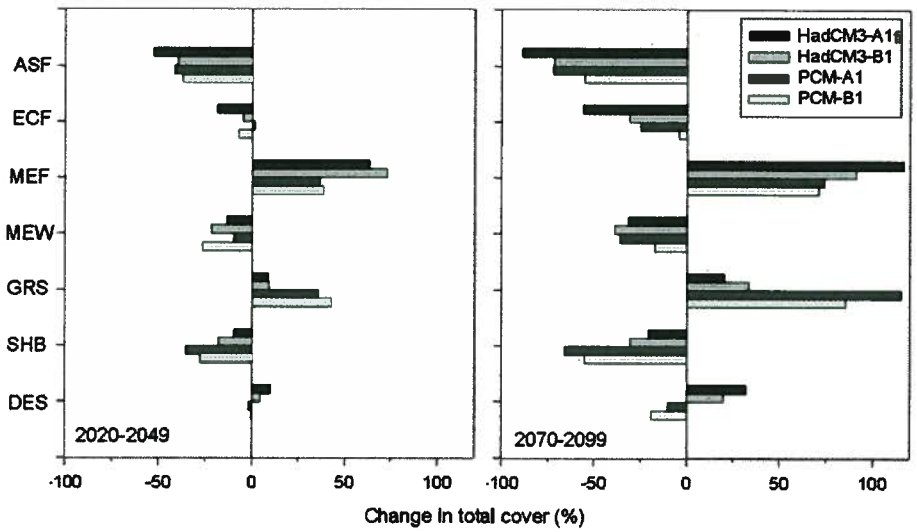

Fig. 3. Statewide change in cover of major vegetation types for 2020–2049 and 2070–2099, relative to simulated distributions for the 1961–1990 reference period. ASF, alpine/subalpine forest; ECF, evergreen conifer forest; MEF, mixed evergreen forest; MEW, mixed evergreen woodland; GRS, grassland; SHB, shrubland; DES, desert. Increasing temperatures drive the reduction in alpine/subalpine forest cover and cause mixed conifer forest to displace evergreen conifer forest in the Sierra Nevada Mountains and the North Coast. Mixed conifer forest in the South Coast expands because of increased humidity and reduced fire frequency. Because of drier conditions and increased fire frequency in inland locations, grassland displaces shrubland and woodland, particularly in the PCM simulations, whereas warmer and drier conditions under HadCM3 cause an expansion of desert cover in the southern Central Valley.

Earlier runoff may also increase the risk of winter flooding (7). Currently, state operators maintain ≈12 km^3 of total vacant space in the major reservoirs to provide winter and early spring flood protection,[n] a volume approximately equal to that stored in the natural snowpack reservoir by April 1st. Capturing earlier runoff to compensate for future reductions in snowpack would take up most of the flood protection space, forcing a choice between winter flood prevention and maintaining water storage for the summer and fall dry period use. Flood risk and freshwater supply are also affected by higher sea levels, which are projected to rise 10–40 cm under B1 and 20–65 cm under A1fi by 2100 (Table 1; see also Fig. 16, which is published as supporting information on the PNAS web site).

Declining Sierra Nevada snowpack, earlier runoff, and reduced spring and summer streamflows will likely affect surface water supplies and shift reliance to groundwater resources, already overdrafted in many agricultural areas in California (24). This could impact 85% of California's population who are agricultural and urban users in the Central Valley, San Francisco Bay Area, and the South Coast, about half of whose water is supplied by rivers of the Central Valley. Under A1fi (both models) and B1 (HadCM3), the projected length, frequency, and severity of extreme droughts in the Sacramento River system during 2070–2099 substantially exceeds what has been experienced in the 20th century. The proportion of years projected to be dry or critical increases from 32% in the historical period to 50–64% by the end of the century under all but the wetter PCM B1 scenario (see Table 2, which is published as supporting information on the PNAS web site). Changes in water availability and timing could disrupt the existing pattern of seniority in month-dependent water rights by reducing the value of rights to mid- and late-season natural streamflow and boosting the value of rights to stored water. The overall magnitude of impacts on water users depends on complex interactions between temperature-driven snowpack decreases and runoff timing, precipitation, future population increases, and human decisions regarding water storage and allocation (see *Impacts on Water Supply* in *Supporting Text*).

Impacts on Agriculture and Vegetation Distribution

In addition to reductions in water supply, climate change could impact California agriculture by increasing demand for irrigation to meet higher evaporative demand, increasing the incidence of pests (25), and through direct temperature effects on production quality and quantity. Dairy products (milk and cream, valued at $3.8 billion annually) and grapes ($3.2 billion annually) are the two highest-value agricultural commodities of California's $30 billion agriculture sector (26). Threshold temperature impacts on dairy production and wine grape quality were calculated by using downscaled temperature projections for key counties, relative to average observed monthly temperatures.[o]

For dairy production, losses were estimated for temperatures above a 32°C threshold (27), as well as for additional losses between 25°C (28) and 32°C. For the top 10 dairy counties in the state (which account for 90% of California's milk production), rising temperatures were found to reduce production by as much as 7–10% (B1) and 11–22% (A1fi) by the end of the century (see Table 3, which is published as supporting information on the PNAS web site). Potential adaptations may become less practical with increasing temperature and humidity (29).

For wine grapes, excessively high temperatures during ripening can adversely affect quality, a major determinant of market value. Assuming ripening occurs at between 1,150 and 1,300 biologically active growing degree days (30), ripening month was determined by summing modeled growing degree days above 10°C from April to October, for both baseline and projected scenarios. Monthly average temperature at the time of ripening was used to estimate potential temperature impacts on quality. For all simulations, average ripening occurs 1–2 months earlier and at higher temperatures, leading to degraded quality and marginal/impaired conditions for all but the cool coastal region

[n]See the U.S. Army Corps of Engineers Flood Control Requirements for California Reservoirs, Sacramento District Water Control Data System, Sacramento, CA (www.spk-wc.usace.army.mil).

[o]See Western U.S. Climate Historical Summaries (Western Regional Climate Center) at www.wrcc.dri.edu/climsum.html.

under all scenarios by the end of the century (see Table 3, which is published as supporting information on the PNAS web site). As with other perennial crops, adaptation options to shift varieties or locations of production would require significant time and capital investment.

The distribution of California's diverse vegetation types also changes substantially over the century relative to historical simulations (Fig. 3; see also Fig. 17, which is published as supporting information on the PNAS web site). Projections of changes in vegetation distribution are those given by MC1, a dynamic general vegetation model that simulates climate-driven changes in life-form mixtures and vegetation types; ecosystem fluxes of carbon, nitrogen, and water; and fire disturbance over time (31). Vegetation shifts driven primarily by temperature, such as reductions in the extent of alpine/subalpine forest and the displacement of evergreen conifer forest by mixed evergreen forest, are consistent across models and more pronounced under A1fi by the end of the century. Changes driven by precipitation and changes in fire frequency are model-dependent and do not exhibit consistent interscenario differences. Most changes are apparent before mid-century, with the exception of changes in desert cover. The shift from evergreen conifer to mixed evergreen forest and expansion of grassland are consistent with previous impact analyses (13), whereas the extreme reduction in alpine/subalpine forest and expansion of desert had not been reported in previous impacts assessments (12, 13).

Conclusions

Consistent and large increases in temperature and extreme heat drive significant impacts on temperature-sensitive sectors in California under both lower and higher emissions scenarios, with the most severe impacts occurring under the higher A1fi scenario. Adaptation options are limited for impacts not easily controlled by human intervention, such as the overall decline in snowpack and loss of alpine and subalpine forests. Although interscenario differences in climate impacts and costs of adaptation emerge mainly in the second half of the century, they are largely entrained by emissions from preceding decades (32). SRES scenarios do not explicitly assume climate-specific policy intervention, and thus this study does not directly address the contrast in impacts due to climate change mitigation policies. However, these findings support the conclusion that climate change and many of its impacts scale with the quantity and timing of greenhouse gas emissions (33). As such, they represent a solid starting point for assessing the outcome of changes in greenhouse gas emission trajectories driven by climate-specific policies (32, 34), and the extent to which lower emissions can reduce the likelihood and thus risks of "dangerous anthropogenic interference with the climate system" (35).

We thank Michael Dettinger and Mary Meyer Tyree for providing assistance with data and analysis, and Frank Davis for providing review of earlier drafts of this manuscript. PCM model results were provided by PCM personnel at the National Center for Atmospheric Research, and HadCM3 model results were provided by Dr. David Viner from the U.K. Met Office's Climate Impacts LINK Project. This work was supported in part by grants from the David and Lucile Packard Foundation, the William and Flora Hewlett Foundation, the Energy Foundation, the California Energy Commission, the National Oceanic and Atmospheric Administration Office of Global Programs, and the Department of Energy.

1. Nakićenović, N., Alcamo, J., Davis, G., de Vries, B., Fenhann, J., Gaffin, S., Gregory, K., Grübler, A., Jung, T. Y., Kram, T., *et al.* (2000) *Intergovernmental Panel on Climate Change Special Report on Emissions Scenarios* (Cambridge Univ. Press, Cambridge, U.K.).
2. Parry, M. (2002) *Global Environ. Change* **12** (3), 149–153.
3. Washington, W. M., Weatherly, J. W., Meehl, G. A., Semtner, A. J., Bettge, T. W., Craig, A. P., Strand, W. G., Arblaster, J., Wayland, V. B., James, R. & Zhang, Y. (2000) *Clim. Dyn.* **16,** 755–774.
4. Gordon, C., Cooper, C., Senior, C. A., Banks, H., Gregory, J. M., Johns, T. C., Mitchell, J. F. B. & Wood, R. A. (2000) *Clim. Dyn.* **16,** 147–168.
5. Pope, V. D., Gallani, M. L., Rowntree, P. R. & Stratton, R. A. (2000) *Clim. Dyn.* **16,** 123–146.
6. Wood, A. W., Maurer, E. P., Kumar, A. & Lettenmaier, D. P. (2002) *J. Geophys. Res.* **107,** 4429, 10.1029/2001JD000659.
7. Dettinger, M. D., Cayan, D. R., Meyer, M. K. & Jeton, A. E. (2004) *Clim. Change* **62,** 283–317.
8. VanRheenan, N. T., Wood, A. W., Palmer, R. N. & Lettenmaier, D. P. (2004) *Clim. Change* **62,** 257–281.
9. Wood, A. W., Leung, L. R., Sridhar, V. & Lettenmaier, D. P. (2004) *Clim. Change* **62,** 189–216.
10. Maurer, E. P., Wood, A. W., Adam, J. C., Lettenmaier, D. P. & Nijssen, B. (2002) *J. Clim.* **15,** 3237–3251.
11. Field, C. B., Daily, G. C., Davis, F. W., Gaines, S., Matson, P. A., Melack, J. & Miller, N. L. (1999) *Confronting Climate Change in California: Ecological Impacts on the Golden State* (Union of Concerned Scientists, Cambridge, MA, and Ecological Society of America, Washington, DC).
12. Wilkinson, R., Clarke, K., Goodchild, M., Reichman, J. & Dozier, J. (2002) *The Potential Consequences of Climate Variability and Change for California: The California Regional Assessment* (U.S. Global Change Research Program, Washington, DC).
13. Wilson, T., Williams, L., Smith, J. & Medelsohn, R. (2003) *Global Climate Change and California: Potential Implications for Ecosystems, Health, and the Economy,* Publication No. 500-03-058CF (California Energy Commission, Public Interest Energy Research Environmental Area, Sacramento).
14. Leung, L. R., Qian, Y., Bian, X., Washington, W. M., Han, J. & Roads, J. O. (2004) *Clim. Change* **62,** 75–113.
15. Snyder, M. A., Bell, J. L., Sloan, L. C., Duffy, P. B. & Govindasamy, B. (2002) *Geophys. Res. Lett.* **29,** 1514–1517.
16. Miller, N. L., Bashford, K. E. & Strem, E. (2003) *J. Am. Water Resour. Assoc.* **39,** 771–784.
17. Kalkstein, L. S. & Davis, R. E. (1989) *Ann. Assoc. Am. Geogr.* **79,** 44–64.
18. Watts, J. D. & Kalkstein, L. S. (2004) *J. Appl. Meteorol.* **43,** 503–513.
19. McGeehin, M. A. & Mirabelli, M. (2001) *Environ. Health Perspect.* **109,** 185–189.
20. Chestnut, L. G., Breffle, W. S., Smith, J. B. & Kalkstein, L. S. (1998) *Environ. Sci. Policy* **1,** 59–70.
21. Knowles, N. & Cayan, D. R. (2002) *Geophys. Res. Lett.* **29,** 1891–1895.
22. Knowles, N. & Cayan, D. R. (2004) *Clim. Change* **62,** 319–336.
23. Gleick, P. H. & Chalecki, E. L. (1999) *J. Am. Water Resour. Assoc.* **35,** 1429–1441.
24. California Department of Water Resources, Division of Planning and Local Assistance (1998) *Bulletin 160–98: California Water Plan* (California Department of Water Resources, Sacramento).
25. Harrington, R. & Stork, N. E., eds. (1995) *Insects in a Changing Environment* (Academic, London).
26. California Agricultural Statistics Service (2002) *California Agriculture Statistical Review* (California Agricultural Statistics Service, Sacramento).
27. Ahmed, M. M. M. & El Amin, A. I. (1997) *J. Arid Environ.* **35,** 737–745.
28. Mellado, M. (1995) *Veterinaria* **26,** 389–399.
29. Pittock, B., Wratt, D., Basher, R., Bates, B., Finlayson, M., Gitay, H., Woodward, A., Arthington, A., Beets, P., Biggs, B., *et al.* (2001) in *Climate Change 2001: Impacts, Adaptation, and Vulnerability* (Cambridge Univ. Press, Cambridge, U.K.).
30. Gladstones, J. (1992) *Viticulture and Environment* (Winetitles, Underdale, South Australia), 310 pp.
31. Lenihan, J., Drapek, R., Bachelet, D. & Neilson, R. (2003) *Ecol. Appl.* **13,** 1667–1681.
32. Swart, R., Mitchell, J., Morita, T. & Raper, S. (2002) *Global Environ. Change* **12,** 155–165.
33. Houghton, J. T., Ding, Y., Griggs, D. J., Noguer, M., van der Linden, P. J. & Xiaosu, D., eds. (2001) *Climate Change 2001: The Scientific Basis* (Cambridge Univ. Press, Cambridge, U.K.).
34. Arnell, N. W., Livermore, M. J. L., Kovats, S., Levy, P. E., Nicholls, R., Parry, M. L. & Gaffin, S. R. (2004) *Global Environ. Change* **14,** 3–20.
35. United Nations (1992) *United Nations Framework Convention on Climate Change* (United Nations, Rio de Janeiro, Brazil).

IOP PUBLISHING ENVIRONMENTAL RESEARCH LETTERS
Environ. Res. Lett. 5 (2010) 014007 (9pp) doi:10.1088/1748-9326/5/1/014007

Implications of incorporating air-quality co-benefits into climate change policymaking

G F Nemet[1,2], T Holloway[1] and P Meier[3]

[1] Nelson Institute Center for Sustainability and the Global Environment (SAGE), University of Wisconsin–Madison, Madison, WI, USA
[2] La Follette School of Public Affairs, University of Wisconsin–Madison, Madison, WI, USA
[3] Energy Institute, University of Wisconsin–Madison, Madison, WI, USA

Received 2 October 2009
Accepted for publication 5 January 2010
Published 22 January 2010
Online at stacks.iop.org/ERL/5/014007

Abstract
We present an analysis of the barriers and opportunities for incorporating air quality co-benefits into climate policy assessments. It is well known that many strategies for reducing greenhouse gas emissions also decrease emissions of health-damaging air pollutants and precursor species, including particulate matter, nitrogen oxides, and sulfur dioxide. In a survey of previous studies we found a range of estimates for the air quality co-benefits of climate change mitigation of \$2-196/tCO_2 with a mean of \$49/tCO_2, and the highest co-benefits found in developing countries. These values, although of a similar order of magnitude to abatement cost estimates, are only rarely included in integrated assessments of climate policy. Full inclusion of these co-benefits would have pervasive implications for climate policy in areas including: optimal policy stringency, overall costs, distributional effects, robustness to discount rates, incentives for international cooperation, and the value of adaptation, forests, and climate engineering relative to mitigation. Under-valuation results in part from uncertainty in climatic damages, valuation inconsistency, and institutional barriers. Because policy debates are framed in terms of cost minimization, policy makers are unlikely to fully value air quality co-benefits unless they can be compared on an equivalent basis with the benefits of avoided climatic damages. While air quality co-benefits have been prominently portrayed as a hedge against uncertainty in the benefits of climate change abatement, this assessment finds that full inclusion of co-benefits *depends on*—rather than substitutes for—better valuation of climate damages.

Keywords: co-benefits, climate policy, air pollution, health

1. Introduction

Changing the energy system in order to stabilize the climate is likely to have a wide variety of effects that are not directly related to greenhouse gas emissions, including human health, macro-economic, geo-political, eco-system, agricultural yields, and employment patterns. Those effects that are favorable to human welfare are often termed 'co-benefits'. The use of the term *benefits* reflects the situation that decisions related to whether, how, and how much to address climate change are typically made with some consideration of the costs and benefits associated with various policy options. These decisions however do not usually consider the full range of effects of actions to address climate change. Among the most important of known co-benefit effects are those associated with air quality and the resulting impacts on human health. Changes in the technologies used to produce and consume energy, as well as the level of energy consumption, have two effects related to air quality. First, many of the changes that would reduce greenhouse gas emissions would reduce other emissions as well, such as nitrogen oxides (NO_x), sulfur dioxide (SO_2), particulate matter, and mercury, and the resulting pollution-related disease. Second, many of these changes would obviate the need for expensive pollution-control equipment—such as flue-gas desulfurization, selective catalytic reduction, and electrostatic precipitators—in order to comply with air quality regulations. How important are air quality (AQ) co-benefits? Why are they not considered in assessments of climate policy design? A primary finding is that the focus on cost minimization—rather than comparison of benefits and costs—diminishes the role of benefits in general. As a result, well-established AQ benefits are not a central part

 © 2010 IOP Publishing Ltd Printed in the UK

NMED - PATZ
REBUTTAL EXHIBIT 11

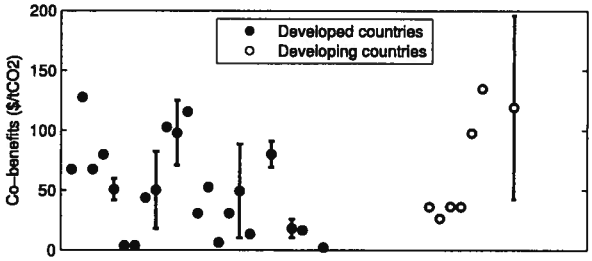

Figure 1. Estimates of the value of air quality co-benefits in developed (left) and developing country studies (right) in 2008$/ton$CO_2$. Within each category, data are reported from left to right by date of study (1991–2010). Absence of values indicates a co-benefit study for which health impacts were assessed, but valuation in $/t$CO_2$ was not.

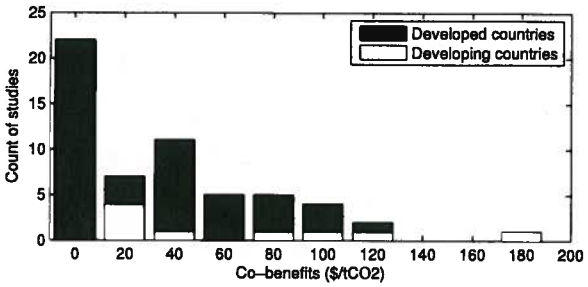

Figure 2. Frequency of values reported in air quality co-benefits studies.

of the climate policy discourse and probably rely on better characterization of climatic benefits in order to be fully valued.

We first review estimates of the value of air quality benefits of climate change policies and in section 3, the extent to which these co-benefits are valued in integrated assessment models. We then discuss the policy implications of including AQ co-benefit considerations in climate policy decision making and explore the reasons why economic policy models tend to ignore, even if they acknowledge, the value of co-benefits. We discuss data and modeling needs to resolve the existing impasse.

2. The value of AQ co-benefits is large

A large set of studies now makes clear that the magnitude of AQ co-benefits of climate change mitigation are non-trivial and have been observed across varied geographies, time periods, and sectors. We surveyed 37 peer-reviewed studies of AQ co-benefits (see the appendix). These studies provided 48 estimates of the economic value of air quality benefits of climate change mitigation, and span diverse geographies, time horizons, valuation techniques, and involve different mixes of economic sectors contributing to mitigation. Because the perspective of this study is on policy making amidst competing social priorities, we restricted our survey to those studies that (1) calculated an economic value of co-benefits, and (2) expressed values in terms of $/ton of CO_2 avoided. This restriction means that we do not include the results from a number of the studies we surveyed, and a larger portion of the studies of developing countries.

In figure 1, studies of developed countries are shown on left and those of developing countries on right. Within each category, data are reported from left to right by date of study (1991–2010), consistent with the studies reported in the appendix tables. Absence of values indicates a co-benefit study for which health impacts were assessed, but valuation in $/t$CO_2$ was not assessed. All values have been converted into constant 2008 dollars. Note that economic valuation was more frequent in developed country studies; 17 out of 24 developed country studies included $/t$CO_2$ estimates compared to 2 out of 13 developing country studies.

Figure 2 shows the frequency of values cited across all studies. The values for developed countries are in black and those for developing countries in white. For the 22 estimates from the 24 developed country studies the range was \$2-128/tCO_2, the median was \$31/tCO_2 and the mean \$44/tCO_2. For the 7 estimates from the 13 developing country studies the range was \$27-196/tCO_2, the median was \$43/tCO_2 and mean was \$81/tCO_2. Values are generally higher in developing countries, although the difference in means is not significant ($0.10 < p < 0.05$) in part due to variation in sector assessed and the dearth of developing country studies that assign economic value to co-benefits.

Heterogeneity in the distribution of study results is partially attributable to constraints on the scalability of AQ co-benefits at more stringent emissions reduction levels. At higher levels of greenhouse gas (GhG) abatement, abatement costs rise but AQ co-benefits remain constant (Burtraw *et al* 2003). Moreover, the apparently higher values in developing country studies result from these countries beginning with higher pollution levels, at which incremental health benefits are large. As emissions reductions become more aggressive, AQ co-benefits play a smaller role. Thus, valuation of AQ co-benefits is most important in the early stages of a long-term climate change mitigation strategy, and most important for developing countries lacking significant air quality management programs.

3. AQ co-benefits are not included in climate policy analyses

Even though the AQ co-benefits of climate change actions are well established, policy analyses typically do *not* account for them. We surveyed 13 major climate policy assessments based on integrated assessment models, selecting based on prominence and their intention to specifically inform policy decisions related to climate change. We drew from those used by the Intergovernmental Panel on Climate Change (IPCC), as well as government sponsored reports to model the impacts of specific policies in the UK and US. With one exception, the models reviewed are integrated assessments in that they combine assessments of both the physical and economic impacts of climate policies. Most of the models listed in table 1 (A, B, D–G, I, K–M) are partial or general equilibrium models, known as *top-down* models, which assess the direct and indirect economic effects of policies. Two (C, H) are systems engineering models that include technological detail and take a *bottom-up* approach. Model J is a benefit-cost analysis. In most cases the objective function is based on minimizing the abatement cost of meeting a climate emissions

Table 1. Treatment of AQ co-benefits in integrated assessment models of climate change policy.

	Venue	Model name	Time	GhG emissions	Value climate impacts	Estimate AQ co-b.	Value AQ co-b.	Include in final values
A	IPCC	IMAGE[a]	2100	Yes	No	No	—	—
B	IPCC	MERGE[a]	2150	Yes	No	No	—	—
C	IPCC	MESSAGE[a]	2100	Yes	No	No	—	—
D	IPCC	MiniCAM[a]	2100	Yes	No	No	—	—
E	IPCC	SGM[a]	2050	Yes	No	No	—	—
F	IPCC	WIAGEM[a]	2100	Yes	No	No	—	—
G	Nordhaus (2008)	DICE-2007[b]	2200	Yes	Yes	No	—	—
H	UK	C.C. Act of 2008 Assessment (MARKAL)[c]	2050	Yes	Yes	Yes	Yes	Yes
I	UK	Stern 2005/PAGE2002[d]	2200	Yes	Yes	Yes	Yes	No
J	US	C.B.O. (2009)[e]	2019	No	No	No	—	—
K	US	EIA NEMS (2008)[f]	2030	Yes	No	No	—	—
L	US	EPA ADAGE (2008)[g]	2050	Yes	No	No	—	—
M	US	EPA IGEM (2008)[g]	2050	Yes	No	No	—	—

[a]IPCC (2007). [b]Nordhaus (2008). [c]DECC (2008). [d]Stern (2006). [e]CBO (2009). [f]EIA (2008). [g]EPA (2008).

goal; climate damage costs are excluded. Only one (I) maximizes welfare by accounting for the benefits of avoided damages. The following section discusses why this final distinction is especially relevant to the treatment of AQ co-benefits.

Although 12 of the 13 models surveyed estimate emissions of greenhouse gases, only three (G, H, I) estimate the value of the resulting climate change damages. The others simply minimize the costs of achieving a specified set of annual emissions targets. Of the three that do estimate both costs and benefits of climate policy, only two (H, I) estimate air quality benefits—and only one of those (H) includes these values in the final cost estimates. The Stern review (I) does discuss AQ co-benefits and even quantifies them in dollar terms as 'up to 1% of GDP' (Stern 2006). But crucially, that study excludes this value in their highly publicized final results of the impacts and costs to address climate change. Only the UK Climate Change Act 2008 Impact Assessment (H in table 1) includes a value for improved air quality (£32b) in their final estimate (DECC 2008).

Beyond these high profile studies, recent work provides examples of more comprehensive inclusion of AQ co-benefits. Ostblom and Samakovlis (2007) include co-benefits in a CGE model for Sweden and find that the costs of climate policy are overstated if they are excluded. Bollen *et al* (2009) adapt a version of model B above to perform a cost-benefit analysis that includes both climatic and AQ impacts; they find the AQ co-benefits twice as large as climatic benefits. Early results from models such as GAINS combine estimates as well (Amann *et al* 2009).

An essential problem hindering inclusion of AQ co-benefits in policy decisions is that debates are framed in terms of minimizing the costs of climate policy. Because the benefits of avoided climate change are not explicitly considered, AQ benefits must somehow be compared to abatement costs[4]. Abatement levels are typically chosen exogenously with very little explicit justification for the specific targets adopted. For example, some targets attempt compliance with the ambiguous objective of avoiding *dangerous interference with the climate system,* as agreed on in the 1992 UN Framework Convention on Climate Change (Kriegler 2007). If full benefit-cost analyses were performed, the valuation of AQ co-benefits would be much simpler, as the addition of AQ co-benefits would imply a more stringent level of pollution abatement. The left panel of figure 3(a) shows that inclusion of air quality impacts would shift the marginal damages cost curve (MDC) upward so that its intersection with the marginal abatement cost curve (MAC) move to the right and as a result, the optimal level of pollution abatement would increase from q^* to q'. In practice, however, optimizing the level of emissions is not the objective of policy makers and is not the approach taken by analysis to inform them.

With exogenously specified targets, the marginal damages of climate change do not influence choices among policy options. Rather, the goal of policy design is to minimize the cost of meeting previously selected abatement levels. Inclusion of AQ co-benefits is less straightforward in this situation because policy debates are focused on the costs of pollution abatement; benefits are not a central part of the policy discourse. From this perspective, AQ co-benefits have to somehow affect the slope or position of the marginal abatement cost curve, rather than the damage curve. For example, the right panel of figure 3(b) shows that addition of AQ co-benefits could be interpreted as shifting the MAC curve downward. The marginal damage curve has been removed from that panel because it does not affect decisions. This shift requires the awkward re-interpretation of the AC as the sum of climate change abatement costs and AQ co-benefits ($MAC_{CC} + MDC_{AQ}$). The shift reduces the cost of climate policy such that the marginal cost, given the exogenously selected abatement level q^*, falls from p^* to p' as a result. The cost of the policy has gotten cheaper for the same level of emissions reductions. Most co-benefits studies and their normative policy claims result from conceiving of the abatement cost curve as this hybrid of climate costs and AQ benefits, even if estimation of p' is rarely explicit. For example, claims of 'no regrets'

[4] While it is optimal to use one policy instrument for each source of market failure, in reality the climate policies in discussion today include dozens of policy instruments within each piece of legislation. In part this is due to the presence of multiple market failures (Jaffe *et al* 2005).

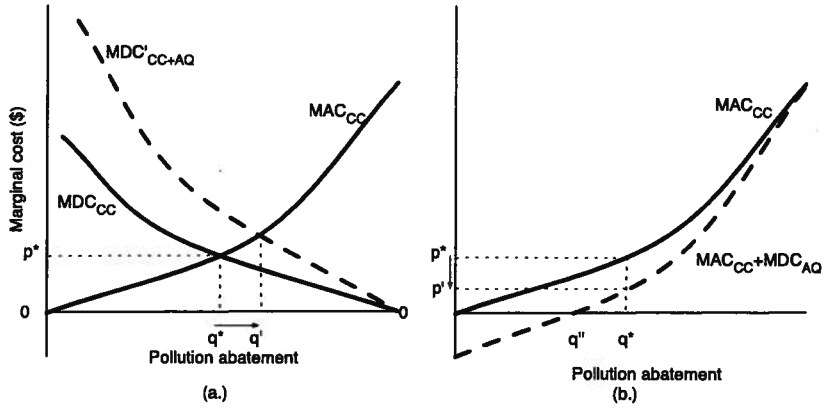

Figure 3. Effect of inclusion of air quality co-benefits on the marginal cost of climate policy. Left panel (a) shows air quality co-benefits interpreted as avoided damages. Right panel (b) shows air quality co-benefits interpreted as reducing abatement costs.

climate policy refer to the existence of abatement opportunities to the left of q'' where policy costs are below zero due to positive co-benefits. Rather, we are given p^* and told it is an overestimate—even in studies as thorough and as prominent as the Stern review. Full valuation of AQ co-benefits requires a more explicit discussion of how these cost impacts are calculated.

4. Implications of including AQ co-benefits

More thorough inclusion of AQ co-benefits would have several important effects on climate policy debates—both on optimal design and on positions held by stakeholders. The first implication is that inclusion of AQ co-benefits will reduce the societal cost of climate policy, as in figure 3(b). Alternatively, co-benefits may justify more stringent climate change policy by increasing the avoided societal damages, as in figure 3(a). Second, co-benefits improve the robustness of stringent climate policy. Acknowledging uncertainty in both the damage function and the abatement cost function, inclusion of AQ co-benefits provides a hedge against lower than expected climate damages or higher than expected mitigation costs. AQ co-benefits also occur earlier than climatic ones, making the social benefits calculation less sensitive to the choice of discount rate, thereby diminishing the significance of using low (Stern and Taylor 2007) or high discount rates (Nordhaus 2007). By increasing the robustness of climate policy to uncertain damages, abatement costs, and discount rates, co-benefits support more aggressive near term climate action even in the face of large uncertainty (Manne 1995).

An extension of this set of arguments on lower costs, higher stringency, and robustness is that inclusion of co-benefits provides stronger incentives for cooperation from developing countries than do climatic benefits alone. Due to lower incomes, an earlier stage of development, and negligible historical contribution to the stock of atmospheric greenhouse gases, rapidly growing developing countries are particularly sensitive to abatement costs and have shown little enthusiasm for reducing emissions. However, reducing their emissions from the trajectory of the last decade is essential to addressing the global problem. Game theoretic models show that the nearer term and more localized AQ co-benefits of climate change mitigation might be sufficiently important to developing countries that they would participate in international agreements (Pittel and Rubbelke 2008). Indeed, in figure 2 the value of AQ co-benefits in developing countries appears higher than in developed countries, although not significantly so given the few valuation studies in developing countries.

A second main implication is that including AQ co-benefits has a distributional effect because it changes the beneficiary of climate change actions. In particular, as the geographic benefits of international offset projects in the energy sector become more local, the value of offset projects for developing countries increases because the value of AQ co-benefits are added to the value of financial transfers from developed countries. As a result, entities in developed countries should expect to pay lower prices for offset projects in developing countries, while the value of domestic mitigation in developed countries will also increase. Thus, the cost of carbon mitigation decreases for both domestic and international abatement measures. A comparison of the value of co-benefits in developed countries in section 2 above (median = $\$31/tCO_2$) to the prices paid for offsets at present ($\sim\$20/tCO_2$) suggests that developed countries may prefer local mitigation, which creates AQ co-benefits, over purchasing international offsets; many international offset projects will be more expensive than domestic projects, even if international offsets would be cheaper with AQ co-benefits valued than without. The valuation of local AQ co-benefits is likely to have a diminishing effect on the flow of offset funds from developed to developing countries. This outcome suggests that the goal of financial transfer from developed to developing countries would be more effectively accomplished through direct support for activities, such as adaptation and poverty alleviation, rather than relying mainly on international offset projects as the transfer mechanism.

A related issue is that the geographic dispersion of the benefits of mitigation will become more closely tied to location of emissions. A fundamental justification behind GHG emissions trading is that the atmosphere is indifferent to the location of emissions since the six greenhouse gases

regulated under the Kyoto protocol are long lived and are well mixed throughout each hemisphere (for methane) or the globe (for others, including CO_2). The broadening of scope from climate benefits to air quality benefits raises the importance of the location of emissions. Given the wide dispersion in the costs to reduce GHG emissions, it is possible that trading could concentrate emissions in locations with high abatement costs (Farrell and Lave 2004). While the development of such *hotspots* does not affect the geographic incidence of climatic damages, it would introduce environmental justice concerns if air pollution health effects become concentrated as a result.

Third, actions that are equivalent in radiative forcing are not equivalent in value. Inclusion of AQ co-benefits increases appeal of transforming energy production and use relative to other means of addressing climate change, which have less pronounced effects on air quality. For example, the appeal of forest preservation will diminish relative to emissions mitigation when AQ co-benefits are included—though of course valuation of other co-benefits such as biodiversity would increase the relative appeal of forests. Similarly, AQ co-benefits reduce the attractiveness of adaptation and climate engineering relative to mitigation. To be sure, adaptation is still necessary, but its role as an appealing alternative to costly mitigation is diminished. Concerns about climate engineering schemes that propose reducing radiative forcing without necessarily changing emissions have been raised due to uncertainties about efficacy and side effects (Bengtsson 2006). Indeed, some solar radiation modification schemes have the potential to reduce air quality (Crutzen 2006, Victor 2008), and even those with no adverse affect must take into account the opportunity cost of missed air quality improvements. The observed under-prioritization of adaptation and climate engineering relative to mitigation (Pielke *et al* 2007) may be partially attributable to concern over the loss of AQ co-benefits, even if not explicitly expressed.

Finally, it is not obvious that all climate change mitigation actions that provide AQ co-benefits will be pursued. Policy makers may simply choose to address AQ directly since it is almost certainly cheaper to reduce local air pollution directly rather than via climate policy (Johnson 2001). This possibility seems especially pertinent in developing countries where, for the reasons discussed above, climate change mitigation has to date been considered a developed country responsibility. It may also be a concern at higher levels of GhG mitigation where abatement costs become expensive and AQ co-benefits start to look relatively small. It may become reasonable for countries, especially developing ones, to consider avoided climate change damages as a co-benefit of efforts to reduce air quality. If high-CO_2-emitting developing countries were to take such a perspective, it would complicate implementation of an international climate agreement. For example, emissions trading between countries would be difficult if one country were to set a national limit on GHG emissions while the other had a national limit on SO_2, NO_x, or other pollutants. Although it may ultimately prove essential to overcoming international collective action problems, it would require a high degree of flexibility and a tolerance for heterogeneity in national implementation plans that goes well beyond what has been agreed upon so far in the international climate regime.

5. Why are AQ co-benefits acknowledged but ignored?

Given these implications, ignoring co-benefits skews policy decisions and leads to sub-optimal social outcomes. Many studies discuss the benefits of a more comprehensive assessment and policy (IPCC 2007, Haines *et al* 2007, Bond 2007). If AQ co-benefits are so substantial and their implications so important, why do not they play a larger role in affecting climate policy design? Several characteristics of AQ co-benefits contribute to their under-valuation.

5.1. Uncertainty in climatic damages and abatement costs

Uncertainty about both the costs and benefits of climate change mitigation reduces the role of air quality benefits in policy debates because it complicates comparisons. This is in contrast to prominent arguments that assert that AQ co-benefits make *no regrets* climate policy possible because the greater certainty of AQ co-benefits reduces the importance of uncertainty over climatic damages. However, the large uncertainty over the benefits of avoided climate change has shaped the policy discourse so that policy design is framed as a problem of cost minimization; benefits are not counted explicitly because estimates are not sufficiently reliable. The resulting marginalization of climatic benefits has had the effect of excluding quantitative representation of benefits in general, including AQ benefits. AQ co-benefits have so far not diminished the importance of climatic uncertainty; rather, deep and persistent climatic uncertainty has led to a policy discourse in which it is extremely difficult for AQ benefits to play a central role.

Cooperation on climate change is difficult in part because the abatement costs in climate policy are so uncertain (Swart *et al* 2009). Claims are made both that climate policy will cost several per cent of gross world product and that climate policy will actually stimulate economic growth (Tol 2009). Estimates reported by the IPCC alone show a range of carbon prices from \$20-100/tCO_2 for 25% emissions reduction from business as usual by 2030 (Nemet 2010). That almost every climate policy proposal involves a quantity-based target rather than price-based target sustains cost uncertainty. In practice, assumptions about base case emissions growth, the supply of loss-cost energy efficiency investments, the cost of renewables, the diffusion of nuclear, and the availability of carbon capture and sequestration technology, as well as other items, leads to large dispersion in abatement costs. In contrast, the technologies involved in air quality improvement are less dynamic, have a longer history, involve a much more limited set of options, and do not require changes to existing infrastructures.

While the overwhelming portion of the discussion on climate policy is focused on abatement costs, the more important source of uncertainty for AQ co-benefits arises from in climate damages. More specifically, estimates of the climate-related damages *avoided* as a result of climate policy are the central concern for policy makers. Estimation of avoided damages involves 'deep uncertainty' because reliable probability distributions of possible outcomes are not available (Lempert 2002, Keller *et al* 2008, Gosling *et al* 2009). One recent survey of published estimates found a range of climate

damages from \$0-33 000/tCO_2, depending on assumptions related to risk aversion, equity, and time preferences (Anthoff *et al* 2009). Of particular concerns is the potential for positive feedbacks, irreversibility and rapid change to the climate system (Torn and Harte 2006). In contrast, estimation of AQ damages is less problematic, in part because the effects of air pollution on human health are nearer term, less geographically dispersed, and are well studied.

Even though damages are the ultimate motivation for climate policy, as shown above, they are not typically included in assessments of climate policy. One interpretation is that we simply distrust the reliability of climate impact studies. An alternative hypothesis is that since the uncertainties are so large and values hinge on choice about small changes in discount rates, that discussion quickly becomes philosophical, and not amenable to policy discourse. Another reason that damage values are infrequently discussed is that willingness to pay to avoid them appears quite low; a contingent valuation study of willingness of US residents to pay for the Kyoto Protocol estimated that households valued the benefits at just under \$191 per household per year (Berrens *et al* 2004), which implies political support for a carbon price in the mid-single digits of \$/tCO_2. More broadly, contingent valuation studies suffer from ignorance about what type of climate people actually want (Dietz and Maddison 2009). Finally, the characteristics of the risks being compared are different (Slovic 1987); the lethal aspects of the health impacts of air pollution may provide a catalyst for regulatory action that, at least at present, is missing in climate change.

5.2. Measurement and valuation

Another reason that AQ co-benefits are typically excluded is that valuation results are sensitive to choices about methodology and parameter values (Bell *et al* 2008). Even if the benefits are widely found to be substantial, standard metrics for economic valuation of health impacts do not exist, which is a particular problem in valuing loss of life and assessing heterogeneous sub-populations. Development of 'Health Impact Assessment' provides one avenue to remedy this problem (Patz *et al* 2008). Valuation of health and life is made worse by disagreement over the appropriate discount rate to use (Stern and Taylor 2007, Nordhaus 2007, Anthoff *et al* 2009). The smaller temporal and geographical scales of AQ impacts relative to climatic impacts make comparison difficult as well. The more diverse set of pollutants that need to be taken into account to optimize the pursuit of AQ and climate benefits, combined with the nearer term impact of AQ impacts, heightens the sensitivity of valuation results to choices of global warming potentials to compare gases (West *et al* 2007, Smith and Haigler 2008). Finally, some have suggested that the transactions and information costs associated with AQ co-benefits are so high that they would offset incremental benefits (Elbakidze and McCarl 2007); however, the values found in section 2 imply that those costs would have to be extremely high. The paucity of studies that value co-benefits in developing countries—for example in figure 1—suggests that the challenges of valuation are even more problematic in those contexts.

5.3. Institutions and epistemic communities

Institutional barriers, in both the scientific and political domains, also discourage inclusion of co-benefits. Scientifically, the networks of institutions and individuals contributing knowledge on air quality have little overlap with those on climate change (Swart 2004). The lack of shared assumptions, methods, and data makes integration of scientific results difficult (Norgaard 2004). The international policy regime reflects a similar separation; the UN Framework Convention on Climate Change and the Convention on Long-Range Transboundary Air Pollution remain separate despite calls for better integration (Holloway *et al* 2003). The adverse consequences of this division of international governance are likely to heighten if countries adopt divergent priorities on climate change and air quality. For example, large developing countries might value avoided climatic damage as a co-benefit of their pursuit of air quality improvement while developed countries might focus on climate impacts directly, with AQ as an ancillary benefit. In effect, climate change may become an 'impure' public good, with private gains from mitigation alleviating free-rider issues (Finus and Ruebbelke 2008). While heterogeneous pursuit of common outcomes might provide a promising context with which to resolve collective action problems, the separation of governance regimes is likely to impede progress. Finally, the implications described above may realign interest group coalitions that are affecting the political process in favor of action on mitigation. The relative decline in the attractiveness of afforestation, adaptation, and climate engineering once AQ co-benefits are taken into account, may threaten the cohesion of coalitions of support of climate policy at the national and international levels. Adding complexity to an already complex regime may reduce salience and consequent political feasibility as well (Young 1989, Rypdal *et al* 2005). This challenge need not be paralyzing; a US Senate committee passed a 'four pollutant bill' for CO_2, SO_2, NO_x, and Hg in 2002 (S.556) and Senators were discussing introducing a similar bill in late-2009.

6. Conclusion

The full inclusion of AQ co-benefits in the design and evaluation of climate policy would almost certainly enhance social outcomes because these co-benefits are large and because policy analysis has not valued them. Moreover, that AQ co-benefits are more local, nearer term, and health related has the potential to enhance incentives for cooperation by engaging actors that are averse to the costs of climate policy or unmotivated by avoided climatic damages. Still, a variety of barriers exist to their inclusion. The framing of the climate policy discourse is likely to continue as one of cost minimization until the benefits of avoided climate change can be more reliably estimated. As a result, a risk remains that AQ co-benefits will be treated as serendipitous and tangential, rather than as driving forces for strong climate policy. Full consideration of AQ co-benefits in policy debates will require improved evaluation techniques for *both* the climatic benefits and the air quality benefits of climate policy. Improving valuation of AQ co-benefits alone is unlikely to promote

more stringent climate policy, even if it helps justify more stringent air quality regulation. In a more general sense, the effort to fully consider the value of co-benefits with vastly different risk characterizations, as well as time and spatial scales, foreshadows challenges in considering other co-benefits of actions to reduce climatic damages. Additional benefits may include effects on crop yields, acid deposition, macro-economic shocks, and geo-political conflict.

Acknowledgments

We thank the Wisconsin Focus on Energy program for financial support and Martin Broyles for research assistance.

Appendix

Table A.1. Studies estimating the co-benefits of climate change mitigation in developed countries.

	Study	Geography	Sectors included	Value of co-benefits (2008$/tCO$_2$)		
				Midrange	High	Low
1	Ayres and Walter (1991)	US	All	68	n.e.	n.e.
2	Ayres and Walter (1991)	Germany	All	128	n.e.	n.e.
3	Pearce (1992)	Norway	All	68	n.e.	n.e.
4	Pearce (1992)	UK	All	80	n.e.	n.e.
5	Alfsen *et al* (1992)	Norway	All	51	60	42
6	Holmes *et al* (1993)	US	Electric	4	n.e.	n.e.
7	Dowlatabadi *et al* (1993)	US	Electric	4	n.e.	n.e.
8	Goulder (1993)	US	All	44	n.e.	n.e.
9	Barker (1993)	UK	All	50	82	18
10	Barker (1993)	US	All	103	n.e.	n.e.
11	Barker (1993)	Norway	All	98	125	71
12	Viscusi *et al* (1994)	US	Electric	116	n.e.	n.e.
13	Rowe (1995)	US	Electric	31	n.e.	n.e.
14	Boyd *et al* (1995)	US	All	53	n.e.	n.e.
15	Palmer and Burtraw (1997)	US	Electric	6	n.e.	n.e.
16	EPA (1997)	US	Electric	31	n.e.	n.e.
17	Mccubbin (1999)	US	Electric	49	89	10
18	Caton and Constable (2000)	Canada	All	13	n.e.	n.e.
19	Syri *et al* (2001)	EU-15	All	n.e.	n.e.	n.e.
20	Han (2001)	Korea	All	80	91	69
21	Syri *et al* (2002)	Finland	All	n.e.	n.e.	n.e.
22	Bye *et al* (2002)	Nordic countries	All	18	26	11
23	Burtraw *et al* (2003)	US	Electric	17	18	15
24	Proost and Regemorter (2003)	Belgium	All	n.e.	n.e.	n.e.
25	Joh *et al* (2003)	Korea	All	2	n.e.	n.e.
26	van Vuuren *et al* (2006)	Europe	All	n.e.	n.e.	n.e.
27	Bollen *et al* (2009)	Netherlands	All	n.e.	n.e.	n.e.
28	Tollefsen *et al* (2009)	Europe	All	n.e.	n.e.	n.e.

Notes n.e. = not estimated in $/CO$_2$ terms. Especially useful previous reviews include: Ekins (1996), Burtraw *et al* (2003), IPCC (2007).

Table A.2. Studies estimating the co-benefits of climate change mitigation in developing countries.

	Study	Geography	Sectors included	Value of co-benefits (2008$/tCO$_2$)		
				Midrange	High	Low
29	Wang and Smith (1999)	China	Electric	n.e.	n.e.	n.e.
30	Cifuentes *et al* (2001)	Brazil	All	n.e.	n.e.	n.e.
31	Cifuentes *et al* (2001)	Mexico	All	n.e.	n.e.	n.e.
32	Bussolo and O'Connor (2001)	India	All	n.e.	n.e.	n.e.
33	O'Connor *et al* (2003)	China	All	n.e.	n.e.	n.e.
34	Dessus and O'Connor (2003)	Chile	All	n.e.	n.e.	n.e.
35	Aunan *et al* (2004)	China	Electric	36	n.e.	n.e.
36	Aunan *et al* (2004)	China	Electric	27	n.e.	n.e.
37	Aunan *et al* (2004)	China	Electric	36	n.e.	n.e.
38	Aunan *et al* (2004)	China	Electric	36	n.e.	n.e.
39	Aunan *et al* (2004)	China	Electric	98	n.e.	n.e.
40	Aunan *et al* (2004)	China	Electric	135	n.e.	n.e.
41	Kan *et al* (2004)	China	All	n.e.	n.e.	n.e.
42	Kan *et al* (2004)	China	All	n.e.	n.e.	n.e.
43	Morgenstern *et al* (2004)	China	Electric	119	196	43
44	West *et al* (2004)	Mexico	All	n.e.	n.e.	n.e.
45	McKinley *et al* (2005)	Mexico	All	n.e.	n.e.	n.e.
46	Li (2006)	Thailand	All	n.e.	n.e.	n.e.
47	Vennemo *et al* (2006)	China	Elec. & Industrial	n.e.	n.e.	n.e.
48	Zhang *et al* (2010)	China	All	n.e.	n.e.	n.e.

Notes n.e. = not estimated in $/CO$_2$ terms. Especially useful previous reviews include: Ekins (1996), Burtraw *et al* (2003), IPCC (2007).

References

Alfsen K H, Brendemoen A and Glomsrod S 1992 Benefits of climate policies: some tentative calculations *Discussion Paper 69* Central Bureau of Statistics, Oslo

Amann M *et al* 2009 *Potentials and Costs for Greenhouse Gas Mitigation in Annex I Countries: Initial Results* (Laxenburg: International Institute for Applied Systems Analysis)

Anthoff D, Tol R S J and Yohe G W 2009 Risk aversion, time preference, and the social cost of carbon *Environ. Res. Lett.* **4** 024002

Aunan K, Fang J H, Vennemo H, Oye K and Seip H M 2004 Co-benefits of climate policy—lessons learned from a study in Shanxi, China *Energy Policy* **32** 567–81

Ayres R U and Walter J 1991 The greenhouse effect: damages, costs and abatement *Environ. Res. Econ.* **1** 237–70

Barker T 1993 *Secondary Benefits of Greenhouse Gas Abatement: The Effects of a UK Carbon/Energy Tax on Air Pollution* (Cambridge: Department of Applied Economics, University of Cambridge)

Bell M, Davis D, Cifuentes L, Krupnick A, Morgenstern R and Thurston G 2008 Ancillary human health benefits of improved air quality resulting from climate change mitigation *Environ. Health* **7** 41

Bengtsson L 2006 Geo-engineering to confine climate change: is it at all feasible? *Clim. Change* **77** 229–34

Berrens R P, Bohara A K, Jenkins-Smith H C, Silva C L and Weimer D L 2004 Information and effort in contingent valuation surveys: application to global climate change using national internet samples *J. Environ. Econ. Manage.* **47** 331–63

Bollen J, van der Zwaan B, Brink C and Eerens H 2009 Local air pollution and global climate change: a combined cost-benefit analysis *Res. Energy Econ.* **31** 161–81

Bond T C 2007 Can warming particles enter global climate discussions? *Environ. Res. Lett.* **2** 045030

Boyd R, Krutilla K and Viscusi W K 1995 Energy taxation as a policy instrument to reduce CO_2 emissions—a net benefit analysis *J. Environ. Econ. Manag.* **29** 1–24

Burtraw D, Krupnick A, Palmer K, Paul A, Toman M and Bloyd C 2003 Ancillary benefits of reduced air pollution in the US from moderate greenhouse gas mitigation policies in the electricity sector *J. Environ. Econ. Manag.* **45** 650–73

Bussolo M and O'Connor D 2001 *Clearing the Air in India: The Economics of Climate Policy With Ancillary Benefits* (Paris: OECD)

Bye B, Kverndokk S and Rosendahl K E 2002 Mitigation costs, distributional effects, and ancillary benefits of carbon policies in the Nordic countries, the UK, and Ireland *Mitig. Adapt. Strateg. Glob. Change* **7** 339–66

Caton R and Constable S 2000 *Clearing the Air: A Preliminary Analysis of Air Quality Co-Benefits from Reduced Greenhouse Gas Emissions in Canada* The David Suzuki Foundation

CBO 2009 *Congressional Budget Office Cost Estimate of H.R. 2454, American Clean Energy and Security Act of 2009* (Washington DC: Congressional Budget Office)

Cifuentes L, Borja-Aburto V H, Gouveia N, Thurston G and Davis D L 2001 Assessing the health benefits of urban air pollution reductions associated with climate change mitigation (2000–2020): Santiago, Sao Paulo, Mexico City, and New York City *Environ. Health Perspect.* **109** 419–25

Crutzen P 2006 Albedo enhancement by stratospheric sulfur injections: a contribution to resolve a policy dilemma? *Clim. Change* **77** 211–20

DECC 2008 *Climate Change Act 2008 Impact Assessment* (London: UK Department of Energy and Climate Change)

Dessus S and O'Connor D 2003 Climate policy without tears: CGE-based ancillary benefits estimates for Chile *Environ. Res. Econ.* **25** 287–317

Dietz S and Maddison D 2009 New frontiers in the economics of climate change *Environ. Res. Econ.* **43** 295–306

Dowlatabadi H, Tschang F and Siegel S 1993 *Estimating the Ancillary Benefits of Selected Carbon Dioxide Mitigation Strategies: Electicity Sector* Climate Change Division, US Environmental Protection Agency

EIA 2008 *Energy Market and Economic Impacts of S.1766, the Low Carbon Economy Act of 2007* (Washington DC: Energy Information Administration)

Ekins P 1996 The secondary benefits of CO_2 abatement: how much emission reduction do they justify? *Ecol. Econ.* **16** 13–24

Elbakidze L and McCarl B A 2007 Sequestration offsets versus direct emission reductions: consideration of environmental co-effects *Ecol. Econ.* **60** 564–71

EPA 1997 *Regulatory Impact Analysis for the Particulate Matter and Ozone National Ambient Air Quality Standards and Proposed Regional Haze Rule* (Washington, DC: US Environmental Protection Agency Office of Air Quality and Planning)

EPA 2008 *EPA's Economic Analysis of the Low Carbon Economy Act of 2007 (S.1766)* (Washington, DC: Environmental Protection Agency)

Farrell A E and Lave L B 2004 Emission trading and public health *Ann. Rev. Public Health* **25** 119

Finus M and Ruebbelke D T G 2008 *Coalition Formation and the Ancillary Benefits of Climate Policy* (Milan: Fondazione Eni Enrico Mattei)

Gosling S, Lowe J, McGregor G, Pelling M and Malamud B 2009 Associations between elevated atmospheric temperature and human mortality: a critical review of the literature *Clim. Change* **92** 299–341

Goulder L 1993 *Economy-Wide Emissions Impacts of Alternative Energy Tax Proposals* Climate Change Division, US Environmental Protection Agency

Haines A, Smith K R, Anderson D, Epstein P R, McMichael A J, Roberts I, Wilkinson P, Woodcock J and Woods J 2007 Energy and health 6—policies for accelerating access to clean energy, improving health, advancing development, and mitigating climate change *Lancet* **370** 1264–81

Han H 2001 *Analysis of the Environmental Benefits of Reductions in Greenhouse Gas Emissions* (Seoul: Korean Environmental Institute)

Holloway T, Fiore A and Hastings M G 2003 Intercontinental transport of air pollution: will emerging science lead to a new hemispheric treaty? *Environ. Sci. Technol.* **37** 4535–42

Holmes R, Keinath D and Sussman F 1993 *Ancillary Benefits of Mitigating Climate Change: Selected Actions from the Climate Change Action Plan* Climate Change Division, US Environmental Protection Agency

IPCC 2007 *Climate change 2007: Mitigation. Contribution of Working group III to the 4th Assessment Report of the Intergovernmental Panel on Climate Change* (Cambridge: Cambridge University Press)

Jaffe A B, Newell R G and Stavins R N 2005 A tale of two market failures: technology and environmental policy *Ecol. Econ.* **54** 164–74

Joh S, Nam Y-M, Shim S, Sung J and Shin Y 2003 Empirical study of environmental ancillary benefits due to greenhouse gas mitigation in Korea *Int. J. Sustain. Dev.* **6** 311–27

Johnson M 2001 'Hidden Health Benefits of Greenhouse Gas Mitigation' offers nothing to policy-makers (eLetter response) *Science* www.sciencemag.org/cgi/eletters/293/5533/1257

Kan H D, Chen B H, Chen C H, Fu Q Y and Chen M 2004 An evaluation of public health impact of ambient air pollution under various energy scenarios in Shanghai, China *Atmos. Environ.* **38** 95–102

Keller K, Yohe G and Schlesinger M 2008 Managing the risks of climate thresholds: uncertainties and information needs *Clim. Change* **91** 5–10

Kriegler E 2007 On the verge of dangerous anthropogenic interference with the climate system? *Environ. Res. Lett.* **2** 5
Lempert R J 2002 A new decision sciences for complex systems *Proc. Natl Acad. Sci. USA* **99** 7309–13
Li J C 2006 A multi-period analysis of a carbon tax including local health feedback: an application to Thailand *Environ. Dev. Econ.* **11** 317–42
Manne A S 1995 The rate of time preference—implications for the greenhouse debate *Energy Policy* **23** 391–4
Mccubbin D 1999 *Co-Control Benefits of Greenhouse Gas Control Policies* US Environmental Protection Agency, Office of Policy
McKinley G *et al* 2005 Quantification of local and global benefits from air pollution control in Mexico City *Environ. Sci. Technol.* **39** 1954–61
Morgenstern R, Krupnick A and Zhang X 2004 The ancillary carbon benefits of SO_2 reductions from a small-boiler policy in Taiyuan, PRC *J. Environ. Dev.* **13** 140–55
Nemet G 2010 Cost containment in climate policy and incentives for technology development *Clim. Change* in press (doi:10.1007/s10584-009-9779-8)
Nordhaus W 2007 Critical assumptions in the Stern review on climate change *Science* **317** 201–2
Nordhaus W 2008 *A Question of Balance: Weighing the Options on Global Warming Policies* (New Haven, CT: Yale University Press)
Norgaard R B 2004 Learning and knowing collectively *Ecol. Econ.* **49** 231–41
O'Connor D, Zhai F, Aunan K, Berntsen T and Vennemo H 2003 *Agricultural and Human Health Impacts of Climate Policy in China: A General Equilibrium Analysis with Special Reference to Guangdong* (Paris: OECD, Development Centre)
Ostblom G and Samakovlis E 2007 Linking health and productivity impacts to climate policy costs: a general equilibrium analysis *Clim. Policy* **7** 379–91
Palmer K and Burtraw D 1997 Electricity restructuring and regional air pollution *Res. Energy Econ.* **19** 139–74
Patz J, Campbell-Lendrum D, Gibbs H and Woodruff R 2008 Health impact assessment of global climate change: expanding on comparative risk assessment approaches for policy making *Ann. Rev. Public Health* **29** 27
Pearce D W 1992 *The Secondary Benefits of Greenhouse Gas Control* (Norwich: The Centre for Social and Economic Research on the Global Environment (CSERGE))
Pielke R, Prins G, Rayner S and Sarewitz D 2007 Lifting the taboo on adaptation *Nature* **445** 597–8
Pittel K and Rubbelke D T G 2008 Climate policy and ancillary benefits: a survey and integration into the modelling of international negotiations on climate change *Ecol. Econ.* **68** 210–20
Proost S and Regemorter D V 2003 Interaction between local air pollution and global warming and its policy implications for Belgium *Int. J. Glob. Environ. Issues* **3** 266–86
Rowe R 1995 *The New York State Externalities Cost Study* (Dobbs Ferry, NY: Hagler Bailly Consulting)
Rypdal K, Berntsen T, Fuglestvedt J S, Aunan K, Torvanger A, Stordal F, Pacyna J M and Nygaard L P 2005 Tropospheric ozone and aerosols in climate agreements: scientific and political challenges *Environ. Sci. Policy* **8** 29–43
Slovic P 1987 Perception of risk *Science* **236** 280–5
Smith K R and Haigler E 2008 Co-benefits of climate mitigation and health protection in energy systems: scoping methods *Ann. Rev. Public Health* **29** 11
Stern N 2006 *Stern Review on the Economics of Climate Change* (Cambridge: Cambridge University Press)
Stern N and Taylor C 2007 Climate change: risk, ethics, and the Stern review *Science* **317** 203–4
Swart R 2004 A good climate for clean air: linkages between climate change and air pollution—an editorial essay *Clim. Change* **66** 263–9
Swart R, Bernstein L, Ha-Duong M and Petersen A 2009 Agreeing to disagree: uncertainty management in assessing climate change, impacts and responses by the IPCC *Clim. Change* **92** 1–29
Syri S, Amann M, Capros P, Mantzos L, Cofala J and Klimont Z 2001 Low-CO_2 energy pathways and regional air pollution in Europe *Energy Policy* **29** 871–84
Syri S, Karvosenoja N, Lehtila A, Laurila T, Lindfors V and Tuovinen J P 2002 Modeling the impacts of the Finnish climate strategy on air pollution *Atmos. Environ.* **36** 3059–69
Tol R S J 2009 The economic effects of climate change *J. Econ. Perspect.* **23** 29–51
Tollefsen P, Rypdal K, Torvanger A and Rive N 2009 Air pollution policies in Europe: efficiency gains from integrating climate effects with damage costs to health and crops *Environ. Sci. Policy* **12** 870–81
Tom M S and Harte J 2006 Missing feedbacks, asymmetric uncertainties, and the underestimation of future warming *Geophys. Res. Lett.* **33** L10703
van Vuuren D P, Cofala J, Eerens H E, Oostenrijk R, Heyes C, Klimont Z, den Elzen M G J and Amann M 2006 Exploring the ancillary benefits of the Kyoto Protocol for air pollution in Europe *Energy Policy* **34** 444–60
Vennemo H, Aunan K, Fang J H, Holtedahl P, Tao H and Seip H M 2006 Domestic environmental benefits of China's energy-related CDM potential *Clim. Change* **75** 215–39
Victor D G 2008 On the regulation of geoengineering *Oxford Rev. Econ. Policy* **24** 322–36
Viscusi W K, Magat W A, Carlin A and Dreyfus M K 1994 Environmentally responsible energy pricing *Energy J.* **15** 23–42
Wang X D and Smith K R 1999 Secondary benefits of greenhouse gs control: health impacts in China *Environ. Sci. Technol.* **33** 3056–61
West J J, Fiore A M, Naik V, Horowitz L W, Schwarzkopf M D and Mauzerall D L 2007 Ozone air quality and radiative forcing consequences of changes in ozone precursor emissions *Geophys. Res. Lett.* **34** L06806
West J J, Osnaya P, Laguna I, Martinez J and Fernandez A 2004 Co-control of urban air pollutants and greenhouse gases in Mexico City *Environ. Sci. Technol.* **38** 3474–81
Young O R 1989 The politics of international regime formation—managing natural-resources and the environment *Int. Org.* **43** 349–75
Zhang D, Aunan K, Martin Seip H, Larssen S, Liu J and Zhang D 2010 The assessment of health damage caused by air pollution and its implication for policy making in Taiyuan, Shanxi, China *Energy Policy* **38** 491–502